PERFORMANCE ASSESSMENT OF SLUDGE-MIXED CEMENT GROUT IN ROCK FRACTURES

Khomkrit Wetchasat

A Thesis Submitted in Partial Fulfillment of the Requirements for the

Doctor of Philosophy of Engineering in Geotechnology

Suranaree University of Technology

Academic Year 2013

การศึกษาศักยภาพของส่วนผสมตะกอนกับซีเมนต์เพื่ออุดรอยแตกหิน

นายคมกริช เวชสัสถ์

วิทยานิพนธ์นี้เป็นส่วนหนึ่งของการศึกษาตามหลักสูตรปริญญาวิศวกรรมศาสตรดุษฎีบัณฑิต

สาขาวิชาเทคโนโลยีธรณี

มหาวิทยาลัยเทคโนโลยีสุรนารี

ปีการศึกษา 2556

PERFORMANCE ASSESSMENT OF SLUDGE-MIXED CEMENT GROUT IN ROCK FRACTURES

Suranaree University of Technology has approved this thesis submitted in partial fulfillment of the requirements for the Degree of Doctor of Philosophy.

Thesis Examining Committee

____

(Dr. Decho Phueakphum)

Chairperson

____

(Prof. Dr. Kittitep Fuenkajorn)

Member (Thesis Advisor)

____

(Prof. Dr. Suksun Horpibulsuk)

Member

____

(Assoc. Prof. Ladda Wannakao)

Member

____

(Dr. Prachya Tepnarong)

Member

____

(Prof. Dr. Sukit Limpijumnong)

Vice Rector for Academic Affairs and Innovation

____

(Assoc. Prof. Flt. Lt. Dr. Kontorn Chamniprasart)

Dean of Institute of Engineering

คมกริช เวชสัสถ์ : การศึกษาศักยภาพของส่วนผสมตะกอนกับซีเมนต์เพื่ออุดรอยแตกหิน (PERFORMANCE ASSESSMENT OF SLUDGE-MIXED CEMENT GROUT IN ROCK FRACTURES) อาจารย์ที่ปรึกษา : ศาสตราจารย์ ดร.กิตติเทพ เฟื่องขจร, 192 หน้า.

วัตถุประสงค์ของการศึกษานี้คือเพื่อประเมินศักยภาพของดินตะกอนผสมกับปูนซีเมนต์ปอร์ตแลนด์ประเภท 1 เพื่อใช้ลดความซึมผ่านของน้ำในรอยแตกของหินทราย รอยแตกถูกทำขึ้นโดยแรงกดในแนวเส้นบนตัวอย่างหินทรายชุดภูกระดึงเพื่อให้หินแตกออกจากกันด้วยแรงดึง ตัวอย่างหินมีขนาด $0.15\times0.15\times0.15$ m ตะกอนจากโรงงานกำจัดตะกอนบางเขนถูกนำมาทดสอบคุณสมบัติเชิงกายภาพและเชิงเคมี มีการหาค่าความหนืดของส่วนผสมเหลวที่น้อยที่สุดแต่ให้ค่ากำลังกดในแกนเดียวที่เหมาะสม ผลทดสอบระบุว่าสัดส่วนที่เหมาะสมของตะกอนต่อซีเมนต์ (S:C) เท่ากับ 1:10, 3:10, 5:10 และเบนทอไนต์ต่อซีเมนต์ (B:C) เท่ากับ 1:10, 2:10, 3:10 ใช้ปริมาณน้ำต่อซีเมนต์เท่ากับ 1:1 เนื่องจากให้ค่าความหนืดของส่วนผสมเหลวไม่เกิน 5 Pa·s และให้ค่ากำลังกดสูงสุด สัดส่วนของ S:C เท่ากับ 3:10 จะให้ค่ากำลังกดเท่ากับ 1.22 MPa และค่าสัมประสิทธิ์ความยืดหยุ่นเท่ากับ 224 MPa ซึ่งต่ำกว่าค่าจาก B:C เล็กน้อย ค่ากำลังเฉือนระหว่างผิวรอยแตกกับส่วนผสมทั้งหมดมีค่าใกล้เคียงกันคืออยู่ในช่วง 0.22 ถึง 0.90 MPa ภายใต้ความเค้นตั้งฉากจาก 0.25 ถึง 1.25 MPa ค่าความซึมผ่านของทุกส่วนผสมจะลดลงในเชิงเวลาซึ่งให้ค่าอยู่ในช่วง 10^{-17} ถึง 10^{-15} m^2 สัดส่วนของ S:C เท่ากับ 5:10 ให้ค่าความซึมผ่านต่ำสุด และของส่วนผสมที่อยู่ในรอยแตกมีระยะการเปิดเผยอเท่ากับ 0.2, 1.0 และ 2.0 cm มีค่าใกล้เคียงกันในช่วง 10^{-16} to 10^{-14} m^2

สาขาวิชา เทคโนโลยีธรณี ลายมือชื่อนักศึกษา ____________________

ปีการศึกษา 2556 ลายมือชื่ออาจารย์ที่ปรึกษา________________

KHOMKRIT WETCHASAT : PERFORMANCE ASSESSMENT OF SLUDGE-MIXED CEMENT GROUT IN ROCK FRACTURES. THESIS ADVISOR : PROF. KITTITEP FUENKAJORN, Ph.D., P.E., 192 PP.

FRACTURE/ ROCK MASS/ PERMEABILITY/ GROUTING/ SLUDGE

The objective of this study is to assess the performance of sludge mixed with the commercial grade Portland cement type I for use in reducing permeability of fractures in sandstone. The fractures are artificially made in Phu Kradung sandstone by applying a line load to induce a splitting tensile crack in 0.15×0.15×0.15 m prismatic blocks. The Bang Khen water treatment sludge is used. The physical and chemical properties of the sludge are examined. This research emphasizes on determining the minimum slurry viscosity and appropriate strength of the grouting materials. The results indicate that the suitable mixing ratios for sludge:cement (S:C) are 1:10, 3:10, 5:10 and for bentonite:cement (B:C) are 1:10, 2:10, 3:10 with water-cement ratio of 1:1 by weight. These proportions yield the lowest slurry viscosity of 5 Pa·s and the highest compressive strength. For S:C = 3:10, the compressive strength and elastic modulus are 1.22 MPa and 224 MPa which are similar to those of bentonite mixed with cement. The shear strength of grouted fractures varies from 0.22 to 0.90 MPa under normal stresses ranging from 0.25 to 1.25 MPa. Permeability of grouting materials is from 10^{-17} to 10^{-15} m^2 and decrease with curing time. S:C of 5:10 give the lowest permeability. Permeabilities of grouted fractures with apertures of 0.2, 1.0 and 2.0 cm range frome 10^{-16} to 10^{-14} m^2.

School of Geotechnology   Student's Signature_________________

Academic Year 2013   Advisor's Signature_________________

TABLE OF CONTENTS

Page

TABLE OF CONTENTS (Continued)

Page

TABLE OF CONTENTS (Continued)

TABLE OF CONTENTS (Continued)

Page

TABLE OF CONTENTS (Continued)

Page

LIST OF TABLES

Table **Page**

LIST OF TABLES (Continued)

Table **Page**

LIST OF FIGURES

Figure **Page**

LIST OF FIGURES (Continued)

Figure **Page**

LIST OF FIGURES (Continued)

Figure **Page**

LIST OF FIGURES (Continued)

Figure **Page**

LIST OF FIGURES (Continued)

Figure **Page**

SYMBOLS AND ABBREVIATIONS

ROMAN ABBREVIATIONS:

A	=	Cross-section area
A, B, m	=	Constants
b	=	Spacing between fracture
B:C	=	Proportion of betonite-mixed cement or betonite:cement
C	=	Porland cement
C_0	=	Constant depends on fracture surface and initial joint aperture
c_p	=	Cohesion
D	=	Diameter of the injection hole at the center of the upper block
e	=	Hydraulic aperture
e_0	=	Hydraulic aperture at zero stress
e_0	=	Initial joint aperture
e_h	=	Hydraulic aperture
F	=	Sheared force
g	=	Acceleration due to gravity
H_c	=	Constant head
K	=	Hydraulic conductivity between smooth and parallel plates
k	=	Intrinsic permeability
k_0	=	Initial fracture permeability at initial normal stress

SYMBOLS AND ABBREVIATIONS (Continued)

K_f	=	Fracture conductivity
K_n	=	Normal stiffness of discontinuity
L	=	Thickness of grouting material in fracture apertures
L/D	=	Length to diameter ratio
m	=	Constant is equal to 1
P	=	Normal load
P_1	=	Effective modulus of the asperities
P_f	=	Maximum load
p_w	=	Water pressure within the discontinuity
Q	=	Flow rate
q	=	Water flow rate through the specimen
r	=	Radius of flow path
r_0	=	Radius of the radius injection hole
s	=	Fracture spacing
S:C	=	Proportion of sludge-mixed cement or sludge:cement.
SG	=	Specific gravity
W:C	=	Water-cement ratio or water:cement

GREEK ABBREVIATIONS:

β	=	Orientation of discontinuity
μ	=	Dynamic viscosity

SYMBOLS AND ABBREVIATIONS (Continued)

τ	=	Shear stress
ρ	=	Slurry density
ν_1	=	Normal deformation of the joint
ν	=	Kinetic viscosity
ν_0	=	Closure of the joint when the hydraulic aperture becomes zero
σ, σ_n	=	Normal stress
σ_0	=	Initial normal stress
σ_c	=	Compressive strength or effective confining stress
σ_{ch}	=	Confining healing pressure in which the permeability is zero
σ_h	=	Horizontal stress applied to the discontinuity
σ_z	=	Vertical stress applied to the discontinuity
δe	=	Change of the joint aperture due to stresses
δe_n	=	Normal deformation component
ΔP	=	Injecting water pressure
ρ_{slurry}	=	density of mixture slurry
ρ_w	=	Density of distilled water at the time of measurement
γ_w	=	Unit weight of water
μ	=	Dynamic viscosity of the water
ϕ_p	=	Angle of internal friction

CHAPTER I

INTRODUCTION

1.1 Background of problems and significance of the study

The increasing amount of the water treatment sludge from the Metropolitan Waterworks Authority (MWA) has called for a permanent solution to dispose of the sludge from four water treatment plants, including Bang Khen, Samsen, Thonburi, and Mahasawat. The water production report of the MWA (2007-2009) indicates that the Bang Khen Water Treatment Plant produces the largest capacity of 3,200,000 m^3/day. The sludge has been collected from the water treatment process (clarifying water system and filtering water system). The increasing sludge is about 162 tons/day. The sludge volume depends on the amount of sediment transported by rain water in the Choa Phraya River basin (Raw water source). The MWA has high expenditure for sludge disposal, especially during heavy rain years at which time there is more sludge deposited and slowly dried. The increase of potable water utilization results in the increase in size and duration of precipitation in sludge lagoon. The sludge in the lagoon has been treated by turning over and drying by sunlight, then becoming sludge cake. The sludge cake is usually taken to fill in abandoned land. After several years, it results in an excessively high deposition. Utilization of the sludge for other purposes is being considered in order to reduce the volumes of the sludge and the cost of disposal

One of the solutions is to mix the sludge with cement slurry for minimizing the groundwater circulation in rock mass. Groundwater in rock mass is one of the key factors governing the mechanical stability of slope embankments, underground mines, tunnels, and dam foundation. A common solution practiced internationally in the construction industry is to use bentonite-mixed with cement as a grouting material to reduce permeability in fractured rock mass. (Castelbaum and Shackelford 2009; Joshi et al. 2010; Malusis et al. 2009). The lack of a true understanding of the permeability characteristics of the sludge-mixed cement in fractured rock makes it difficult to predict the water flow in geological structures under the complex hydro-geological environments. Knowledge and experimental evidences about the permeability of the sludge-mixed cement in fractured rock under varied stress conditions have been rare.

1.2 Research objectives

The objectives of this study are to assess the performance of the Bang Khen water treatment sludge mixed with the commercial grade Portland cement for reducing permeability in saturated fractured rock in the laboratory and to compare the results with the bentonite-mixed cement in terms of the mechanical and hydraulic properties.

1.3 Research methodology

1.3.1 Literature review

Literature review is carried out to study the experimental researches on the water treatment sludge, grouting materials, and permeability of single fracture. The sources of information are from text books, journals, technical reports and conference papers. A summary of the literature review will be given in the thesis.

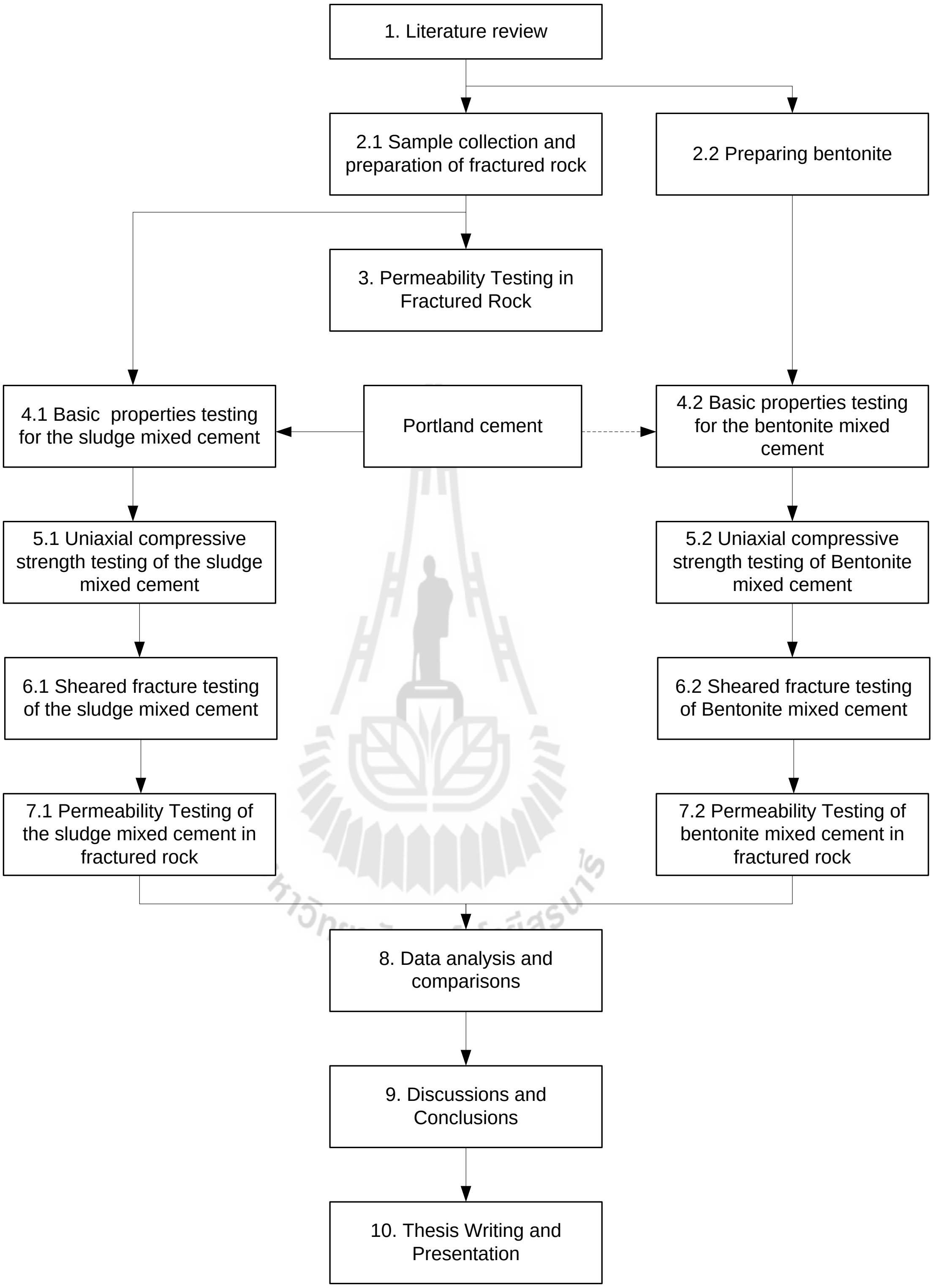

Figure 1.1 Research plan

1.3.2 Sample collection and preparation

The grouting materials used in this research are 1) the water treatment sludge with particle sizes less than 75 μm, 2) commercial grade bentonite for comparing with the sludge test results, 3) commercial grade Portland cement type I for mixing with the sludge and bentonite, and 4) sandstone samples from Phu Kradung formation. Sample preparation is carried out in the Geomechanics Research (GMR) Laboratory at Suranaree University of Technology. The fractures are artificially made by applying a line load at the center to induce a splitting tensile crack in 152.4×152.4×152.4 mm^3 blocks of sandstones. The fracture area is 152.4×152.4 mm^2. A minimum of eighteen sandstone specimens is tested for the three portions of sludge-mixed cement and bentonite-mixed cement under normal stresses ranging from 0.25 to 1.25 MPa. The sludge is collected from the Bang Khen Water Treatment Plant, the Metropolitan Waterworks Authority.

1.3.3 Permeability testing of fractures

Before grouting with sludge-mixed cement or bentonite-mixed cement into the artificial fracture of the sandstone specimens, the fracture permeability needed to be measured. The fracture permeability is used to compare with the permeability of grouting materials for both sludge and bentonte. Constant head flow tests are performed to determine the fracture permeability of sandstone specimens under normal stresses. The normal stresses are ranging from 0.25 to 1.25 MPa. Results simulate stress under various depths which can affect the permeability of grouting materials in fractured sandstone.

1.3.4 Basic properties testing of grouting materials

The objective of basic property test is to determine the density, viscosity, and permeability of sludge-mixed cement and bentonite-mixed cement. Sludge and bentonite-mixed cement ratios vary from 1:10, 2:10, 3:10, 4:10, to 5:10 for selecting the optimum mixing content. Similarities and differences of the results will be compared.

1.3.5 Uniaxial compressive strength testing of grouting materials

The objective of the uniaxial compressive strength tests is to determine the uniaxial compressive strength and elastic modulus of grouting material specimens. Grouting materials are sludge-mixed cement and bentonite-mixed cement. The test procedure is similar to the ASTM standards (ASTM C938, D4832 and C39). Sludge and bentonite-mixed cement ratios vary from 1:10, 2:10, 3:10, 4:10, to 5:10 for determining the strength and the elastic modulus.

1.3.6 Sheared fracture testing of grouting materials

The objective of the sheared fracture tests is to determine the shear strength of grouting material in sandstone fracture. Grouting materials are sludge and bentonite-mixed cement. The experimental procedure is similar to the ASTM standard (D5607). The constant normal stresses are 0.25, 0.5, 1.0 and 1.25 MPa. The shear stress is applied while the shear displacement and head drop is monitored for every 0.2 mm of shear displacement. Similarities and differences of the results are compared with other researches.

1.3.7 Permeability testing of grouting materials in rock fractures

The objective of permeability test of grouting materials in rock fractures is to determine the permeability of sludge-mixed cement and bentonite-mixed cement in artificial fractures. The grouting materials are used to fill the fractures. The constant normal stresses are 0.25, 0.5, 1.0 and 1.25 MPa.

1.3.8 Data analysis and comparisons

The research results are analyzed to optimize the grout mix ratios in terms of the mechanical and hydraulic properties. The results from the analysis are used in the comparison with other researches.

1.3.9 Discussions and conclusions

Discussions of the results are described to determine the reliability and accuracy of the measurements. Performance of the new grouting material is discussed based on the test results. Similarities and discrepancies of the grouting material in terms of the mechanical and hydraulic properties are discussed to apply the sludge-mixed cement in the fields.

1.3.10 Conclusions and thesis writing

All research activities, methods, and results are documented and complied in the thesis. The research or findings will be published in the conference proceedings or journals.

1.4 Scope and limitations of the study

The scope and limitation of the research include as follows.

a. This research emphasizes on studying the mechanical and hydraulic properties of water treatment sludge-mixed cement as a grouting material to reduce permeability in fractured rock mass.

b. Laboratory tests of water treatment sludge-mixed cement include constant head flow tests and uniaxial compression test.

c. Portland cement type I is used. (ASTM C150)

d. The particle sizes of the sludge are less than 0.075 mm (sieve no. 200).

e. The sludge-to-cement (by dry weight) ratios of 1:10, 2:10, 3:10, 4:10, and 5:10 are primarily selected.

f. Laboratory testing will be conducted on specimens from Phu Kradung sandstone. The fracture area of the specimens is 152.4×152.4 mm

g. All tested fractures are artificially made in the laboratory.

h. The constant normal stresses on the fracture range from 0.25 to 1.25 MPa.

i. Mixing, curing and testing of the cement and mixtures follows, as much as practical, the ASTM and the API standards.

1.5 Thesis contents

Chapter I introduces the thesis by briefly describing the background of problems and significance of the study. The research objectives, methodology, scope and limitations are identified. **Chapter II** summarizes the results of the literature review. **Chapter III** describes the sample and mixture preparations. **Chapter IV to VI** describes the results from the laboratory experiments. The experiments are divided into 4 tests, including 1) Viscosity and density of mixtures tests 2) Uniaxial compressive testing 3) Shearing resistance between grout and fracture 4) Permeability of grouting materials and 5) Permeability of grouting materials in rock fractures. **Chapter VII and VIII** discusses and concludes the research results, and provides recommendations for future research studies.

CHAPTER II

LITERATURE REVIEW

2.1 Introduction

This chapter summarizes the results of literature review carried out to improve an understanding of the permeability in fractured rock mass, which include recent research results and utilization of the water treatment sludge.

2.2 Experimental researches on the water treatment sludge

Laothong (2003) studies the sludge cake from the water treatment process at Wang Noi Power Plant. The results indicate that the sludge is a nonhazardous waste. These are 300 tons of the sludge per month, costing 2.48 baht/kg or 460,000 baht per month for disposal. The utilization of the sludge cake can reduce operation cost of the power plant. The sludge is found to be loamy sand. Four sludge cake utilization alternatives have been explored, including cement replacement in mortar, laterite replacement in interlocking block, clay replacement in baked clay brick and ceramic wares. The results indicate that the best alternative is laterite replacement in interlocking block with the proportion of 2:2:5 by weight (cement:sludge:laterite). The laterite at the optimum gives the 28 days compressive strength of 82.14 kg/m^2, which is greater than 70 kg/m^2 required by the Thai Industrial Standard (TIS). With the interlocking block alternative, although the production cost of 3.83 baht/kg was higher than disposal cost of 1.35 baht/kg, the product could be sold at the price of about 6 to 8 baht. Utilization of sludge cake in making interlocking block is being considered to be a feasible alternative.

Suriyachat et al. (2004) study the basic properties of the water treatment sludge. The results indicate that the liquid limit is 77.96%, plastic limit is 50.76%, shrinkage limit is 11.15%, the plasticity index is 27.20%, and the maximum density is 1.33 g/cm^3. The correlation between permeability coefficient and the moisture content is found when the moisture content is low with high permeability coefficient. This is probably a result of a rearrangement of molecules at the particle surfaces by the action of adsorbing water leading to a formation of gain-soil bridges. The optimum moisture content of 29% is suitable for the minimum coefficient of permeability. The coefficient of permeability is similarly to the clay used in the ceramic industry.

The chemical compositions of the sludge and clay from the pottery in central and northern parts of Thailand suggest that the sludge properties are similar to the clay properties of these manufacturers. The analysis of chemical compositions shows that the amount of Fe_2O_3 is between 4 and 5%, including the optimal values of SiO_2 and Al_2O_3 as it is similar to red clay. This is an important raw material used in the ceramic industry.

Laboratory experiments in ceramic product made of the sludge are in the areas of pottery and jewelry. Those must be mixed with sand. To obtain a beautiful shape it must have the sand portion of 30%, but it takes several times for fermentation of the clay. The initially result showed that the water treatment sludge could be used as a raw material in the ceramic industry. It makes to achieve a renewable and reused in the manufacturing of integrated and sustainable natural materials.

Bunjongsiri and Bunjongsiri (2005) studyd the content of clay mix with sludge from community wastewater treatment to make brick. There are six ratios of clay and sludge from community wastewater treatment: 3:1, 7:3, 6.5:3.5, 3:2, 5.5:4.5 and 3:7. The experiment indicated the quantity of the heavy metal in the brick (mg/kg) and two ratios of 1:3 and 3:7 by leachate extraction procedure. The quantities in mg/kg of the heavy metal were 240.84 and 490.07 for copper, 17.66 and 59.16 for lead, 0.636 and 0.96 for cadmium, 667.87 and 973.28 for manganese, 167.44 and 157.45 for chromium and 136.82 and 337.75 for zinc. The bricks could not reach the industrial standard of TIS 77-2531. The ratio of 3:1 represents the best value close to the industrial standard as the value of compressive strength was 15.05 kg/cm^2. The density was 1.10 g/cm^3. Tolerance of length, wide, and thickness was 5.24, 6.16, and 9.35% respectively. The weight was 388.60 g and the absorber was 36.23%.

Poonsawat and Lertpocasombut (2006) study the properties of tile bodies to produce clay plan roofing tile by using sludge from Bang Khen and Mahasawat water treatment plants as a raw material. The tile bodies are consisted of 70 to 100% of the sludge and 0 to 30% of quartz and feldspar. They are fired at 1,000, 1,050 and 1,100°C. The results indicate that the plasticity index of the sludge from Bang Khen water treatment plant is higher than those from Mahasawat water treatment plant. Temperature increases the strength, shrinkage and bulk density and decreases water absorption and porosity. At 1,100°C, the ratios of 90:5:5 (Bang Khen sludge:quartz:feldspar) and 85:5:10 (Mahasawat sludge:quartz:feldspar) are suitable for making clay plan roofing tile.

Kongthong and Lertpocasombut (2006) study adsorption by using sludge from Bang Khen water treatment plant. Research objective was aimed to reduce color remaining of effluent wastewater from dye industries. Fifty mg/l of three solutions (basic, reactive, and disperse dyes) is used as initial concentration. Sludge ash which is obtained after burning at 500°C and dried sludge is used as an adsorbent. The pH results showed no effect on the adsorption of the basic and re-active dyes while disperse to dye is effectively adsorbed at pH 4. Equilibrium time and isotherm of the adsorption are determined and found that the dried sludge gave good results compared to the sludge ash in basic dye adsorption. It is in contrast to the disperse dye adsorption. The results are not found in re-active dye adsorption either using dried sludge or sludge ash.

Adamant et al. (2006) determine the mechanical and durability of mortar to replace cement with dry sludge ash from Bang Khen water treatment plant. This research studies the chemical compositions and physical properties of the dry sludge ash, including the flow value, and compressive strength. Durability against the sulfuric attack which is tested by using a sulfuric solution with pH of 1.0, and sodium sulfate (Na_2SO_4). Binder materials containing various proportions between the sludge ash and Portland cement, 0, 10, 20, and 30% by weight are prepared with the water to the binder material ratios of 0.50, 0.55, and 0.60. The results indicate that the dry sludge ash increased with decreasing flow value, compressive strength, and weight loss due to sulfuric acid attack.

Sa-ngiumsak and Cheerarot (2008) determine the properties of artificial aggregates made from the water treatment sludge. The aggregates containing various proportions between the sludge and clay, 100:0, 80:20, 60:40, 40:60, 20:80 and 0:100 by weight were prepared by molding and firing at 800, 1,000, and 1,200°C for 24-hour firing time. Then compressive strength of an artificial aggregate is tested. Some mixtures are chosen to test abrasion, stability in sodium sulfate, and absorption. Finally, the compressive strength of concrete containing the artificial aggregates is tested. The results showed that the compressive strength of the artificial aggregates increased with increasing firing temperature and amount of sludge. The aggregates with the ratio of sludge to clay of 60:40 fired at 1,200°C had the highest compressive strength of 490 ksc. The aggregate fired at 1,200°C had the highest compressive strength while the aggregate fired at 800 and 1,000°C gave similar compressive strengths. When the amount of the sludge increased, the water absorption, abrasion, and stability in sodium sulfate of the aggregates decreased. Comparing with natural aggregates, the water absorption of all proportions of the artificial aggregates was higher than that of the natural aggregates. The abrasion and stability in sodium sulfate were low. The concrete containing the artificial aggregates had higher compressive strength than the concrete containing natural aggregates.

2.3 Permeability of Single Fracture

The main factors controlling fluid flow through a single fracture are the surface roughness, apertures, orientation of fractures, normal and shear stresses, and unloading behavior. Out of these controlling factors, the aperture is the major parameter, which is a function of external stress, fluid pressure and geometrical properties of the fracture (Indraratna and Ranjith, 2001).

The conductivity of a single fracture is given by the ‘cubic law’: (Witherspoon et al., 1980; Indraratna and Ranjith, 2001; Ranjith and Viete, 2011)

$$K_f = ge^3/12\nu b \tag{2.1}$$

where K_f = fracture conductivity (m/s), e = hydraulic aperture (m), g = acceleration due to gravity (m/s^2), ν = kinematic viscosity, which is 1.01×10^{-6} (m^2/s) for pure water at 20°C, and b is the spacing between fracture (m).

For a smooth, planar joint having an aperture of magnitude *e*, the fracture permeability (k) for laminar flow is given by (Barton et al., 1985)

$$k = e^2/12 \tag{2.2}$$

The joint aperture *e* is mainly dependent on the normal and shear stress acting on the joint. Assuming the rock matrix to be isotropic and linear elastic, obeying Hooke's law, the following aperture-stress relationship can be formulated: (Rutqvist, 1995; Indraratna and Ranjith, 2001)

$$e = e_0 \pm \delta e \tag{2.3}$$

where e_0 is the initial joint aperture and δe is the change of the joint aperture due to stresses (i.e., both normal and shear components) acting on the joint. In conventional rock mechanics, the normal deformation component is given by Jaeger and Cook (1979):

$$\delta e_n = (1/K_n)(\sigma_z \cos\beta + \sigma_h \sin\beta) \tag{2.4}$$

where K_n = normal stiffness of discontinuity, σ_z = vertical stress applied to the discontinuity, σ_h = horizontal stress applied to the discontinuity, and β = orientation of discontinuity.

Considering the water pressure to be acting perpendicular to the joint surface, the equation can be modified to obtain (Indraratna and Ranjith, 2001)

$$\delta e_n = (1/K_n)(\sigma_1 \cos\beta - \sigma_3 \sin\beta - p_w) \quad (2.5)$$

where p_w = water pressure within the discontinuity.

Combining the above equations for planar and smooth joints, the permeability of a single fracture is given by

$$k = (e_0 + \delta e_n)^2/12 \quad (2.6)$$

Based on the initial hydraulic aperture and the closure of joint, Detoumay (1980) suggested the following relationship to determine the fracture permeability:

$$k = e_0^2(1-\nu/\nu_0)^2/12 \quad (2.7)$$

where e_0 = hydraulic aperture at zero stress, ν_0 = closure of the joint when the hydraulic aperture becomes zero and ν = normal deformation of the joint.

Snow (1968) observed an empirical model to describe the fracture fluid flow variation against the normal stress, as described by

$$k = k_0 + K_n(e^2/s)(\sigma - \sigma_0) \quad (2.8)$$

where k_0 = initial fracture permeability at initial normal stress (σ_0), K_n = normal stiffness, s = fracture spacing and e = hydraulic aperture.

Jones (1975) suggested the following empirical relation between the fracture permeability and the normal stress:

$$k = C_0[\log(\sigma_{ch}/\sigma_c)]^3 \tag{2.9}$$

where σ_{ch} = confining healing pressure in which the permeability is zero and σ_c = effective confining stress. The constant (C_0) depends on the fracture surface and the initial joint aperture.

Nelson (1975) suggested the following empirical relation between the fracture permeability and the normal stress:

$$k = A + B\sigma_c^{-m} \tag{2.10}$$

where A, B and m are constants which are determined by regression analysis. These constants may vary from one rock to another, and even for the same rock type, depending on the topography of the fracture surface.

Gangi (1978) reports a theoretical model for fracture permeability as a function of the confining pressure, as represented by

$$k = k_0[1 - (\sigma_c/P_1)^m]^3 \tag{2.11}$$

where P_1 = effective modulus of the asperities and m = constant which describes the distribution function of the asperity length. This expression gives a better prediction if the effect of surface roughness on flow is negligible, which of course is not reasonable in practice.

2.4 Experimental researches on grouting materials

Huang (1997) investigates the properties of cement-fly ash grout mixtures as barriers for isolation of hazardous and low-level radioactive wastes. The fly ash was used to replace 30 percent by mass of cement. Three additives, including bentonite, silica fume, and polypropylene fiber were used individually in the grout mixes to improve the properties of the grouts in different aspects. The flow ability, bleeding, and setting time of freshly mixed grouts were determined; and the unconfined compressive strength, pore size distribution, and water permeability were determined for hardened grouts at various curing durations up to 120 days. Finally, the durability of cement-fly ash grouts was carefully examined in terms of the changes in their physical properties after different levels of exposure to sulfate attack and wet-dry cycles.

Owaidat et al. (1999) reported that the U.S. Army Corps of Engineers had recently implemented a levee-strengthening program along the banks of the American River in Sacramento, California. During the rainy season, the existing levee system protected major commercial and residential areas of this metropolitan area. One of the main components of this program was the construction of slurry walls through the existing levee to improve stability by preventing seepage through and beneath the levee. Since conventional soil-bentonite (SB) slurry walls had little shear strength, which would jeopardize the stability, of the existing levees, and cement-bentonite (CB) slurry walls were significantly more expensive, soil-cement-bentonite (SCB) slurry walls were being utilized for this strengthening program. This research described a case study on the design, construction and performance of an underground SCB barrier wall, which was used to isolate river water seeping into the American

River levee and its foundation soils. Challenges to barrier performance included achieving a maximum allowable hydraulic conductivity of 5×10^{-7} cm/s while having a minimum unconfined compressive strength of 15 psi.

Kashir and Yanful (2000) reported that the use of slurry walls to contain oxidized tailings and provide cutoff below tailings dams were generally a cost-effective way of preventing environmental degradation due to seepage of acid water from tailing's areas. Long-term environmental protection dictated that the slurry wall materials been compatible with the acid water. Six percent bentonite by weight was added separately to two natural soils to represent slurry wall backfill materials, which were then permeated with several pore volumes of acid mine drainage (AMD) in the laboratory. Results using both flexible wall and fixed wall permeameters were similar. The carbonate-rich backfill gave an average hydraulic conductivity (K) of 1×10^{-9} cm/s, buffered the AMD at circumneutral pH, and kept effluent metal concentrations to very low values, for example, less than 0.05 mg/l zinc. The carbonate-free backfill also maintained low K (average 3×10^{-9} cm/s) during AMD permeation, it could not neutralize the AMD as effluent pH decreased to approximately 3.5, and metal concentrations reached those of the influent or permeant after about 17 pore volumes.

Fransson (2001) describes a rock volume suitable for a grouting field test at the Äspö Hard Rock Laboratory, Sweden. Fixed interval length transmissivities and the corresponding number of fractures from geological mapping of a probe hole were used to calculate a probability of conductive fractures for analyses of data from individual boreholes. The transmissivity and specific capacity of the boreholes were compared to examine the robustness of the specific capacity. From the findings of the study, the probability of conductive fractures from probe hole data, the specific capacity and fracture frequency of individual boreholes were sufficient to construct a simplified model of the fracture and the rock volume. The median specific capacity of the boreholes was a good description of the effective cross-fracture transmissivity. The field test was also carried out to demonstrate the usefulness of the methodology for improving the analyses of data from the hydraulic tests and geological mapping for a grouting fan.

Ryan and Day (2002) state that Soil-Cement-Bentonite (SCB) slurry walls had been used with increasing frequency in recent years to provide barriers to the lateral flow of groundwater in situations where the strength of a normal soil-bentonite (SB) wall would be inadequate to carry foundation loads. The addition of cement to the backfill blended allows the backfill to set and from a more rigid system that could support greater overlying loads. Construction and quality control for the SCB wall were more demanding than that needed for the SB walls. Backfill mixing, sampling and testing of this type of wall involve more exacting procedures. Recommendations were made for methods to carry out pre-job design mix testing and in-field quality control testing for the most reliable results. Designing the SCB backfill was a complex issue involving conflicting actions of the various materials involved. While the SCB wall provides additional strength, permeability was one property that generally suffers in comparison to the SB walls. A normal permeability specification would be a maximum of 1×10^{-6} cm/sec. With special attention to materials and procedures, a specification of a maximum 5×10^{-7} could be achieved. The results were presented that the strengths of the SCB were in the range of 15-300 psi.

Rahmani (2004) stated that grouting had been used over the past two centuries to increase the strength, decrease the deformation and reduce the permeability of soils or fractured rocks. Due to its significance in engineering and science predicting grout effectiveness in fractured rocks was of interest. There were different approaches to estimate the effectiveness of grouting, one of which was numerical modeling. Numerical models could simulate a distribution of grout inside fractures by which the effectiveness of grout could be estimated. Few numerical studies had been carried out to model grout penetration in fractured rocks. Due to complexities of modeling grout and fracture most of these studies had either used simplifying assumptions or been bound to small sizes of fractures, both resulting in unrealistic simulations.

Then the current work is aimed to eliminate some of the simplifying assumptions and to develop a model that could improve the reliability of the results. In reality, grouts were believed to behave as a Bingham fluid, but many models did not consider a full Bingham fluid flow solution due to its complexity. Real fractures had rough surfaces with randomly varying apertures. However, some models considered fractures as planes with two parallel sides and a constant aperture. In this work the Bingham fluid flow equations were solved numerically over a stochastically varying aperture fracture. To simplify the equations and decrease the computational time the current model substituted two-dimensional elements by one-dimensional pipes with equivalent properties. The model was capable of simulating the time penetration of grout in a mesh of fracture over a rather long period of time. The results of the model could be used to predict the grout penetration for different conditions of fractures or grout (Rahmani, 2004).

Baik et al. (2007) described that compacting bentonite had been considered as a candidate buffer material in the underground repository for the disposal of high-level radioactive waste. An erosion of bentonite particles caused by a groundwater flow at the interface of a compacting bentonite, and fractured granite was studied experimentally under various geochemical conditions. The experimental results showed that bentonite particles could be eroded from a compacted bentonite buffer by a flowing groundwater depending upon the contact time, the flow rate of the groundwater, and the geochemical parameters of the groundwater such as the pH and ionic strength. A gel formation of the bentonite was observed to be a dominant process in the erosion of bentonite particles, although an intrusion of bentonite into a rock fracture also contributed to the erosion. The concentration of the eroded bentonite particles eroded by a flowing groundwater was increased with an increasing flow rate of the groundwater. It was observed from the experiments that the erosion of the bentonite particles was considerably affected by the ionic strength of a groundwater, although the effect of the pH was not great within the studied pH range from 7 to 10. An erosion of the bentonite particles in a natural groundwater was also observed to be considerable, and the eroded bentonite particles were expected to be stable at the given groundwater condition. The erosion of the bentonite particles by a flowing groundwater did not significantly reduce the physical stability and thus the performance of a compacted bentonite buffer. However, it was expected that an erosion of the bentonite particles due to a groundwater flow will generate bentonite particles in a given groundwater condition, which could serve as a source of the colloids facilitating radionuclide migration through rock fractures.

Butron et al. (2010) presented a new pre-excavation grouting concept to prevent dripping and reduced the inflow into a railway tunnel. For this purpose, the tunnel's roof was driped-sealed using colloidal silica and the walls and invert of the tunnel were grouted with cement. The grouting design process followed a structured approach with pre-investigations of core-drilled boreholes providing parameters for the layout. Water pressure tests and pressure volume time recordings were used for the evaluation. Results showed that the design was successful: the total transmissivity was reduced from 4.9×10^{-8} m^2/s to the measurement limit (1.6×10^{-8} m^2/s), and the dripping was reduced to eight spots from the roof. Improved rock characterization showed that the grout hole separation was within the transmissivity correlation length and that grouting efficiency depends to a large extent on the dimensionality of the flow system of the rock mass.

CHAPTER III

SAMPLE PREPARATIONS

3.1 Introduction

This chapter describes basic characteristics of materials tested in this study. Materials used in this experiment consist of sludge, bentonite, Portland cement and sandstone samples.

3.2 Sludge preparation

Sludge samples used in this research have been donated by Metropolitan Waterworks Authority. They are collected from sludge dewatering plant of Bang Khen Water Treatment Plant located in Bangkok Metropolis (Figures 3.1). Sludge is drained from the bottom of the clarifiers and backwash water from the filter beds. Sludge is pumped to the sludge dewatering plant. Dried sludge is a moist, brown, rough, fine-grained soil. Sludge samples are collected and packed in a moisture barrier bag. The 1,000 kg in bags is transported to Geomechanics Research Laboratory of Suranaree University of Technology, Nakhon Ratchasima province (Figures 3.2).

Dried sludge cake is taken out and dried under sunlight (Figure 3.3). The moisture is removed one more time in a hot-air oven at 140°C for at least 24 hours or until its weight remains constant. The dried sludge is sieved through a mesh no. 200. The packed sludge retaining on the mesh of the size is grounded by a milling machine

(Figure 3.4), and sieved through the mesh again. Dried sludge from the oven (Figure 3.5) is stored in a plastic box with a tight lid to prevent moisture.

One of the basic physical properties of the sludge is the distribution of the grain size particles. The distribution of different grain sizes affects the engineering properties of soil. Grain size analysis provides the grain size distribution, and it is required in classifying the soil. This test is performed to determine the percentage of different grain sizes contained within sludge. Sieve analysis is performed to determine the distribution of the coarser particles, and the hydrometer method is used to determine the distribution of the finer particles. Testing of these samples follows, as much as practical, the ASTM standards (D4543). Results of these tests can be shown in Figure 3.6. Comparison the grain sizes distribution obtained here with those from the Department of Primary Industries and Mines (DPIM) shows that they are slightly different due to the different sludge sampling periods. Sludge form Bang Khen Water Treatment Plant is likely to have different properties for different seasons. The test method of the ASTM standard (D854) used for determination of the specific gravity of solids passing a sieve indicates that the sludge has a specific gravity of 2.56.

The Atterberg's limits are index properties of soil. Depending on the water content of the soil, it may appear in four states: solid, semi-solid, plastic and liquid. In each state the consistency and behavior of a soil is different and thus so are its engineering properties. The Atterberg limits can be used to distinguish between silt and clay, and it can distinguish between different types of silts and clays. Thus, sludge has been tested to find these indexes by using the ASTM D4318 and D2487 (ASTM

2010e, 2010f). The results are listed in Table 3.1. The sludge samples are classified according to the Unified Soil Classification System is in the MH (elastic silt).

Sludge samples from sludge dewatering plan of Bang Khen contain more than 52 percent silicon dioxide (SiO_2) and 24 percent aluminum oxide (Al_2O_3) that chemical composition is determined based on X-ray fluorescence spectrometer (reported from National Metal and Materials Technology Center, National Science and Technology Development Agency database). X-ray fluorescence (XRF) is used to study the chemical compositions of the materials. The objective of analysis is to determine oxide concentrations in samples with X-ray fluorescence spectrometer, Philips PW-2404. Samples used in this analysis are sludge and bentonite powders. Test method is semi-quantitative X-ray fluorescence spectrometry analysis. Laboratory conducted here are under 25±5°C and relative humidity of 60±10%. The sample were mixed with binder ($C_{38}H_{76}N_2O_2$, sample:binder, 4:0.8 by weight). They were pressed to form pellets with 3.2 cm diameter. Results of oxide concentrations in the sludge samples are shown in Table 3.2.

3.3 Bentonites

Bentonite is an engineering material as excellent sealant material because of its low permeability, desirable swelling and self-healing characteristic, sorptive qualities and longevity in nature. Bentonite is used extensively for grouting material to reduce permeability in fractured rock mass. Bentonite mixed with cement is made to hold themselves, and not piping with the water pressure while curing in the rock fractures (Akgün and Daemen, 1999; Fuenkajorn and Daemen, 1996; Svermova et al., 2003; Metcalfe and Walker, 2004). The bentonite used in this study is from American

Colloid Company, United States of America. This is the widely used in the drilling industry, oil exploration, natural gas and mineral deposits. Tables 3.1 and 3.2 summarize the chemical compositions and engineering properties of the bentonite tested in this study.

3.4 Portland cement

Portland cement type I is used in conforms to the ASTM (C150). Portland cement can be purchased readily, low cost and widely used in the construction construction. Portland cement of INSEE Thong brand, bag cement 40 kg, used in this study is from the City Cement Public Company Limited, Thailand. The cement is kept in plastic box sealed to prevent moisture, cool-dry area.

Porland cement of INSEE Thong brand conforms to the ASTM C91 standard which is autoclave expansion of 0.001%, setting time (by Gillmore Method) for initial of 145 minutes and final of 245 minutes. The mortar compressive strength for 7 and 28 days is 13 and 15.5 MPa. The amount of air content in mortar is 15.5%, with water retention value of 78.5% (percentage of original flow). Table 3.3 summaries the chemical compositions of Portland cement type I, which is the same type used in this study.

3.5 Rock samples

The selection criteria for rock sample are that the rock should be homogeneous, low permeability and availability as much as possible. This is to minimize the intrinsic variability of the test results. The sandstone samples are used and collected from Phu Kradung formation. Sample preparations are carried out in the

Geomechanics Research (GMR) laboratory facility at Suranaree University of Technology. Sample preparations have been carried out for series for constant head flow testing (Figure 3.7) and direct shear test (Figure 3.8).

3.5.1 Sample preparation for constant head flow test under various normal stresses

Sandstone samples for the constant head test are prepared to have prismatic blocks of sandstone. Preparation of these samples follows the suggested methods proposed by Navarro (2010). The fractures are artificially made by applying a line load at the center to induce a splitting tensile crack in 152.4×152.4×152.4 mm^3 prismatic blocks. The fracture area is 152.4×152.4 mm^2. The injection hole at the center of the upper block is 8 mm in diameter. A minimum of sixty sandstone specimens are tested for constant head flow test with both three portions of sludge-mixed cement and bentonite-mixed cement under normal stress ranging from 0.25 - 1.25 MPa.

3.5.2 Sample preparation for direct shear test under various normal stresses

Sandstone samples for the constant head test are prepared to have cylindrical shape. Preparation of these samples follows the ASTM standards (D4543) with a nominal dimension of 100 mm in diameter and 100 nm long. The fractures are artificially made by applying a line load at the center of length to induce a splitting tensile crack. The fracture area is 7,854 mm^2. A minimum of forty sandstone specimens are tested for direct shear test under normal stress ranging from 0.25 - 1.25 MPa.

Table 3.1 Atterberg's limits and specific gravity of sludge and bentonite.

Atterberg Limits	**Bentonite (%weight)**		**Sludge (%weight)**	
	SUT [1]	**US[2]**	**SUT [1]**	**KU[3]**
Liquid limit	357	478	55	69
Plastic limit	44	28	22	42
Plasticity index	313	449	23	28
Specific gravity	2.50	-	2.56	-

Note: [1]SUT = Suranaree University of Technology Laboratory,

[2]after Castelbaum and Shackelford (2009)

[3]after Kanchanamai (2003)

Table 3.2 Results of oxide concentrations in the bentonite and sludge samples.

Oxide	Concentration (% weight)			
	Bentonite		Sludge	
	SUT [1]	ACC [2]	SUT	TU [3]
Na_2O	1.63	2.2	0.22	0.37
MgO	2.44	1.3	0.96	1.43
Al_2O_3	19.85	19.8	23.47	25.76
SiO_2	61.93	61.3	52.37	59.44
P_2O_5	0.05	-	0.34	0.30
SO_3	1.27	-	0.55	0.37
Cl	N/D [4]	-	0.07	-
K_2O	0.44	0.4	1.55	2.39
CaO	1.27	0.6	0.79	0.91
TiO_2	0.19	0.1	0.79	0.83
V_2O_5	N/D	-	0.02	-
Cr_2O_3	N/D	-	0.02	-
MnO	0.02	-	0.22	-
Fe_2O_3	4.45	3.9	6.33	7.84
CuO	0.01	-	0.01	-
Rb_2O	N/D	-	0.01	-
SrO	0.03	-	0.01	-
Y_2O_3	0.01	-	<0.01	-
ZrO_2	0.03	-	0.03	-
Nb_2O_5	0.01	-	<0.01	-
BaO	0.03	-	0.01	-
CeO_2	0.04	-	N/D	-
LOI. at 1,025 °C	6.29	-	12.20	3.06
Total	100	-	100	-

Note: [1]SUT = Suranaree University of Technology Laboratory,

[2]ACC = American Colloid Company Technical Data,

[3]TU = Tummasart University Laboratory (after Hadsanan et al., 2006)

[4]N/D = Not detectable

Table 3.3 Results of oxide concentrations in Porland cement. (Ali, 2008)

Silicon dioxide (SiO_2)	20.58
Aluminum oxide (Al_2O_3)	5.71
Ferric oxide (Fe_2O_3)	2.94
Calcium oxide (CaO)	64.76
Magnesium oxide (MgO)	0.87
Potassium oxide (K_2O)	0.67
Sulfer trioxide (SO_3)	2.63
Sodium oxide (Na_2O)	0.14
Titanium Oxide (TiO_2)	0.29
Phosphorus oxide (P_2O_5)	0.06
Loss on ignition (LOI)	0.96

Figure 3.1 Sludge from sludge dewatering plant of Bang Khen Water Treatment Plant located in Bangkok Metropolis.

Figure 3.2 Sludge samples packed in a moisture barrier bag.

(a)

(b)

Figure 3.3 Sludge is dehydrated by drying under sunlight.

Figure 3.4 Sludge cakes are cracked by a milling machine.

Figure 3.5 Sludge in a hot-air oven at 140°C for at least 24 hours or until its weight remains constant.

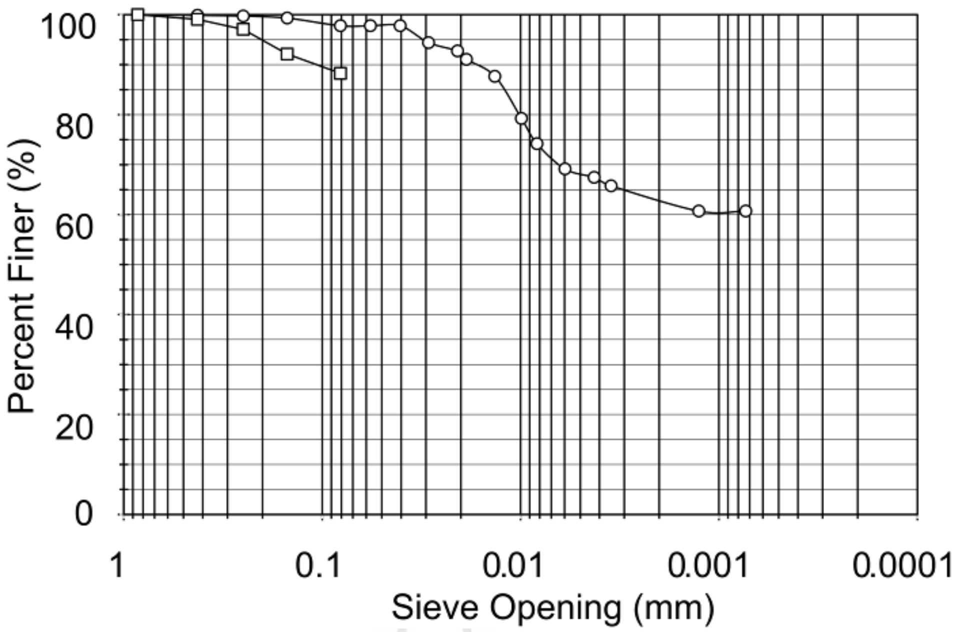

Figure 3.6 Grain size distribution of water treatment sludge compared SUT and DPIM test results.

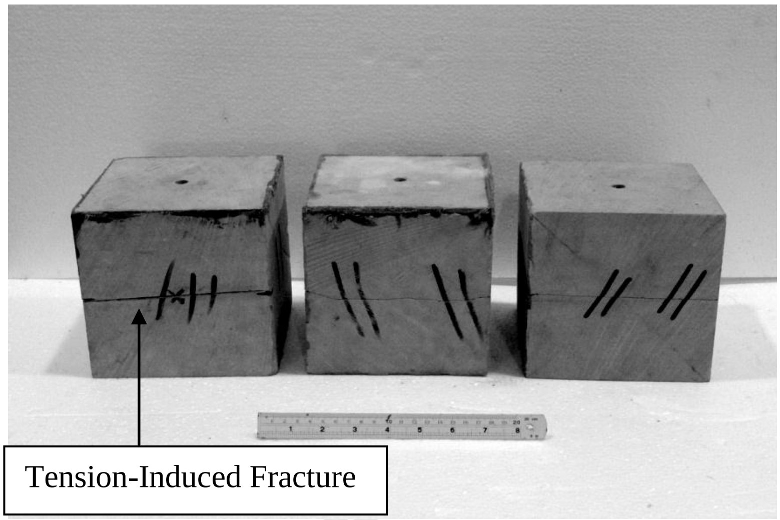

Figure 3.7 Some sandstone samples with 152.4×152.4×152.4 mm^3 prismatic blocks for series for constant head flow testing.

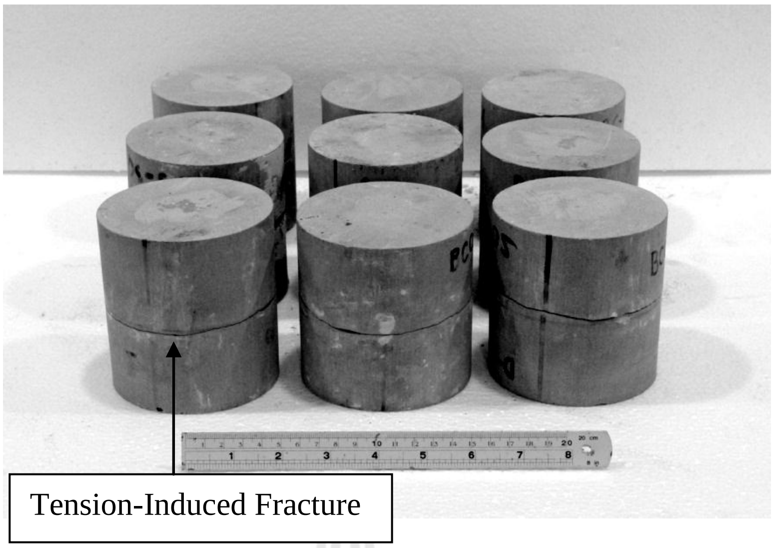

Figure 3.8 Sandstone samples with a nominal dimension of 100 mm in diameter and 100 nm long for direct shear testing.

CHAPTER IV

GROUT PREPARATIONS

4.1 Introduction

This chapter describes the methods and results of laboratory experiments used to determinate the most suitable mixing ratios for grouting in rock fracture.

4.2 Viscosity and density of mixtures

The objectives of these tests are to determine proportioning of mixtures and methods to be used to test the mechanical and hydraulic properties in the next step. These results lead to the determination that the most suitable mixing ratios of sludge-mixed cement should be proportional for grouting in rock fracture. Viscosity measurement follows, as much as practical, the ASTM standard (D2196). Apparatus used in these experiment consist of :

1) Sludge (Figure 4.1),

2) Bentonite (Figure 4.2),

3) Porland cement (Figure 4.3),

4) Distilled water,

5) Digital weight scale with maximum capacity of 2,000 g and accuracy to ±0.01 g. (Figure 4.4),

6) Mixer, Kitchenaid Professional 600 6QT 575 watt stand mixer, with maximum capacity of 5,000 cm^3 and 6 speed control (Figure 4.5),

7) Viscometer,Bookfield viscometer RV 203 Watt 50 Hz (Figure 4.6)

8) Digital thermometer HIP C0905019480 with accuracy to ±0.1°C (Figure 4.7).

4.2.1 Test methods

The preliminary selection in proportions of mixtures are determined and given by using viscosity values. Proportions of mixtures, S:C and B:C, are 0:10, 1:10, 2:10, 3:10, 4:10, 5:10, 6:10, 7:10, 8:10, 9:10 and 10:10 with W:C ratios ranging from 4:10, 8:10, 10:10 and 12.5:10. Slurry of mixtures in 1,000 cm^3 by weight used here are shown in Table 4.1. Test procedure also follow:

1) Material balance of the four types defined, proportion. Then pack into plastic bags type bag and tie securely (Figure 4.8).

2) The material is weighed and then put together in a plastic bag and tie tightly. Make a homogeneous mixture by shaking several times.

3) Pour the distilled water in the bag to weigh it down and turn the mixer speed up to 275 rpm. Mixing of all grouts is accomplished using a blade paddle mixer as suggested in ASTM standard C938.

4) Pour the mixed material in Section 2) into the mix to run at the same time. If there is additional material should be poured within a two-minute timer and start pouring the mixture into distilled water. I measured the room temperature.

5) In a homogeneous mix for 3 minutes to complete mixing at 275 rpm, then turn off the mixer.

6) Determine the density and viscosity of the mixture slurry by using standard ASTM standard (D2196). Pour in a beaker with a volume of the mixture is equal to exactly 500 cc (Figure 4.9).

7) Weigh the beaker with the mixture. Subtract the weight of the beaker from the results and then divided by the volume of the mixture (500 cc) is the density of mixture slurry.

8) Specific gravity (SG) of the mixture is calculated from equation

$$SG = \rho_{slurry} / \rho_{w} \tag{4.1}$$

where ρ_{slurry} is a density of mixture slurry, and ρ_{w} is density of distilled water at the time of measurement. The results of the test density and specific gravity are summarized in Table 4.2.

Viscosity test is performed after the weighing of ingredients in the measuring beaker with a volume of 500 cc, which is continuing immediately. The viscosity of the mixture, which is resistant to flow, can be determined by a rotational viscometer, Brookfield model RV dial reading viscometer. Spindle set (RV-1 through RV-7) is selected for this test. Testing of viscosity follows the ASTM standard D2196.

1) For the mixture of given viscosity, the resistance is greater as the spindle size and rotational speed increase. The minimum viscosity ranged, is obtained by using the largest spindle at the highest speed; the maximum range by using the smallest spindle at the slowest speed.

2) The sample is placed in Glass Beaker (500 cm^3) under viscometer (Figure 4.10).

3) Weigh and temperature of each sample are recorded to determine a slurry density.

4) Releasing the brake once the viscometer is rotating smoothly and time for 60 seconds. Brake firmly is depressed and the viscometer is turned off during continuing to hold the brake down. Values on the viscometer gauge are read and recorded. Recording the number of the spindles are used.

5) Calculating the viscosity in centipoises by multiplying the meter reading by the multiplier corresponding to the particular spindle used.

The reading of the test Viscosity Brookfield is in units of centipoise (cP) or equal mPa·s in dynamic viscosity. The dynamic viscosity is converted to the kinetic viscosity by equation (4.2).

$$\mu = \rho \cdot \nu \tag{4.2}$$

where μ is dynamic viscosity, ν is the kinetic viscosity, and ρ is slurry density.

4.2.2 Test results

Figure 4.11 shows dynamic viscosity of bentonite-cement and sludge-cement mixtures for different W:C ratios. The results of mixture ratios by weight of the total volume of 1,000 cc are listed in Table 4.2. The results of slurry density tests in beakers of 500 cc are listed in Table 4.2. The results of slurry viscosity tests are listed in Table 4.3.

Table 4.1 Mixture ratios by weight of the total volume of 1,000 cc.

Binder	W:C	S:C or B:C	Weight (g)		
			Cement	Sludge or Bentonite	Water
Sludge	8:10	1:10	636	64	509
	8:10	2:10	595	119	476
	8:10	3:10	558	167	446
	8:10	4:10	526	210	421
	8:10	5:10	497	249	398
	8:10	6:10	471	283	377
	8:10	7:10	448	314	359
	10:10	1:10	564	56	564
	10:10	2:10	531	106	531
	10:10	3:10	502	151	502
	10:10	4:10	476	190	476
	10:10	5:10	452	226	452
	10:10	6:10	431	258	431
	10:10	7:10	411	288	411
	10:10	8:10	393	315	393
	10:10	9:10	377	339	377
	10:10	10:10	362	362	362
	12.5:10	1:10	495	49	618
	12.5:10	2:10	469	94	586
	12.5:10	3:10	446	134	558
	12.5:10	4:10	425	170	532
	12.5:10	5:10	406	203	508
	12.5:10	6:10	389	233	486
	12.5:10	7:10	373	261	466
	12.5:10	8:10	358	287	448
	12.5:10	9:10	345	310	431
	12.5:10	10:10	332	332	415

Table 4.1 Mixture ratios by weight of the total volume of 1,000 cc (continued).

Binder	W:C	S:C or B:C	Weight (g)		
			Cement	Sludge or Bentonite	Water
Bentonite	10:10	1:10	570	57	570
	10:10	2:10	542	108	542
	10:10	3:10	516	155	516
	40:10	1:10	210	21	841
	40:10	2:10	206	41	825
	40:10	3:10	203	61	810
	40:10	4:10	199	80	795
	40:10	5:10	195	98	781
	40:10	6:10	192	115	767
	40:10	7:10	189	132	754
	40:10	8:10	185	148	741
	40:10	9:10	182	164	729
	40:10	10:10	179	179	717
Cement	8:10	0:10	684	0	547
	10:10	0:10	602	0	602
	12.5:10	0:10	537	0	644
	40:10	0:10	214	0	858

Table 4.2 Results of slurry density tests in beakers of 500 cc.

Binder	W:C	S:C or B:C	Slurry Temperature (°C)	Slurry Weight (g)	Slurry Density (g/cc)	Water Density (g/cc)	Specific Gravity
Sludge	8:10	1:10	28.4	766.6	1.53	0.9961	1.54
	8:10	2:10	28.7	777.6	1.56	0.9960	1.56
	8:10	3:10	29.6	787.5	1.58	0.9958	1.58
	8:10	4:10	29.3	825.3	1.65	0.9959	1.66
	8:10	5:10	31	872.7	1.75	0.9953	1.75
	8:10	6:10	31.5	836.4	1.67	0.9952	1.68
	8:10	7:10	31.5	888.0	1.78	0.9952	1.78
	10:10	1:10	28.6	733.5	1.47	0.9961	1.47
	10:10	2:10	30.4	734.6	1.47	0.9955	1.48
	10:10	3:10	30.2	742.0	1.48	0.9956	1.49
	10:10	4:10	31.5	774.8	1.55	0.9952	1.56
	10:10	5:10	30.3	794.5	1.59	0.9956	1.60
	10:10	6:10	28.9	818.8	1.64	0.9960	1.64
	10:10	7:10	30.6	811.9	1.62	0.9955	1.63
	10:10	8:10	30.3	825.1	1.65	0.9956	1.66
	10:10	9:10	30.6	846.9	1.69	0.9955	1.70
	10:10	10:10	30.6	930.3	1.86	0.9955	1.87
	12.5:10	1:10	27.6	685.6	1.37	0.9963	1.38
	12.5:10	2:10	28.4	695.6	1.39	0.9961	1.40
	12.5:10	3:10	28.8	725.9	1.45	0.9960	1.46
	12.5:10	4:10	29.3	713.3	1.43	0.9959	1.43
	12.5:10	5:10	30.9	760.4	1.52	0.9954	1.53
	12.5:10	6:10	29.8	727.1	1.45	0.9957	1.46
	12.5:10	7:10	29.3	728.6	1.46	0.9959	1.46
	12.5:10	8:10	29.8	754.0	1.51	0.9957	1.51
	12.5:10	9:10	30.3	762.7	1.53	0.9956	1.53
	12.5:10	10:10	30.8	777.8	1.56	0.9954	1.56

Table 4.2 Results of slurry density tests in beakers of 500 cc (continued).

Binder	W:C	S:C or B:C	Slurry Temperature (°C)	Slurry Weight (g)	Slurry Density (g/cc)	Water Density (g/cc)	Specific Gravity
Bentonite	10:10	1:10	28.2	705.4	1.41	0.9962	1.42
	10:10	2:10	27.9	725.0	1.45	0.9963	1.46
	10:10	3:10	29.4	757.1	1.51	0.9958	1.52
	40:10	1:10	28.9	584.9	1.17	0.9960	1.17
	40:10	2:10	29.3	554.9	1.11	0.9959	1.11
	40:10	3:10	28.8	583.4	1.17	0.9960	1.17
	40:10	4:10	28.6	585.3	1.17	0.9961	1.18
	40:10	5:10	29.8	577.6	1.16	0.9957	1.16
	40:10	6:10	28.6	571.5	1.14	0.9961	1.15
	40:10	7:10	29.1	583.2	1.17	0.9959	1.17
	40:10	8:10	29	575.5	1.15	0.9959	1.16
	40:10	9:10	29.1	586.9	1.17	0.9959	1.18
	40:10	10:10	28.8	589.8	1.18	0.9960	1.18
Cement	8:10	0:10	29	769.5	1.54	0.9959	1.55
	10:10	0:10	29.1	723.3	1.45	0.9959	1.45
	12.5:10	0:10	27.6	725.4	1.45	0.9963	1.46
	40:10	0:10	27.9	584.7	1.17	0.9963	1.17

Table 4.3 Results of slurry viscosity tests.

Binder	W:C	S:C or B:C	Temperature (°C)			Slurry Density (kg/m^3)	Dynamic Viscosity (mPa·s)	Kinematic Viscosity (10^{-4} m^2/s)
			Air	Water	Slurry			
Sludge	8:10	1:10	27.6	27.5	28.4	1.53	14,260	0.93
	8:10	2:10	27.6	27.5	28.7	1.56	20,360	1.31
	8:10	3:10	28.1	27.5	29.6	1.58	31,350	1.99
	8:10	4:10	27.9	27.8	29.3	1.65	51,200	3.10
	8:10	5:10	28.3	28.6	31	1.75	72,000	4.13
	8:10	6:10	31.3	28.8	31.5	1.67	99,200	5.93
	8:10	7:10	30.8	29.4	31.5	1.78	132,000	7.43
	10:10	1:10	31.3	27.5	28.6	1.47	8,170	0.56
	10:10	2:10	30.8	27.5	30.4	1.47	10,400	0.71
	10:10	3:10	32.3	27.5	30.2	1.48	15,750	1.06
	10:10	4:10	31.1	27.5	31.5	1.55	25,650	1.65
	10:10	5:10	31.5	27.5	30.3	1.59	41,720	2.63
	10:10	6:10	31.5	27.5	28.9	1.64	62,330	3.81
	10:10	7:10	29.8	28.8	30.6	1.62	92,400	5.69
	10:10	8:10	31.3	27.5	30.3	1.65	130,320	7.90
	10:10	9:10	30.2	28.8	30.6	1.69	171,330	10.12
	10:10	10:10	31.7	27.5	30.6	1.86	260,000	13.97
	12.5:10	1:10	28.7	27.5	27.6	1.37	2,360	0.17
	12.5:10	2:10	27.9	27.8	28.4	1.39	3,680	0.26
	12.5:10	3:10	28.6	27.8	28.8	1.45	5,170	0.36
	12.5:10	4:10	27.8	27.5	29.3	1.43	6,990	0.49
	12.5:10	5:10	31.8	27.5	30.9	1.52	10,610	0.70
	12.5:10	6:10	29.8	29.4	29.8	1.45	15,700	1.08
	12.5:10	7:10	29.8	29.3	29.3	1.46	21,170	1.45
	12.5:10	8:10	30.0	29.7	29.8	1.51	26,970	1.79
	12.5:10	9:10	30.1	29.4	30.3	1.53	38,200	2.50
	12.5:10	10:10	30.6	29.5	30.8	1.56	53,600	3.45

Table 4.3 Results of slurry viscosity tests (continued).

Binder	W:C	S:C or B:C	Temperature (°C)			Slurry Density (kg/m^3)	Dynamic Viscosity (mPa·s)	Kinematic Viscosity (10^{-4} m^2/s)
			Air	Water	Slurry			
Bentonite	10:10	1:10	27.8	27.8	28.2	1.41	30,930	2.19
	10:10	2:10	27.7	27.5	27.9	1.45	106,000	7.31
	10:10	3:10	28.7	28.8	29.4	1.51	346,400	22.88
	40:10	1:10	30.1	27.5	28.9	1.17	480	0.04
	40:10	2:10	30.5	27.5	29.3	1.11	960	0.09
	40:10	3:10	30.5	27.5	28.8	1.17	1,380	0.12
	40:10	4:10	30.3	17.5	28.6	1.17	3,020	0.26
	40:10	5:10	30.4	27.5	29.8	1.16	6,290	0.54
	40:10	6:10	30.4	29.4	28.6	1.14	13,580	1.19
	40:10	7:10	30.4	29.4	29.1	1.17	26,530	2.27
	40:10	8:10	29.6	29.4	29.0	1.15	43,000	3.74
	40:10	9:10	30.3	29.4	29.1	1.17	80,700	6.88
	40:10	10:10	29.6	29.4	28.8	1.18	160,670	13.62
Cement	8:10	0:10	31.4	27.5	29.0	1.54	10,380	0.67
	10:10	0:10	30.8	27.9	29.1	1.45	6,230	0.43
	12.5:10	0:10	31.0	27.5	27.6	1.45	1,770	0.12
	40:10	0:10	29.8	27.5	27.9	1.17	170	0.01

Figure 4.1 Sludge sample packed in a plastic box with a lid to prevent moisture.

Figure 4.2 American Colloid Bentonite used in this study.

Figure 4.3 Bag of Portland cement 40 kg is used in this study.

Figure 4.4 Digital weight scale with maximum capacity for 2000 grams and accuracy to ±0.01 gram.

Figure 4.5 Mixer, Kitchenaid Professional 600 6QT 575 watt stand mixer, with maximum capacity for 5,000 cm^3 and 6 speed control.

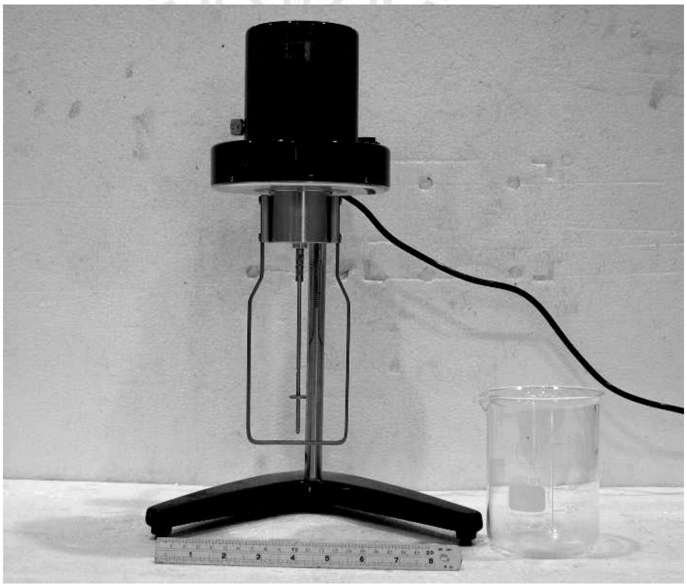

Figure 4.6 Viscometer, Bookfield viscometer RV 203 Watt 50 Hz.

Figure 4.7 Digital thermometer HIP C0905019480 with accuracy to ±0.1°C.

(a)

(b)

(c)

Figure 4.8 Grouting materials in plastic bags are prepared for mix proportion (a) cement and water, (b) cement, water and sludge, and (c) bentonite, cement and water.

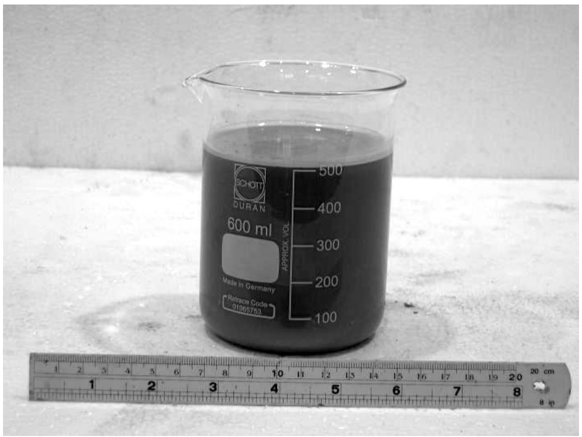

(a)

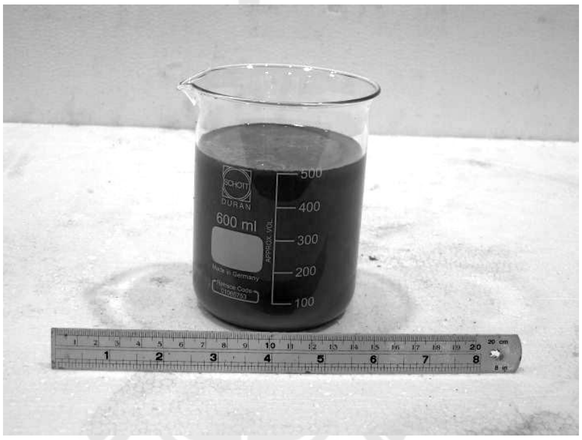

(b)

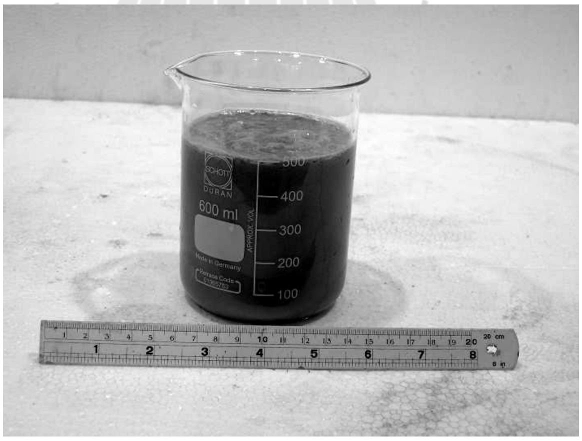

(c)

Figure 4.9 Slurry volume of 500 cc in beakers for the density and viscosity tests (a) cement paste (b) sludge-cement slurry, and (c) bentonite-cement slurry.

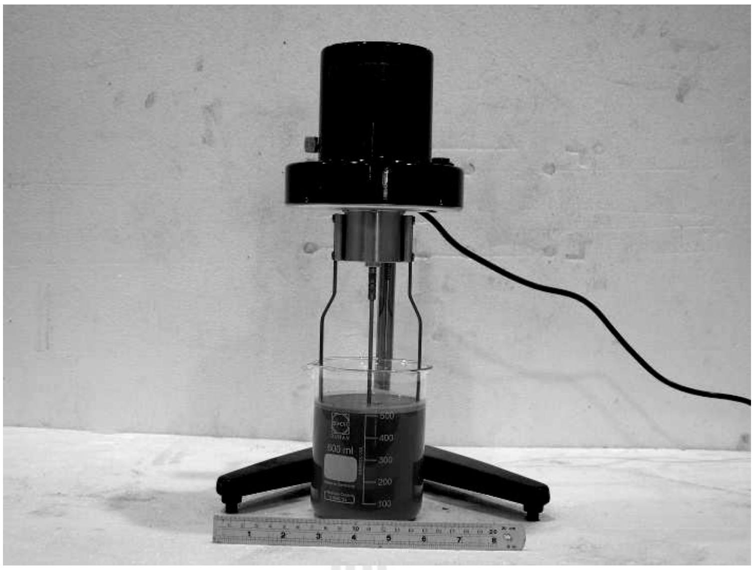

Figure 4.10 Brookfield model RV dial reading viscometer is used for viscosity and slurry density tests.

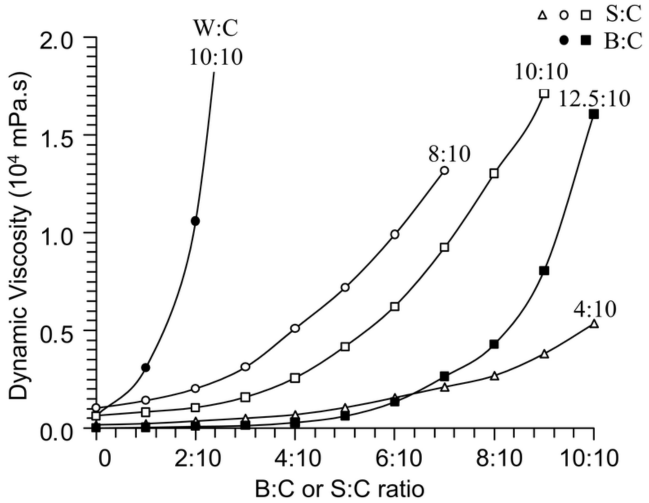

Figure 4.11 Dynamic viscosity of bentonite-cement and sludge-cement mixtures for different W:C ratios.

CHAPTER V

MECHANICAL PROPERTIES TESTING

5.1 Introduction

This chapter describes the methods and results of laboratory tests used to determinate the maximum compressive strength, elastic modulus, and Poisson's ratio for the six proportions of grouting materials selected from Chapter IV. Pure cement is tested in term of mechanical properties. Preparation of these samples follows, as much as practicable, the ASTM standards (ASTM D7012). Direct shear testing is performed to determine the maximum shear force occurs at the interface among the surfaces of the grouting material and surface of fractured sandstone.

5.2 Uniaxial compressive strength testing

The objectives of the uniaxial compressive strength tests are, 1) to evaluate the basic mechanical properties of grouting material specimens of two-inch in diameter at three days curing. They are used as an index to confirm that the proportions of S:C and B:C mixtures are appropriate selection of the viscosity of mixture slurry form Chapter IV, and 2) to determine the uniaxial compressive strength, Poison's ratio and elastic modulus of grouting material specimens of four-inch in diameter at three days curing. This is a part of the material characterization. The material parameters are sample size, weight, density, failure load, and mode of failure, etc. These parameters are monitored, recorded and analyzed. The suitable mixing ratios for the S:C and B:C mixtures are selected and compared.

5.2.1 Test methods

Preparation of these samples follows, as much as practical, the ASTM D7012, C938 and C39 (ASTM 2010a, 2010b, 2010c). The uniaxial compressive strength test is carried out at the ages of 3 days curing. Cylindrical specimens of 50.8 mm diameter are prepared for the basic uniaxial compressive strength test. During the test, cylindrical specimens of 101.6 mm diameter, the axial deformation and lateral deformation are monitored. The maximum loaded at the failure is recorded. The compressive strength (σ_C), Poisson's ratio (ν), elastic modulus (E) are determined for sludge and bentonite-mixed cement ratios vary from 1:10, 2:10, 3:10, 4:10, to 5:10.

Equipment and Apparatus

1) Rubber stopper for PVC pipe of 2 inches in diameter.

2) Point Loaded-Uniaxial Tester, model PLT-75, provide up to 30 tons of load.

3) Cutter, model 51 ZE-LG3-570A Tile Cutter, with speed 2,950 r/min can be cut with a maximum 51 mm thick.

Initially uniaxial compressive strength test procedure follows as below:

1) The mixture slurry from the preparation in Chapter IV is placed in a 54 mm PVC mold with rubber stopper plugged at the bottom (Figure 5.1). Joint connection should not leak out between PVC pipe and rubber stopper.

2) They are cured under water at room temperature (ASTM standard C192).

3) All specimens are cured for three days before testing. They are out of the mold and cut to a L/D ratio of about 2.0 to 2.5 (about 4 to 6 inches in length) (Figures 5.2 and 5.3).

4) Specimens are tested with a loading rate of 1 MPa/s for uniaxial compressive strength test (Figure 5.4).

5) During the test, the failure modes are monitored (Figure 5.5). The maximum loaded at the failure is recorded. The compressive strength (σ_C) is determined and compared for suitable mixing ratios.

The mixtures from the preparation (in Chapter IV) and the results from initially uniaxial compressive strength test are used for selected suitable mixing ratios. The suitable mixing ratios for the S:C mixtures are 1:10, 3:10, 5:10 and for the B:C mixtures are 1:10, 2:10, 3:10 both with the W:C of 1:1 by weight. Uniaxial compressive strength test procedure follows as below:

1) The mixture slurry from the preparation (in section 5.1) is placed in a PVC mold of 101.6 mm diameter and 203.2 mm long (Figure 5.6).

2) They are cured under water at room temperature (ASTM standard C39).

3) All specimens are cured for three days before testing. They are out of the mold and cut to L/D ratio of about 2.0. Summary of parameters and results for basic mechanical testing are listed in Table 5.1.

4) Uniaxial compressive strength tests have been performed on specimens with loading rate of 1 MPa/s (ASTM D7012).

5) During the test, axial and diametric deformations are monitored. Dial gauges are the resolutions of ±0.01 mm.

6) The maximum loaded at the failure is recorded. The cylindrical specimen is loaded vertically using the compression machine shown in Figure 5.7. Figure 5.8 shows failure modes for each specimen.

The failure stress is calculated by dividing the axial load by the cross-section area of specimen. The compressive strength (σ_c) is determined from the maximum load (P_f) divided by the original cross-section area (A):

$$\sigma_c = P_f/A \tag{5.3}$$

5.2.2 Test results

The results of the uniaxial compressive strengths for B:C and S:C mixtures with W:C = 10:10, 8:10, 12.5:10, 40:10 at 3 days of curing are shown in Figure 5.9. Parameters and results of uniaxial compressive strength test on the C, B:C and S:C mixtures specimens of 50.8 mm and 101.6 mm diameter with W:C = 1:1 are summarized in Table 5.2.

The results of the S:C and B:C show that the chemical reaction between cement and water with the large cast are better than the small cast. Figures 5.10 and 5.11 show the uniaxial compressive strength and elastic modulus for the S:C and B:C with W:C = 1:1. The uniaxial compressive strength and elastic modulus for the specimens with the diameter of 101.6 mm are summarized in Tables 5.3 and 5.4. The uniaxial compressive strength for the specimens with the diameter of 50.8 mm is summarized in Table 5.5. The maximum compressive strengths for the S:C and B:C mixtures are similar.

5.3 Shearing resistance between grout and fracture

The objective of the fracture shear test is to determine the direct shear strength of grouting material in sandstone fracture. Grouting materials are sludge- and bentonite-mixed cement. The experimental procedure is similar to the ASTM standard

(D5607). The constant normal stresses are 0.25, 0.5, 0.75, 1.0 and 1.25 MPa. The shear stresses are applied while the shear displacement and head drop is monitored for every 0.2 mm of shear displacement. Similarities and differences of the results are compared. The mixtures from the preparation in Chapter IV and the results from tasks 5.2 are used for selected suitable mixing ratios.

5.3.1 Test methods

Proportions of S:C mixtures are 0:10, 3:10, 5:10, and for B:C mixtures are 1:10, 2:10, 3:10 with W:C ratio of 10:10 by weight. Preparation of these samples follows, as much as practical, the ASTM C938 (ASTM 2010b). The PVC molded of 101.68 mm diameter is attributed to the rock samples with a nominal dimension of 100 mm in diameter and 100 nm long. The fractures are artificially made by applying a line load at the center of length to induce splitting tensile crack. Some sandstone specimens and surface sandstone of 101.6 mm diameter prepared for direct shear testing are shown in Figures 5.12 and 5.13. The grouting material in the PVC mold has 50.8 mm thick that occur between the two rock samples (Figure 5.14). The grouting materials are placed into the cylindrical PVC mold. The shear strength tested, is carried out at the ages of 3 days curing. Laboratory arrangement for the three-ring shear test equipment is shown in Figure 5.15 (Sonsakul and Fuenkajorn, 2013). The constant normal stresses used, are 0.25, 0.5, 0.75, 1.0 and 1.25 MPa. The shear stressed, is applied while the shear displacement and dilation are monitored for every 0.2 mm of shear displacement. The failure modes are recorded. The test results are presented in forms of the shear strength as a function of normal stress as follows:

$$\tau = F/2A \tag{5.4}$$

$$\sigma_n = P/A \tag{5.5}$$

where τ is the shear stress, F is sheared force, A is cross section area, σ_n is normal stress, P is normal load.

The results are presented in the form of the Coulomb's criterion. The line tangent to each of these circles defines the Coulomb's criterion and can be expressed by:

$$\tau = c_p + \sigma\tan\phi_p \tag{5.6}$$

where τ and σ are the shear stress and normal stress, ϕ_p is the angle of internal friction, and c_p is cohesion.

5.3.2 Test results

Figure 5.16 shows some samples after testing. Table 5.6 lists the result of shear strength. Shearing resistance between cement grout and fracture with W:C=1:1 are shown in Figures 5.17 to 5.23. The results in the form of the Coulomb's criterion are shown in Figure 5.24. Table 5.7 lists the Coulomb's parameters.

Table 5.1 Summary of parameters and results for basic mechanical testing.

Types	Sample no.	Length (mm)	Diameter (mm)	L/D	Weight (kg)	Density (g/cc)
C	C9-1	202.7	107.6	1.88	1.53	0.83
	C9-2	201.0	106.9	1.88	1.50	0.83
	C9-3	206.4	106.4	1.94	1.49	0.81
	C9-4	203.3	107.0	1.90	1.54	0.84
	C9-5	202.6	107.6	1.88	1.55	0.84
B:C=0.1	BC20-1	204.3	107.8	1.89	2.46	1.32
	BC20-2	204.7	106.2	1.93	2.45	1.35
	BC20-3	204.1	107.7	1.90	2.43	1.31
	BC20-4	204.3	105.9	1.93	2.42	1.34
	BC20-5	205.0	105.6	1.94	2.54	1.41
B:C=0.2	BC21- 1	202.0	107.1	1.89	2.60	1.43
	BC21- 2	204.4	106.5	1.92	2.56	1.41
	BC21- 3	196.8	106.8	1.84	2.43	1.38
	BC21 - 4	205.6	106.8	1.93	2.44	1.32
	BC21 - 5	207.5	106.3	1.95	2.50	1.36
B:C =0.3	BC9-6	207.5	106.3	1.95	2.45	1.33
	BC9-7	207.5	106.3	1.95	2.50	1.36
	BC9-8	207.5	106.3	1.95	2.43	1.32
	BC9-9	207.5	106.3	1.95	2.44	1.32
	BC9-10	207.5	106.3	1.95	2.43	1.32

Table 5.1 Summary of parameters and results for basic mechanical testing (continued).

Types	Sample no.	Length (mm)	Diameter (mm)	L/D	Weight (kg)	Density (g/cc)
S:C=0.1	SC40-1	202.7	105.4	1.92	3.50	1.98
	SC40-2	202.9	106.3	1.91	3.30	1.83
	SC40-3	204.4	106.9	1.91	3.60	1.96
	SC40-4	204.6	106.9	1.91	3.45	1.88
	SC40-5	204.4	107.3	1.90	3.50	1.89
S:C=0.3	SC22-6	203.9	107.4	1.90	3.21	1.74
	SC22-7	206.6	107.4	1.92	3.24	1.73
	SC22-8	203.2	108.3	1.88	3.50	1.87
	SC22-9	205.3	107.0	1.92	3.41	1.85
	SC22-10	205.2	106.7	1.92	3.44	1.88
S:C=0.5	SC21-6	205.5	106.6	1.93	3.20	1.74
	SC21-7	207.0	105.7	1.96	3.25	1.79
	SC21-8	208.8	107.3	1.95	3.35	1.77
	SC21-9	208.2	108.1	1.93	3.40	1.78
	SC21-10	208.4	106.4	1.96	3.50	1.89

Table 5.2 Summary of uniaxial compressive strength test results on the C, B:C and S:C mixtures specimens of 50.8 mm diameter.

Binder	W:C	S:C or B:C	Number of	Uniaxial Compressive
Sludge	8:10	1:10	5	1.39 ± 0.19
	8:10	2:10	15	2.77 ± 0.20
	8:10	3:10	8	2.75 ± 0.12
	8:10	4:10	5	2.72 ± 0.14
	10:10	1:10	2	0.79 ± 0.12
	10:10	2:10	13	0.95 ± 0.11
	10:10	3:10	3	1.22 ± 0.10
	10:10	4:10	3	1.13±0.17
	10:10	5:10	3	1.10 ± 0.34
	10:10	6:10	3	1.02± 0.00
	10:10	8:10	3	0.88± 0.01
	10:10	10:10	3	0.81± 0.00
	12.5:10	2:10	5	0.62 ± 0.02
	12.5:10	4:10	5	0.52 ± 0.09
	12.5:10	5:10	15	0.44 ± 0.01
Bentonite	10:10	1:10	10	1.05±0.10
	10:10	2:10	7	1.83 ± 0.00
	10:10	3:10	9	1.77 ± 0.09
	40:10	1:10	5	0.19 ± 0.05
	40:10	2:10	5	0.07 ± 0.03
	40:10	3:10	5	0.08 ± 0.02
	40:10	4:10	5	0.04 ± 0.00
	40:10	5:10	5	0.05 ± 0.02
Cement	8:10	0:10	5	1.14±0.10
	10:10	0:10	5	0.85 ± 0.00
	12.5:10	0:10	5	0.70 ± 0.10
	40:10	0:10	5	0.41±0.03

Table 5.3 Summary of uniaxial compressive strength test results on the C, B:C and S:C mixtures specimens of 101.6 mm diameter with W:C = 1:1.

Types	Number of Samples	Mixing Ratio	Uniaxial Compressive Strength (MPa)
C	5	0:10	1.40 ± 0.27
B:C	5	1:10	1.59 ± 0.28
B:C	5	2:10	2.09 ± 0.26
B:C	5	3:10	1.92 ± 0.05
S:C	5	1:10	1.35 ± 0.06
S:C	5	3:10	1.77 ± 0.21
S:C	5	5:10	1.52 ± 0.19

Table 5.4 Poisson’s ratio and elastic modulus from uniaxial compressive strength testing.

Types	Number of Samples	Mixing Ratio	Poisson’s Ratio	Elastic Modulus (MPa)
C	5	0:10	0.18	212
B:C	5	1:10	0.17	193
B:C	5	2:10	0.14	275
B:C	5	3:10	0.16	228
S:C	5	1:10	0.15	190
S:C	5	3:10	0.21	224
S:C	5	5:10	0.16	261

Table 5.5 Summary of uniaxial compressive strength test results on the C, B:C and S:C mixtures specimens of 50.8 mm diameter with W:C = 1:1.

Types	Number of Samples	Mixing Ratio	Uniaxial Compressive Strength (MPa)
C	4	-	0.85 ± 0.00
B:C	2	1:10	1.05 ± 0.10
B:C	2	2:10	1.83 ± 0.00
B:C	2	3:10	1.77 ± 0.09
S:C	2	1:10	0.79 ± 0.12
S:C	3	3:10	1.22 ± 0.10
S:C	3	5:10	1.10 ± 0.34

Table 5.6 Summary of direct shear strength test results on the C, B:C and S:C mixtures specimens with W:C = 1:1.

Normal Stress (MPa)	Peak Shear Stress (MPa)						
	Pure Cement	S:C =1:10	S:C =3:10	S:C =5:10	B:C =1:10	B:C =2:10	B:C =3:10
0.25	0.62	0.36	0.31	0.34	0.37	0.22	0.25
0.50	0.68	0.49	0.42	0.46	0.53	0.34	0.37
0.75	0.77	0.62	0.55	0.60	0.65	0.43	0.47
1.00	0.86	0.74	0.68	0.71	0.77	0.52	0.56
1.25	0.90	0.83	0.77	0.80	0.85	0.63	0.67
1.50	0.93	0.90	0.83	0.86	0.90	0.74	0.80

Table 5.7 Summary of shear strength parameters calibrated from direct shear tests using Coulomb's criteria.

Sample No.	c_p (MPa)	$\tan\phi_p$	ϕ_p (degrees)	R^2
Pure Cement	0.563	0.263	14.7	0.962
S:C=1:10	0.275	0.436	23.6	0.985
S:C=3:10	0.213	0.435	23.5	0.988
S:C=5:10	0.255	0.428	23.2	0.985
B:C=1:10	0.306	0.424	23.0	0.968
B:C=2:10	0.121	0.410	22.3	0.998
B:C=3:10	0.143	0.430	23.3	0.996

Figure 5.1 PVC mold has an inner diameter of 50.8 mm with a rubber stopper on the bottom.

Figure 5.2 Core sample is cut to obtain the desired length with ZE-LG3-570A Tile Cutter.

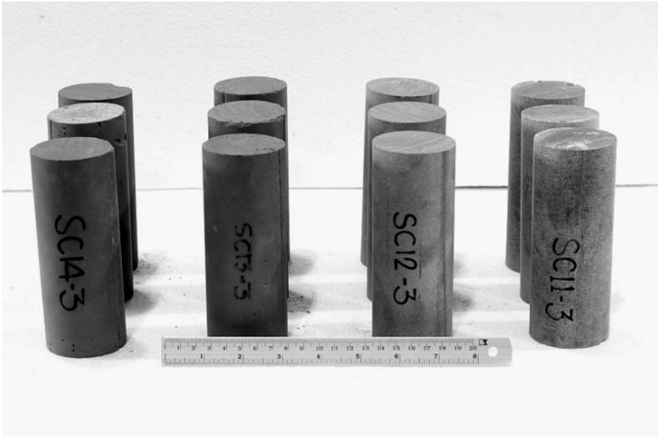

(a)

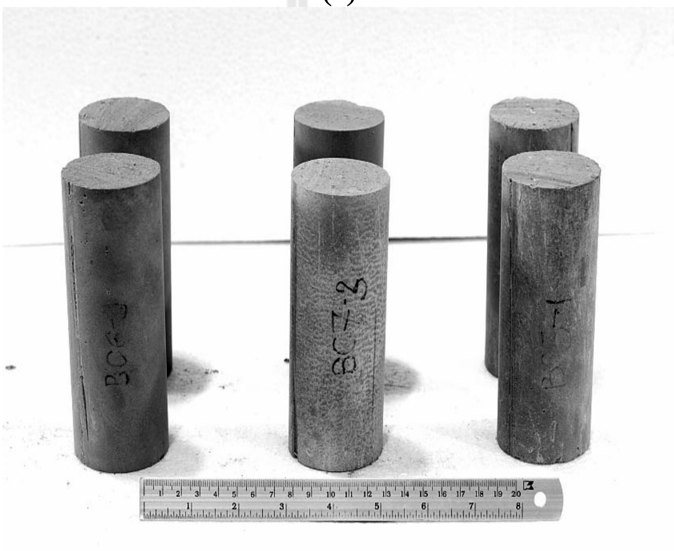

(b)

Figure 5.3 Some specimens prepared for basic mechanical testing (a) sludge-mixed cement, and (b) bentonite-mixed cement.

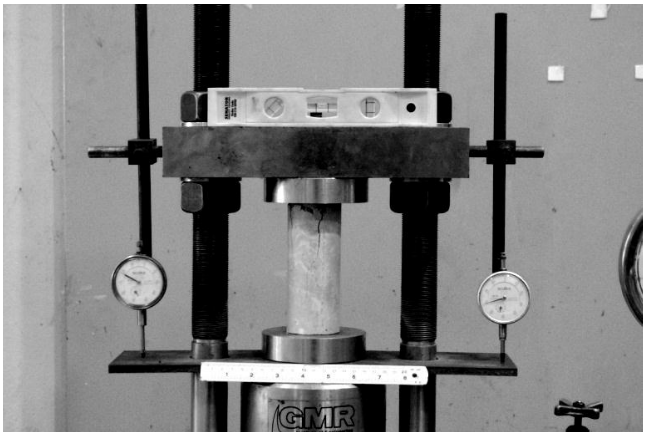

(a)

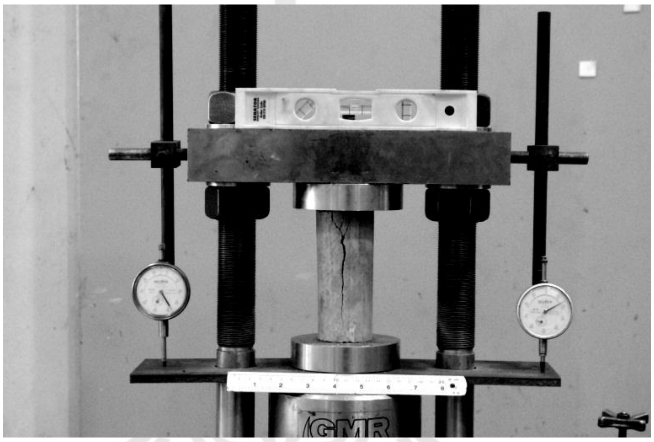

(b)

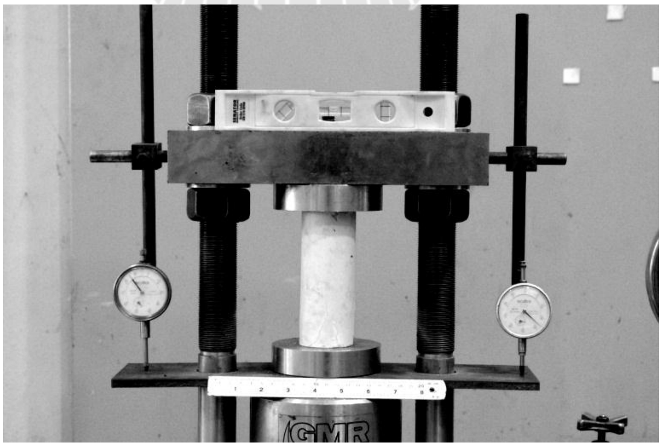

(c)

Figure 5.4 Uniaxial compressive strength test with constant loading rate. The cylindrical specimen is loaded vertically using the compression machine, (a) cement, (b) sludge-mixed cement, and (c) bentonite-mixed cement.

(a)

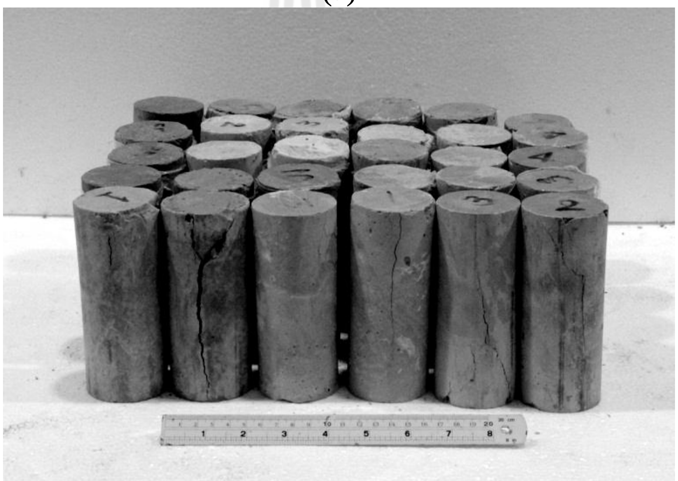

(b)

Figure 5.5 Specimens (a) sludge-mixed cement, and (b) bentonite-mixed cement after failure under loading with constant stress rate of 1 MPa/s.

Figure 5.6 PVC mold has an inner diameter of 101.6 mm with 203.2 mm in length.

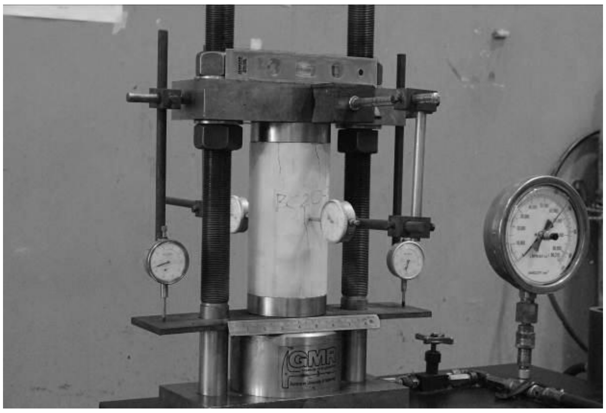

(a)

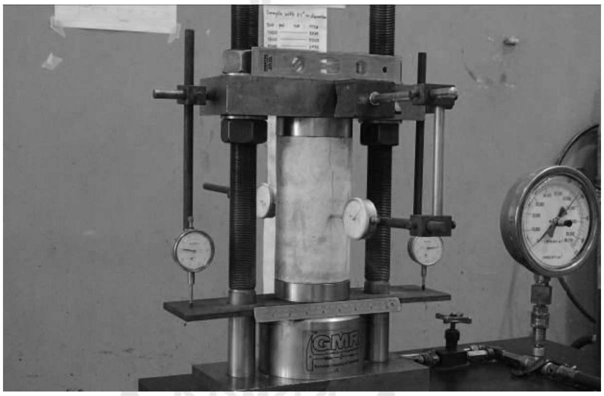

(b)

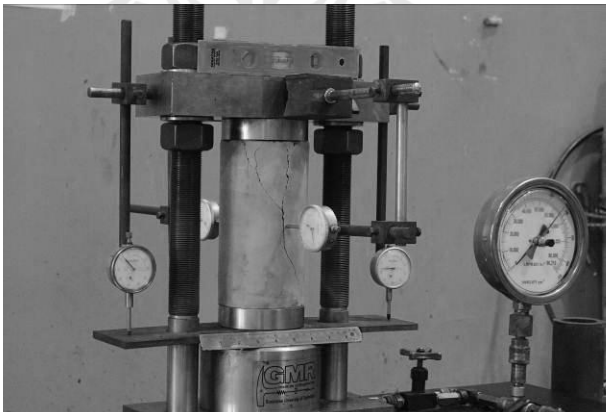

(c)

Figure 5.7 Uniaxial compressive strength test with constant loading rate. The cylindrical specimen is loaded vertically using the compression machine, (a) B:C = 2:10, (b) C:W = 1:1, and (c) S:C = 3:10.

(a)

(b)

(c)

Figure 5.8 Specimens of 101.6 mm diameter (a) sludge-mixed cement, and (b) bentonite-mixed cement after failure under loading with constant stress rate of 1 MPa/s.

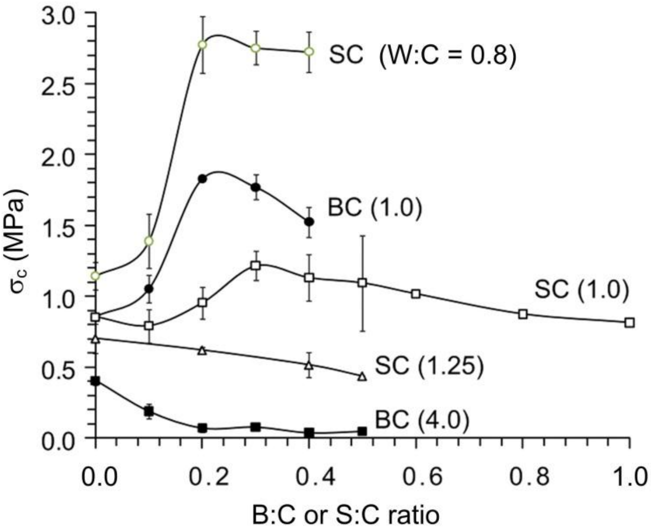

Figure 5.9 Uniaxial compressive strengths for B:C and S:C mixtures with W:C = 10:10, 8:10, 12.5:10, 40:10 at 3 days of curing.

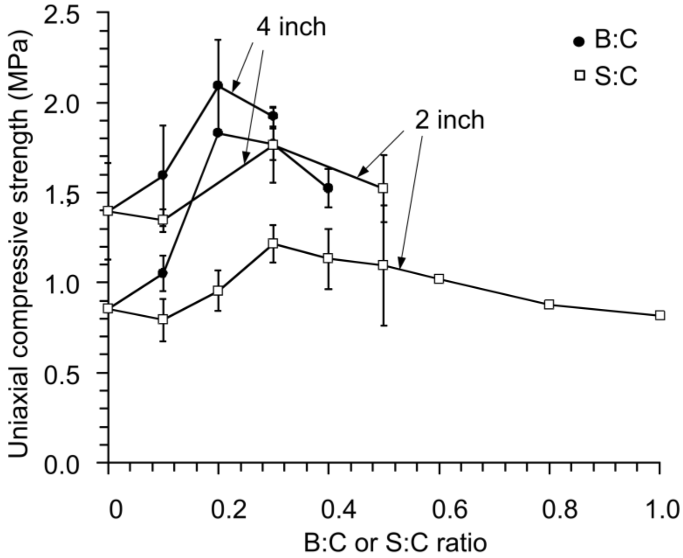

Figure 5.10 Uniaxial compressive strengths for B:C and S:C with W:C = 1:1.

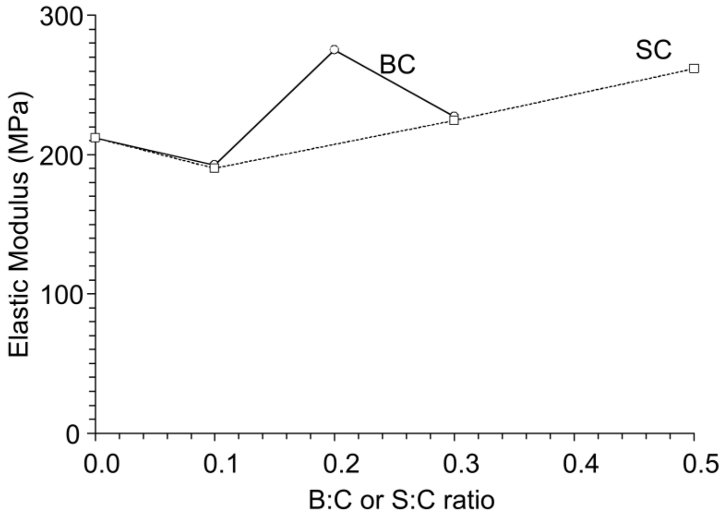

Figure 5.11 Comparisons of elastic modulus between B:C and S:C mixtures.

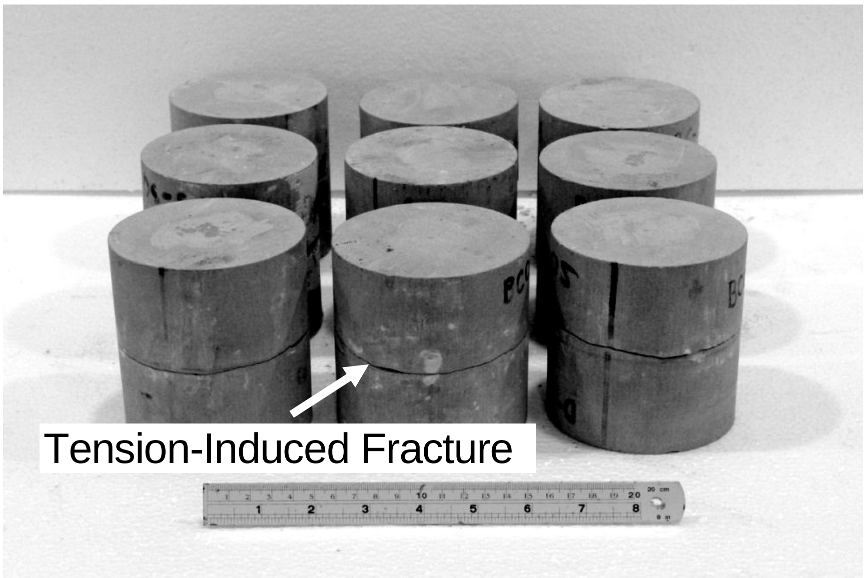

Figure 5.12 Some sandstone specimens of 101.6 mm diameter prepared for direct shear testing.

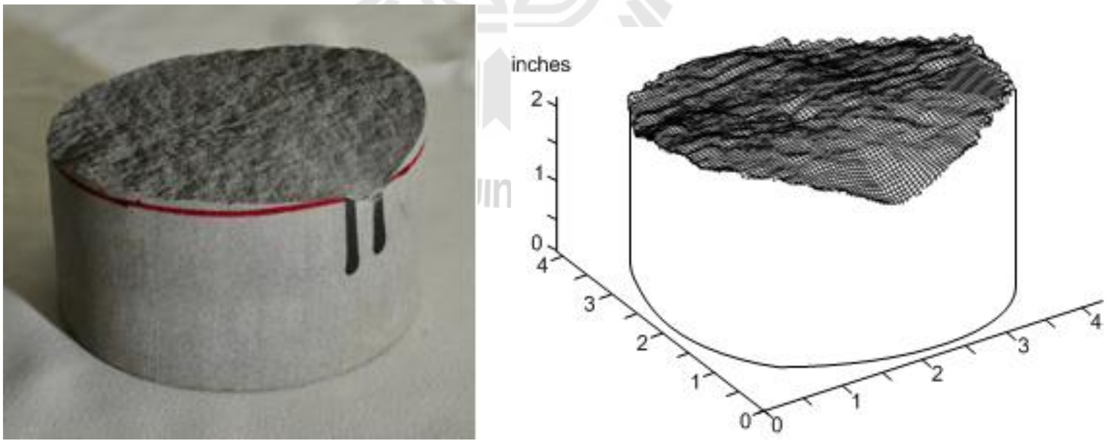

Figure 5.13 Surface sandstone specimen prepared for direct shear testing (left) and surface sandstone model of laser scan (right).

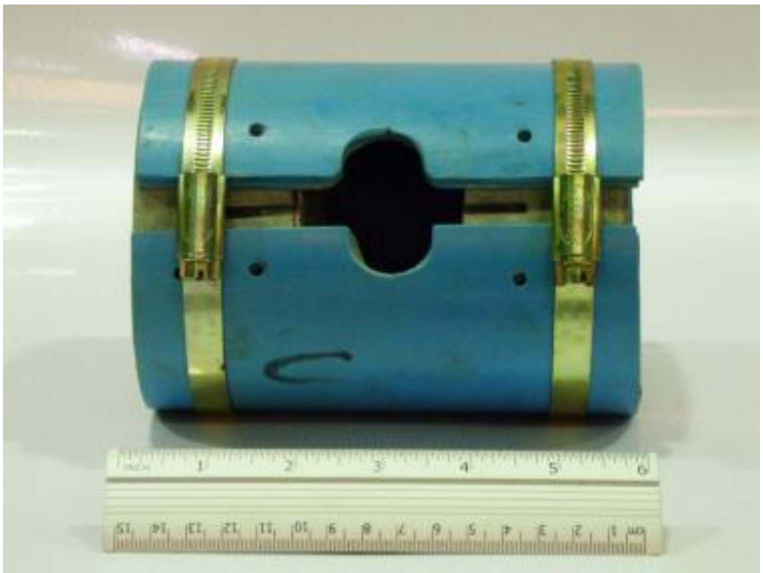

Figure 5.14 PVC mold has an inner diameter of 101.6 mm for direct shear testing.

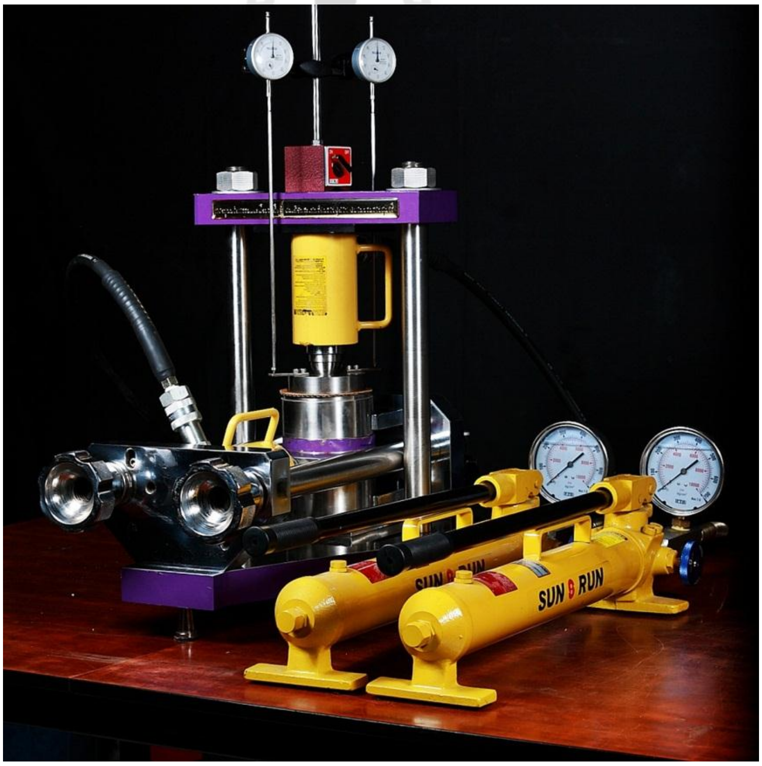

Figure 5.15 Laboratory arrangements for three-ring direct shear test.

Figure 5.16 Some specimens of grouting material in sandstone fracture after failure under shearing between grout and fracture.

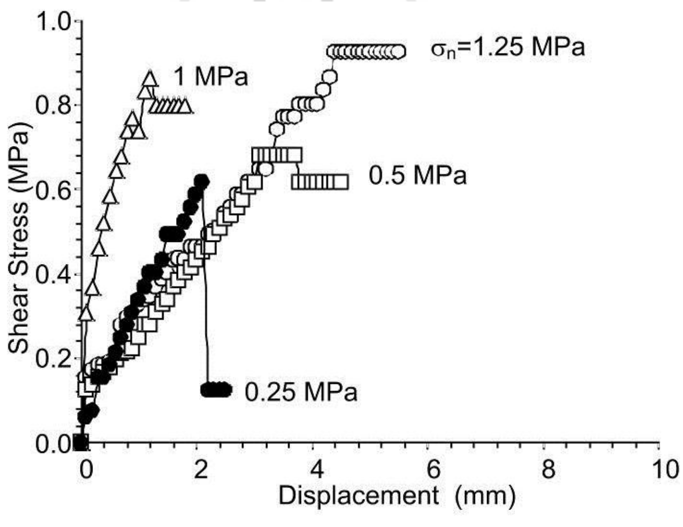

Figure 5.17 Shearing resistance between cement grout and fracture with W:C=1:1.

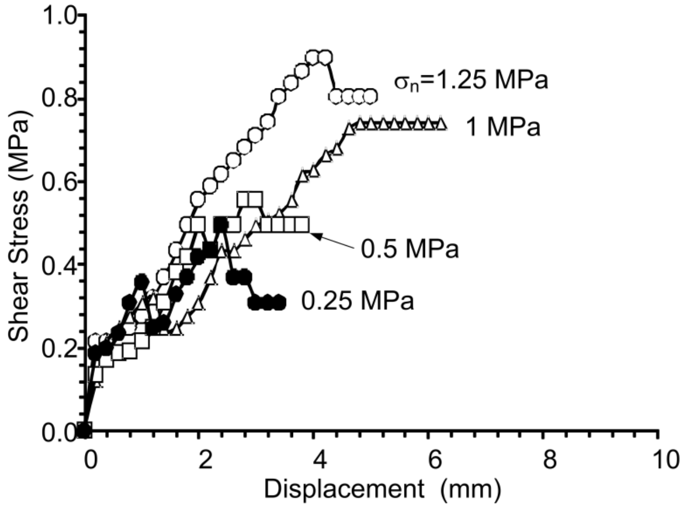

Figure 5.18 Shearing resistance between S:C=1:10 mixture grout and fracture with W:C=1:1.

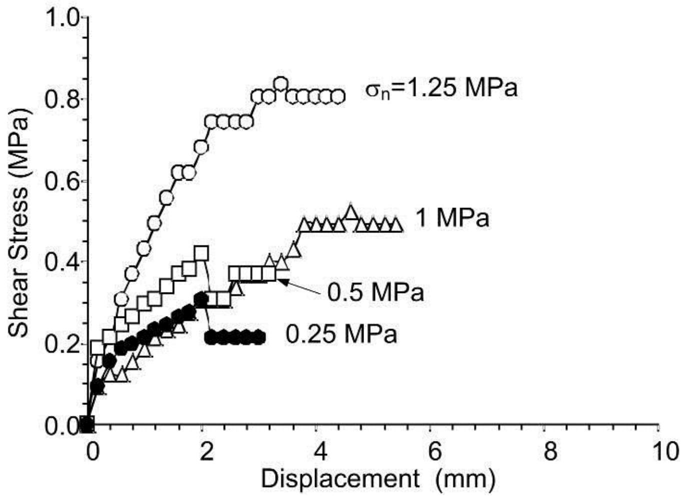

Figure 5.19 Shearing resistance between S:C=3:10 mixture grout and fracture with W:C=1:1.

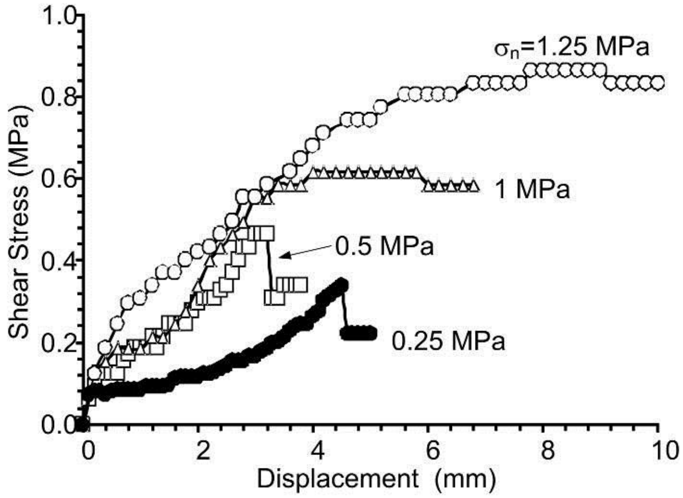

Figure 5.20 Shearing resistance between S:C=5:10 mixture grout and fracture with W:C=1:1.

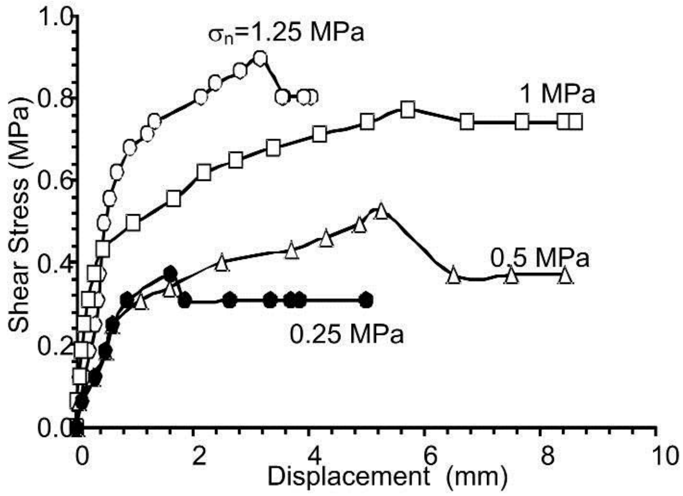

Figure 5.21 Shearing resistance between B:C=1:10 mixture grout and fracture with W:C=1:1.

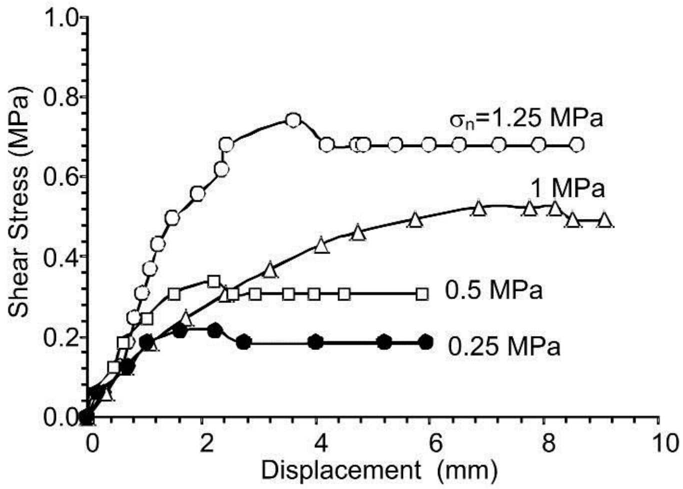

Figure 5.22 Shearing resistance between B:C=2:10 mixture grout and fracture with W:C=1:1.

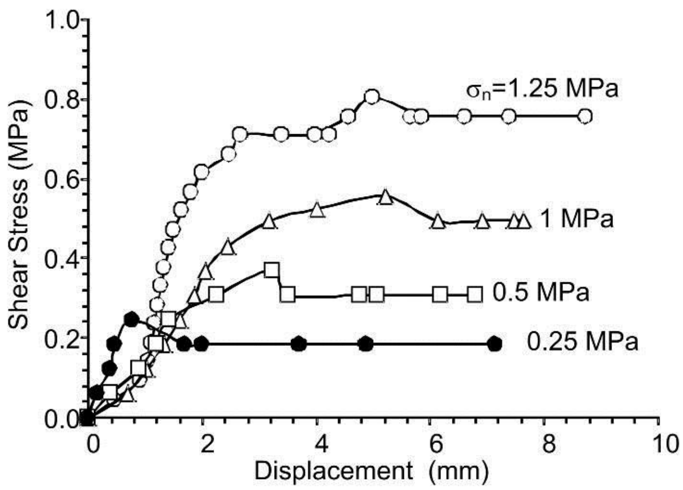

Figure 5.23 Shearing resistance between B:C=3:10 mixture grout and fracture with W:C=1:1.

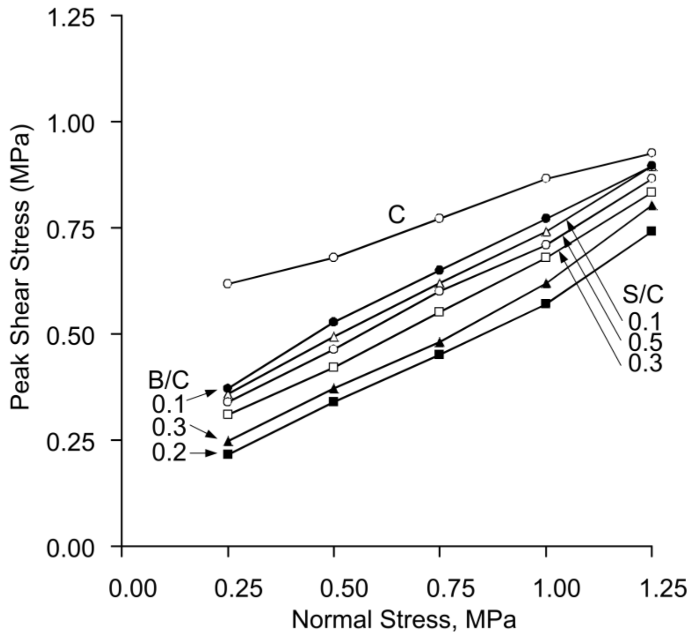

Figure 5.24 Normal stress and peak shear stress.

CHAPTER V

MECHANICAL PROPERTIES TESTING

5.1 Introduction

This chapter describes the methods and results of laboratory tests used to determinate the maximum compressive strength, elastic modulus, and Poisson's ratio for the six proportions of grouting materials selected from Chapter IV. Pure cement is tested in term of mechanical properties. Preparation of these samples follows, as much as practicable, the ASTM standards (ASTM D7012). Direct shear testing is performed to determine the maximum shear force occurs at the interface among the surfaces of the grouting material and surface of fractured sandstone.

5.2 Uniaxial compressive strength testing

The objectives of the uniaxial compressive strength tests are, 1) to evaluate the basic mechanical properties of grouting material specimens of two-inch in diameter at three days curing. They are used as an index to confirm that the proportions of S:C and B:C mixtures are appropriate selection of the viscosity of mixture slurry form Chapter IV, and 2) to determine the uniaxial compressive strength, Poison's ratio and elastic modulus of grouting material specimens of four-inch in diameter at three days curing. This is a part of the material characterization. The material parameters are sample size, weight, density, failure load, and mode of failure, etc. These parameters are monitored, recorded and analyzed. The suitable mixing ratios for the S:C and B:C mixtures are selected and compared.

5.2.1 Test methods

Preparation of these samples follows, as much as practical, the ASTM D7012, C938 and C39 (ASTM 2010a, 2010b, 2010c). The uniaxial compressive strength test is carried out at the ages of 3 days curing. Cylindrical specimens of 50.8 mm diameter are prepared for the basic uniaxial compressive strength test. During the test, cylindrical specimens of 101.6 mm diameter, the axial deformation and lateral deformation are monitored. The maximum loaded at the failure is recorded. The compressive strength (σ_C), Poisson's ratio (ν), elastic modulus (E) are determined for sludge and bentonite-mixed cement ratios vary from 1:10, 2:10, 3:10, 4:10, to 5:10.

Equipment and Apparatus

1) Rubber stopper for PVC pipe of 2 inches in diameter.

2) Point Loaded-Uniaxial Tester, model PLT-75, provide up to 30 tons of load.

3) Cutter, model 51 ZE-LG3-570A Tile Cutter, with speed 2,950 r/min can be cut with a maximum 51 mm thick.

Initially uniaxial compressive strength test procedure follows as below:

1) The mixture slurry from the preparation in Chapter IV is placed in a 54 mm PVC mold with rubber stopper plugged at the bottom (Figure 5.1). Joint connection should not leak out between PVC pipe and rubber stopper.

2) They are cured under water at room temperature (ASTM standard C192).

3) All specimens are cured for three days before testing. They are out of the mold and cut to a L/D ratio of about 2.0 to 2.5 (about 4 to 6 inches in length) (Figures 5.2 and 5.3).

4) Specimens are tested with a loading rate of 1 MPa/s for uniaxial compressive strength test (Figure 5.4).

5) During the test, the failure modes are monitored (Figure 5.5). The maximum loaded at the failure is recorded. The compressive strength (σ_C) is determined and compared for suitable mixing ratios.

The mixtures from the preparation (in Chapter IV) and the results from initially uniaxial compressive strength test are used for selected suitable mixing ratios. The suitable mixing ratios for the S:C mixtures are 1:10, 3:10, 5:10 and for the B:C mixtures are 1:10, 2:10, 3:10 both with the W:C of 1:1 by weight. Uniaxial compressive strength test procedure follows as below:

1) The mixture slurry from the preparation (in section 5.1) is placed in a PVC mold of 101.6 mm diameter and 203.2 mm long (Figure 5.6).

2) They are cured under water at room temperature (ASTM standard C39).

3) All specimens are cured for three days before testing. They are out of the mold and cut to L/D ratio of about 2.0. Summary of parameters and results for basic mechanical testing are listed in Table 5.1.

4) Uniaxial compressive strength tests have been performed on specimens with loading rate of 1 MPa/s (ASTM D7012).

5) During the test, axial and diametric deformations are monitored. Dial gauges are the resolutions of ±0.01 mm.

6) The maximum loaded at the failure is recorded. The cylindrical specimen is loaded vertically using the compression machine shown in Figure 5.7. Figure 5.8 shows failure modes for each specimen.

The failure stress is calculated by dividing the axial load by the cross-section area of specimen. The compressive strength (σ_c) is determined from the maximum load (P_f) divided by the original cross-section area (A):

$$\sigma_c = P_f/A \tag{5.3}$$

5.2.2 Test results

The results of the uniaxial compressive strengths for B:C and S:C mixtures with W:C = 10:10, 8:10, 12.5:10, 40:10 at 3 days of curing are shown in Figure 5.9. Parameters and results of uniaxial compressive strength test on the C, B:C and S:C mixtures specimens of 50.8 mm and 101.6 mm diameter with W:C = 1:1 are summarized in Table 5.2.

The results of the S:C and B:C show that the chemical reaction between cement and water with the large cast are better than the small cast. Figures 5.10 and 5.11 show the uniaxial compressive strength and elastic modulus for the S:C and B:C with W:C = 1:1. The uniaxial compressive strength and elastic modulus for the specimens with the diameter of 101.6 mm are summarized in Tables 5.3 and 5.4. The uniaxial compressive strength for the specimens with the diameter of 50.8 mm is summarized in Table 5.5. The maximum compressive strengths for the S:C and B:C mixtures are similar.

5.3 Shearing resistance between grout and fracture

The objective of the fracture shear test is to determine the direct shear strength of grouting material in sandstone fracture. Grouting materials are sludge- and bentonite-mixed cement. The experimental procedure is similar to the ASTM standard

(D5607). The constant normal stresses are 0.25, 0.5, 0.75, 1.0 and 1.25 MPa. The shear stresses are applied while the shear displacement and head drop is monitored for every 0.2 mm of shear displacement. Similarities and differences of the results are compared. The mixtures from the preparation in Chapter IV and the results from tasks 5.2 are used for selected suitable mixing ratios.

5.3.1 Test methods

Proportions of S:C mixtures are 0:10, 3:10, 5:10, and for B:C mixtures are 1:10, 2:10, 3:10 with W:C ratio of 10:10 by weight. Preparation of these samples follows, as much as practical, the ASTM C938 (ASTM 2010b). The PVC molded of 101.68 mm diameter is attributed to the rock samples with a nominal dimension of 100 mm in diameter and 100 nm long. The fractures are artificially made by applying a line load at the center of length to induce splitting tensile crack. Some sandstone specimens and surface sandstone of 101.6 mm diameter prepared for direct shear testing are shown in Figures 5.12 and 5.13. The grouting material in the PVC mold has 50.8 mm thick that occur between the two rock samples (Figure 5.14). The grouting materials are placed into the cylindrical PVC mold. The shear strength tested, is carried out at the ages of 3 days curing. Laboratory arrangement for the three-ring shear test equipment is shown in Figure 5.15 (Sonsakul and Fuenkajorn, 2013). The constant normal stresses used, are 0.25, 0.5, 0.75, 1.0 and 1.25 MPa. The shear stressed, is applied while the shear displacement and dilation are monitored for every 0.2 mm of shear displacement. The failure modes are recorded. The test results are presented in forms of the shear strength as a function of normal stress as follows:

$$\tau = F/2A \tag{5.4}$$

$$\sigma_n = P/A \tag{5.5}$$

where τ is the shear stress, F is sheared force, A is cross section area, σ_n is normal stress, P is normal load.

The results are presented in the form of the Coulomb's criterion. The line tangent to each of these circles defines the Coulomb's criterion and can be expressed by:

$$\tau = c_p + \sigma\tan\phi_p \tag{5.6}$$

where τ and σ are the shear stress and normal stress, ϕ_p is the angle of internal friction, and c_p is cohesion.

5.3.2 Test results

Figure 5.16 shows some samples after testing. Table 5.6 lists the result of shear strength. Shearing resistance between cement grout and fracture with W:C=1:1 are shown in Figures 5.17 to 5.23. The results in the form of the Coulomb's criterion are shown in Figure 5.24. Table 5.7 lists the Coulomb's parameters.

Table 5.1 Summary of parameters and results for basic mechanical testing.

Types	Sample no.	Length (mm)	Diameter (mm)	L/D	Weight (kg)	Density (g/cc)
C	C9-1	202.7	107.6	1.88	1.53	0.83
	C9-2	201.0	106.9	1.88	1.50	0.83
	C9-3	206.4	106.4	1.94	1.49	0.81
	C9-4	203.3	107.0	1.90	1.54	0.84
	C9-5	202.6	107.6	1.88	1.55	0.84
B:C=0.1	BC20-1	204.3	107.8	1.89	2.46	1.32
	BC20-2	204.7	106.2	1.93	2.45	1.35
	BC20-3	204.1	107.7	1.90	2.43	1.31
	BC20-4	204.3	105.9	1.93	2.42	1.34
	BC20-5	205.0	105.6	1.94	2.54	1.41
B:C=0.2	BC21- 1	202.0	107.1	1.89	2.60	1.43
	BC21- 2	204.4	106.5	1.92	2.56	1.41
	BC21- 3	196.8	106.8	1.84	2.43	1.38
	BC21 - 4	205.6	106.8	1.93	2.44	1.32
	BC21 - 5	207.5	106.3	1.95	2.50	1.36
B:C =0.3	BC9-6	207.5	106.3	1.95	2.45	1.33
	BC9-7	207.5	106.3	1.95	2.50	1.36
	BC9-8	207.5	106.3	1.95	2.43	1.32
	BC9-9	207.5	106.3	1.95	2.44	1.32
	BC9-10	207.5	106.3	1.95	2.43	1.32

Table 5.1 Summary of parameters and results for basic mechanical testing (continued).

Types	Sample no.	Length (mm)	Diameter (mm)	L/D	Weight (kg)	Density (g/cc)
S:C=0.1	SC40-1	202.7	105.4	1.92	3.50	1.98
	SC40-2	202.9	106.3	1.91	3.30	1.83
	SC40-3	204.4	106.9	1.91	3.60	1.96
	SC40-4	204.6	106.9	1.91	3.45	1.88
	SC40-5	204.4	107.3	1.90	3.50	1.89
S:C=0.3	SC22-6	203.9	107.4	1.90	3.21	1.74
	SC22-7	206.6	107.4	1.92	3.24	1.73
	SC22-8	203.2	108.3	1.88	3.50	1.87
	SC22-9	205.3	107.0	1.92	3.41	1.85
	SC22-10	205.2	106.7	1.92	3.44	1.88
S:C=0.5	SC21-6	205.5	106.6	1.93	3.20	1.74
	SC21-7	207.0	105.7	1.96	3.25	1.79
	SC21-8	208.8	107.3	1.95	3.35	1.77
	SC21-9	208.2	108.1	1.93	3.40	1.78
	SC21-10	208.4	106.4	1.96	3.50	1.89

Table 5.2 Summary of uniaxial compressive strength test results on the C, B:C and S:C mixtures specimens of 50.8 mm diameter.

Binder	W:C	S:C or B:C	Number of	Uniaxial Compressive
Sludge	8:10	1:10	5	1.39 ± 0.19
	8:10	2:10	15	2.77 ± 0.20
	8:10	3:10	8	2.75 ± 0.12
	8:10	4:10	5	2.72 ± 0.14
	10:10	1:10	2	0.79 ± 0.12
	10:10	2:10	13	0.95 ± 0.11
	10:10	3:10	3	1.22 ± 0.10
	10:10	4:10	3	1.13±0.17
	10:10	5:10	3	1.10 ± 0.34
	10:10	6:10	3	1.02± 0.00
	10:10	8:10	3	0.88± 0.01
	10:10	10:10	3	0.81± 0.00
	12.5:10	2:10	5	0.62 ± 0.02
	12.5:10	4:10	5	0.52 ± 0.09
	12.5:10	5:10	15	0.44 ± 0.01
Bentonite	10:10	1:10	10	1.05±0.10
	10:10	2:10	7	1.83 ± 0.00
	10:10	3:10	9	1.77 ± 0.09
	40:10	1:10	5	0.19 ± 0.05
	40:10	2:10	5	0.07 ± 0.03
	40:10	3:10	5	0.08 ± 0.02
	40:10	4:10	5	0.04 ± 0.00
	40:10	5:10	5	0.05 ± 0.02
Cement	8:10	0:10	5	1.14±0.10
	10:10	0:10	5	0.85 ± 0.00
	12.5:10	0:10	5	0.70 ± 0.10
	40:10	0:10	5	0.41±0.03

Table 5.3 Summary of uniaxial compressive strength test results on the C, B:C and S:C mixtures specimens of 101.6 mm diameter with W:C = 1:1.

Types	Number of Samples	Mixing Ratio	Uniaxial Compressive Strength (MPa)
C	5	0:10	1.40 ± 0.27
B:C	5	1:10	1.59 ± 0.28
B:C	5	2:10	2.09 ± 0.26
B:C	5	3:10	1.92 ± 0.05
S:C	5	1:10	1.35 ± 0.06
S:C	5	3:10	1.77 ± 0.21
S:C	5	5:10	1.52 ± 0.19

Table 5.4 Poisson's ratio and elastic modulus from uniaxial compressive strength testing.

Types	Number of Samples	Mixing Ratio	Poisson's Ratio	Elastic Modulus (MPa)
C	5	0:10	0.18	212
B:C	5	1:10	0.17	193
B:C	5	2:10	0.14	275
B:C	5	3:10	0.16	228
S:C	5	1:10	0.15	190
S:C	5	3:10	0.21	224
S:C	5	5:10	0.16	261

Table 5.5 Summary of uniaxial compressive strength test results on the C, B:C and S:C mixtures specimens of 50.8 mm diameter with W:C = 1:1.

Types	Number of Samples	Mixing Ratio	Uniaxial Compressive Strength (MPa)
C	4	-	0.85 ± 0.00
B:C	2	1:10	1.05 ± 0.10
B:C	2	2:10	1.83 ± 0.00
B:C	2	3:10	1.77 ± 0.09
S:C	2	1:10	0.79 ± 0.12
S:C	3	3:10	1.22 ± 0.10
S:C	3	5:10	1.10 ± 0.34

Table 5.6 Summary of direct shear strength test results on the C, B:C and S:C mixtures specimens with W:C = 1:1.

Normal Stress (MPa)	Peak Shear Stress (MPa)						
	Pure Cement	S:C =1:10	S:C =3:10	S:C =5:10	B:C =1:10	B:C =2:10	B:C =3:10
0.25	0.62	0.36	0.31	0.34	0.37	0.22	0.25
0.50	0.68	0.49	0.42	0.46	0.53	0.34	0.37
0.75	0.77	0.62	0.55	0.60	0.65	0.43	0.47
1.00	0.86	0.74	0.68	0.71	0.77	0.52	0.56
1.25	0.90	0.83	0.77	0.80	0.85	0.63	0.67
1.50	0.93	0.90	0.83	0.86	0.90	0.74	0.80

Table 5.7 Summary of shear strength parameters calibrated from direct shear tests using Coulomb's criteria.

Sample No.	c_p (MPa)	$\tan\phi_p$	ϕ_p (degrees)	R^2
Pure Cement	0.563	0.263	14.7	0.962
S:C=1:10	0.275	0.436	23.6	0.985
S:C=3:10	0.213	0.435	23.5	0.988
S:C=5:10	0.255	0.428	23.2	0.985
B:C=1:10	0.306	0.424	23.0	0.968
B:C=2:10	0.121	0.410	22.3	0.998
B:C=3:10	0.143	0.430	23.3	0.996

Figure 5.1 PVC mold has an inner diameter of 50.8 mm with a rubber stopper on the bottom.

Figure 5.2 Core sample is cut to obtain the desired length with ZE-LG3-570A Tile Cutter.

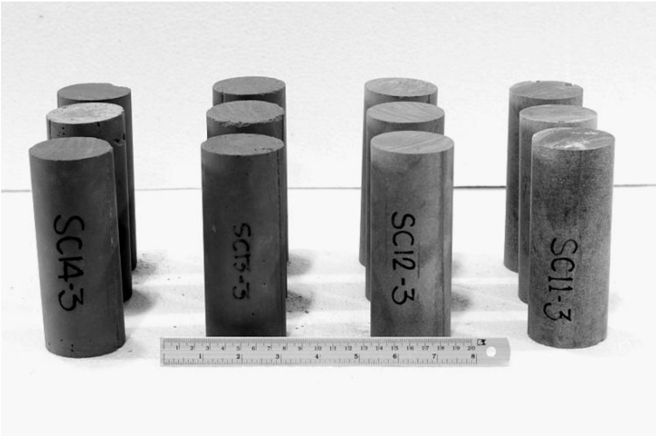

(a)

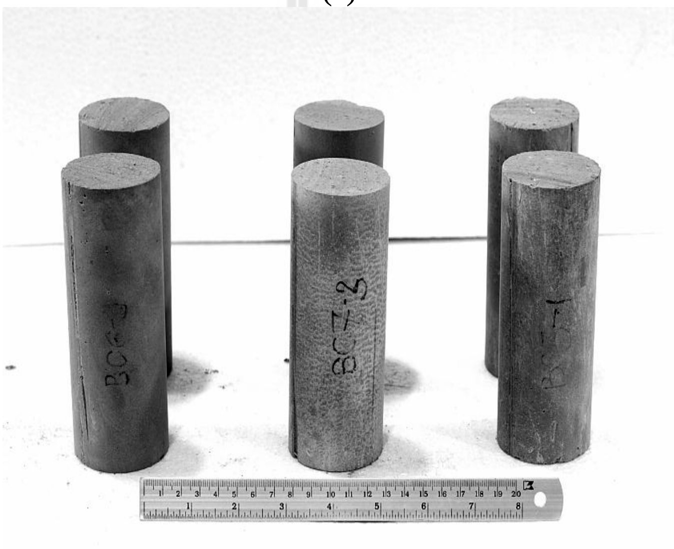

(b)

Figure 5.3 Some specimens prepared for basic mechanical testing (a) sludge-mixed cement, and (b) bentonite-mixed cement.

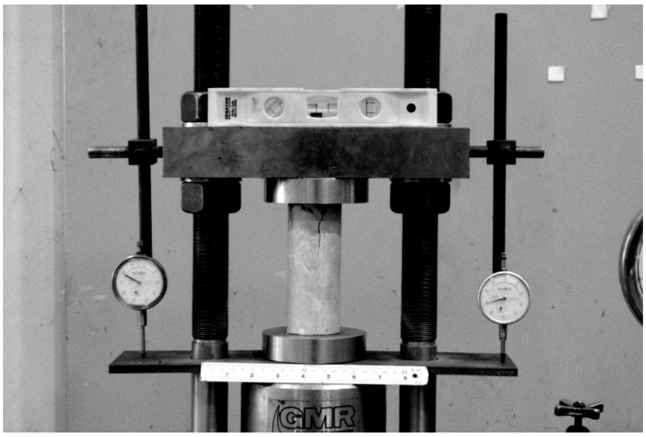

(a)

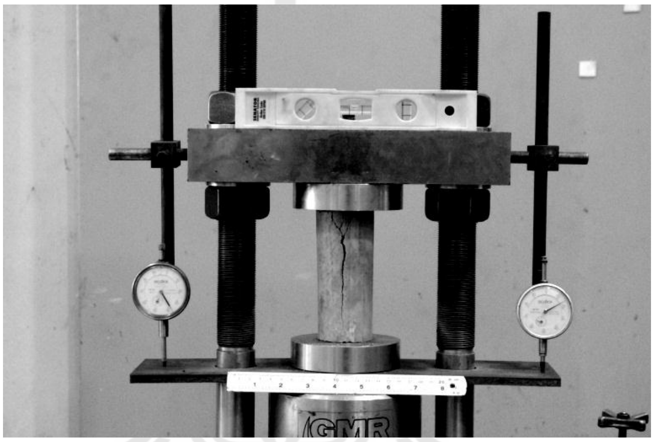

(b)

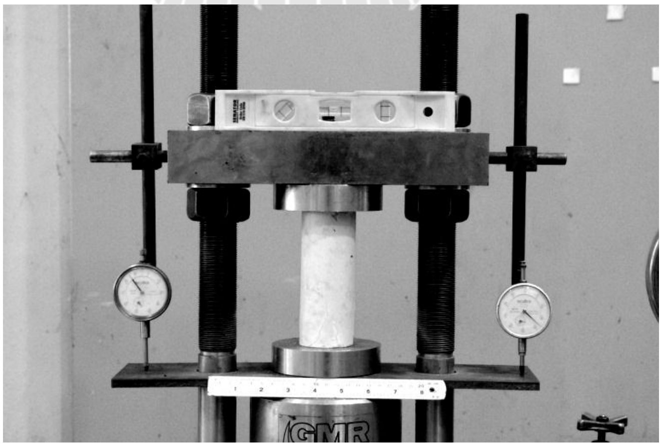

(c)

Figure 5.4 Uniaxial compressive strength test with constant loading rate. The cylindrical specimen is loaded vertically using the compression machine, (a) cement, (b) sludge-mixed cement, and (c) bentonite-mixed cement.

(a)

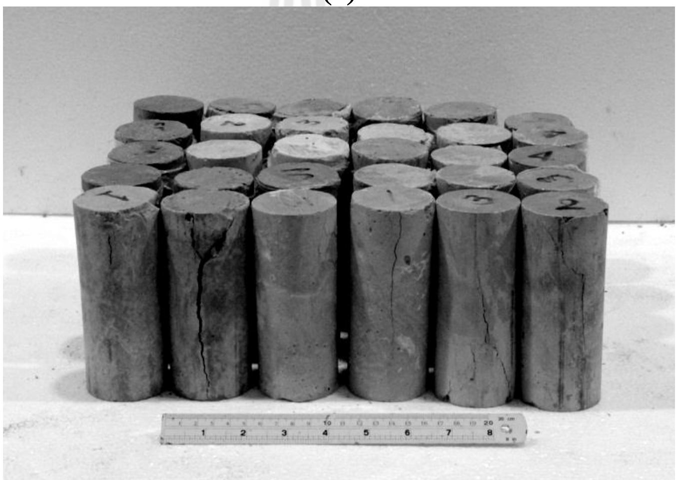

(b)

Figure 5.5 Specimens (a) sludge-mixed cement, and (b) bentonite-mixed cement after failure under loading with constant stress rate of 1 MPa/s.

Figure 5.6 PVC mold has an inner diameter of 101.6 mm with 203.2 mm in length.

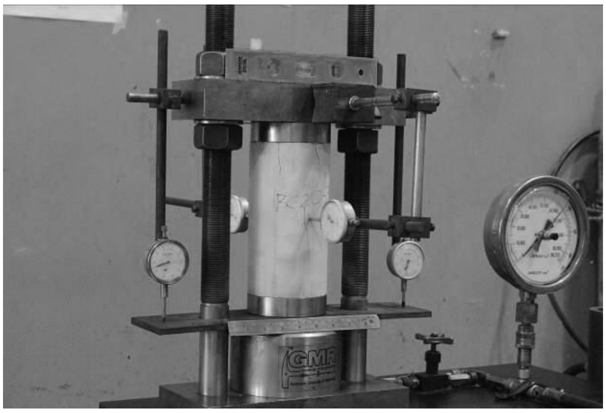

(a)

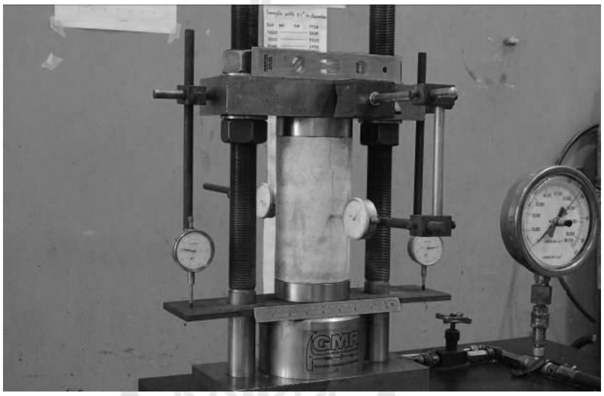

(b)

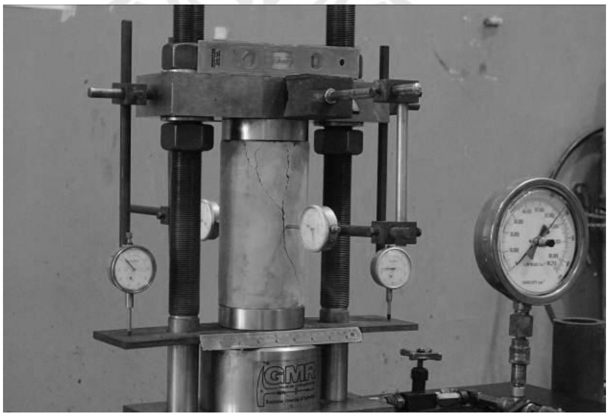

(c)

Figure 5.7 Uniaxial compressive strength test with constant loading rate. The cylindrical specimen is loaded vertically using the compression machine, (a) B:C = 2:10, (b) C:W = 1:1, and (c) S:C = 3:10.

(a)

(b)

(c)

Figure 5.8 Specimens of 101.6 mm diameter (a) sludge-mixed cement, and (b) bentonite-mixed cement after failure under loading with constant stress rate of 1 MPa/s.

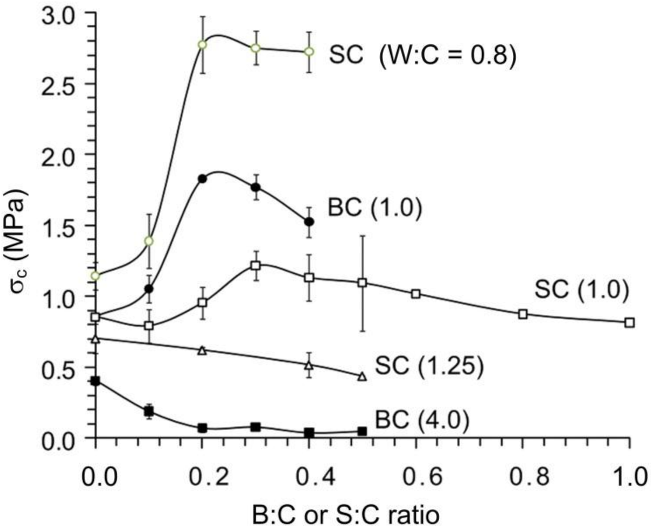

Figure 5.9 Uniaxial compressive strengths for B:C and S:C mixtures with W:C = 10:10, 8:10, 12.5:10, 40:10 at 3 days of curing.

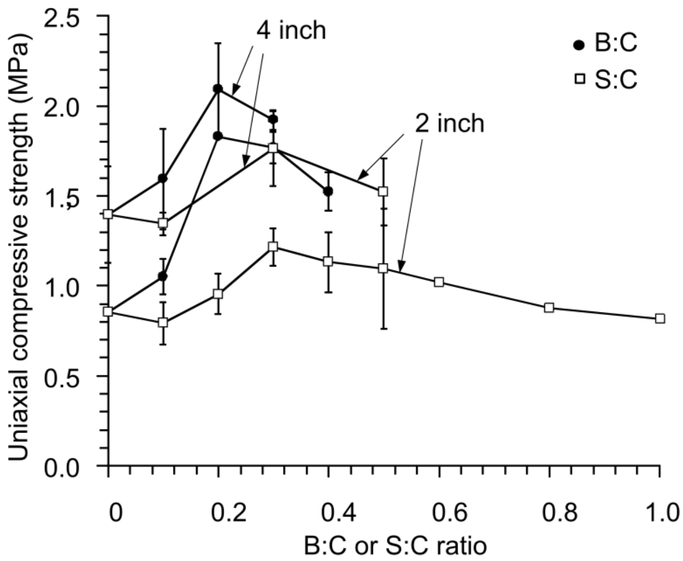

Figure 5.10 Uniaxial compressive strengths for B:C and S:C with W:C = 1:1.

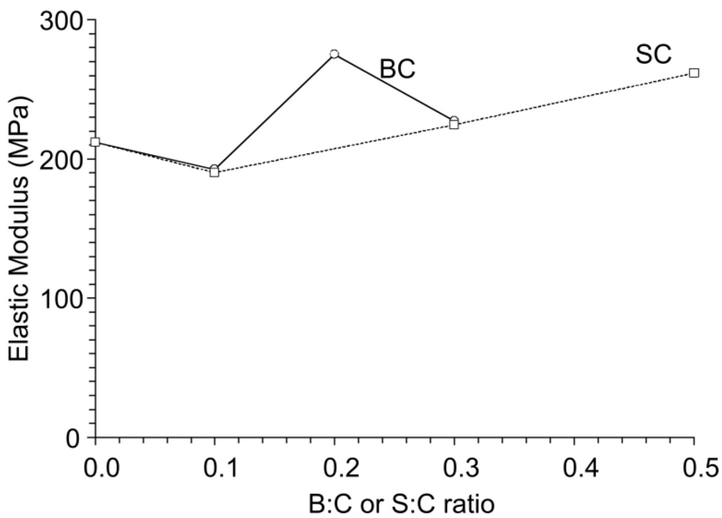

Figure 5.11 Comparisons of elastic modulus between B:C and S:C mixtures.

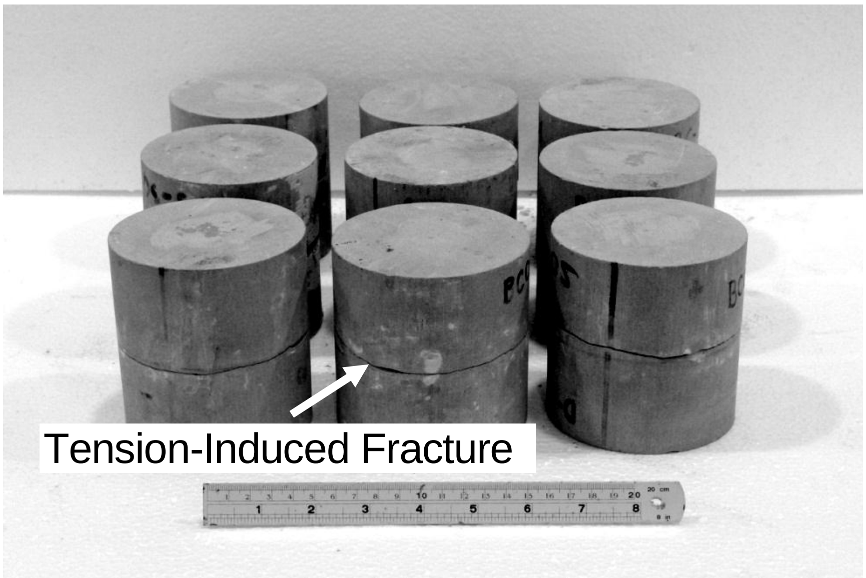

Figure 5.12 Some sandstone specimens of 101.6 mm diameter prepared for direct shear testing.

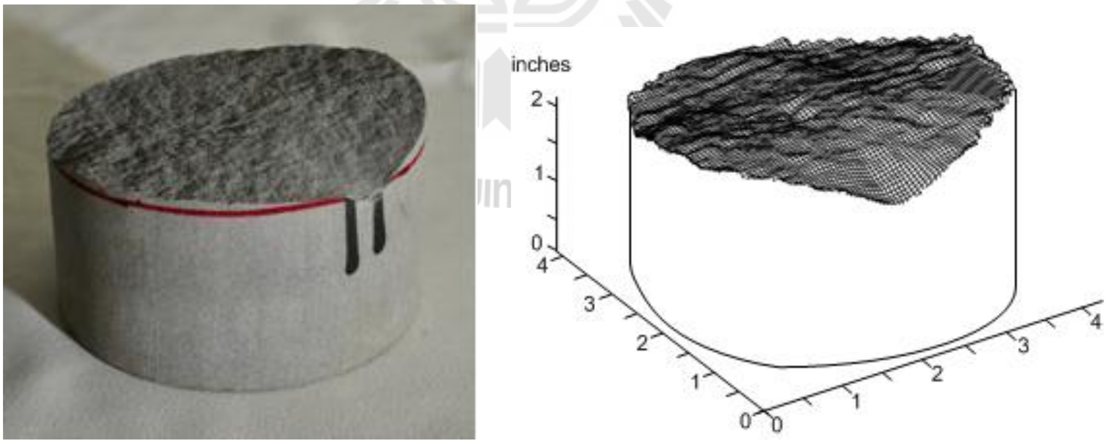

Figure 5.13 Surface sandstone specimen prepared for direct shear testing (left) and surface sandstone model of laser scan (right).

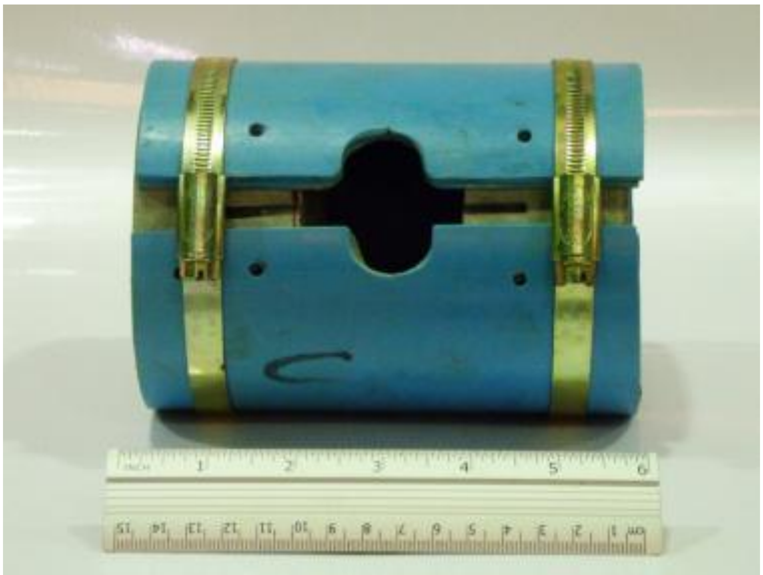

Figure 5.14 PVC mold has an inner diameter of 101.6 mm for direct shear testing.

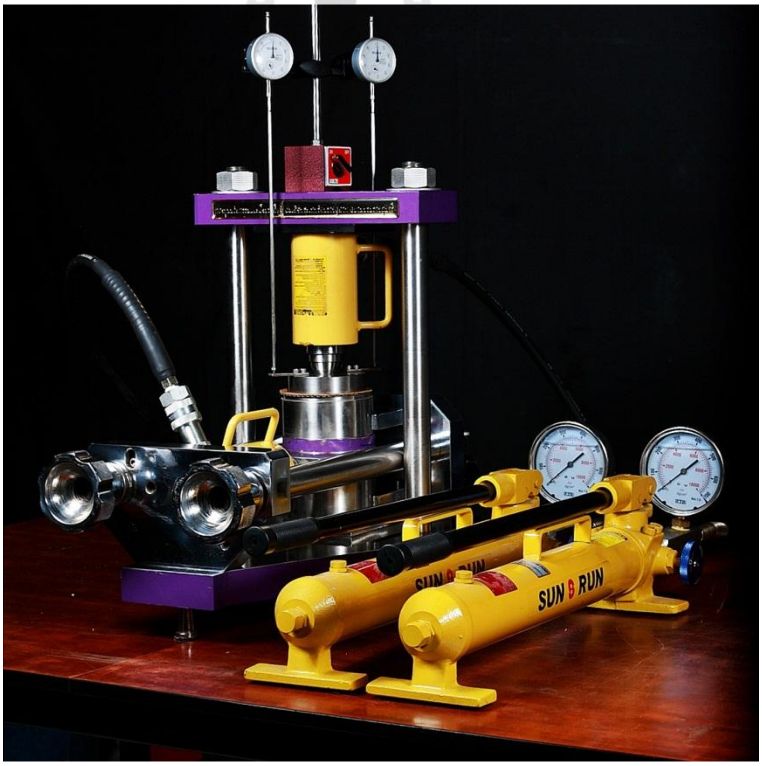

Figure 5.15 Laboratory arrangements for three-ring direct shear test.

Figure 5.16 Some specimens of grouting material in sandstone fracture after failure under shearing between grout and fracture.

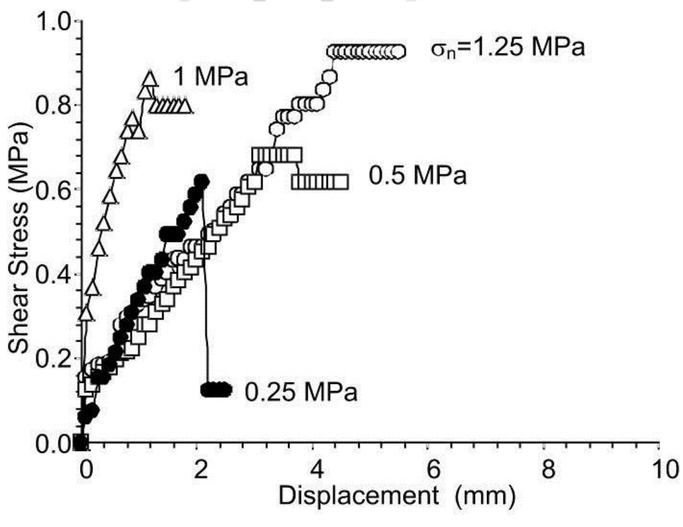

Figure 5.17 Shearing resistance between cement grout and fracture with W:C=1:1.

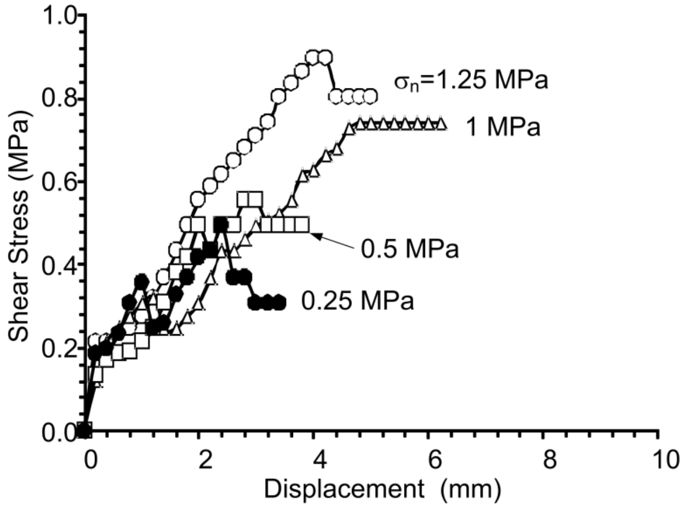

Figure 5.18 Shearing resistance between S:C=1:10 mixture grout and fracture with W:C=1:1.

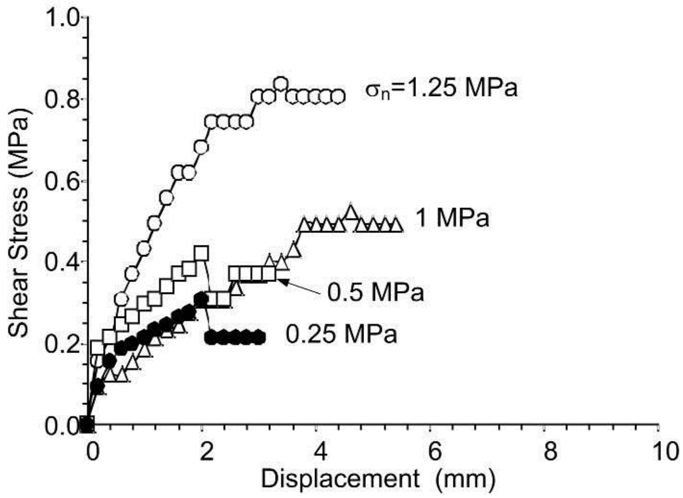

Figure 5.19 Shearing resistance between S:C=3:10 mixture grout and fracture with W:C=1:1.

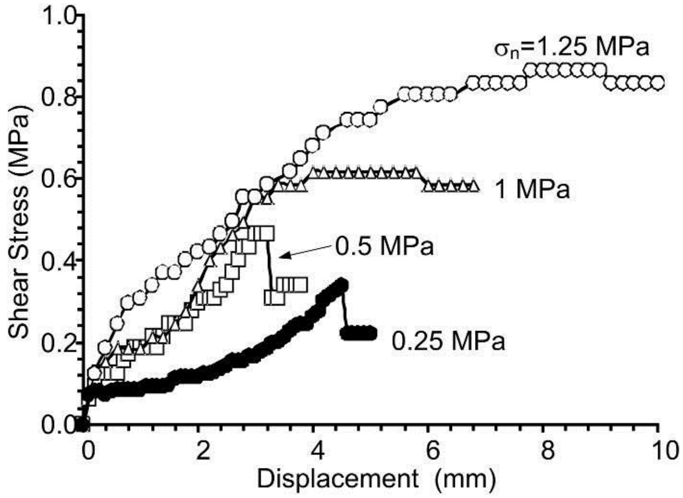

Figure 5.20 Shearing resistance between S:C=5:10 mixture grout and fracture with W:C=1:1.

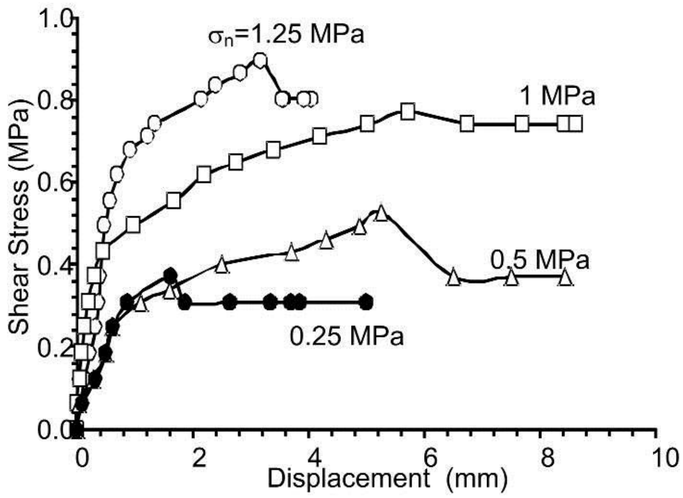

Figure 5.21 Shearing resistance between B:C=1:10 mixture grout and fracture with W:C=1:1.

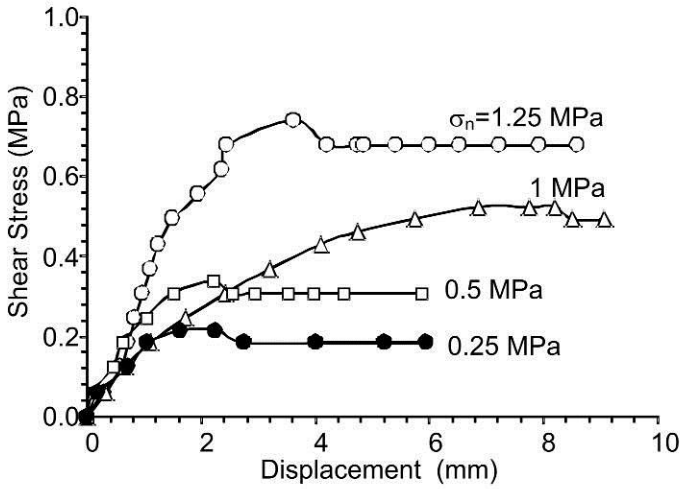

Figure 5.22 Shearing resistance between B:C=2:10 mixture grout and fracture with W:C=1:1.

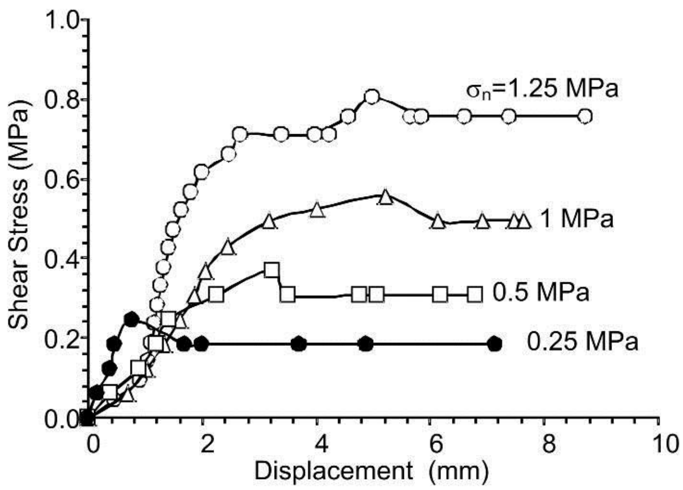

Figure 5.23 Shearing resistance between B:C=3:10 mixture grout and fracture with W:C=1:1.

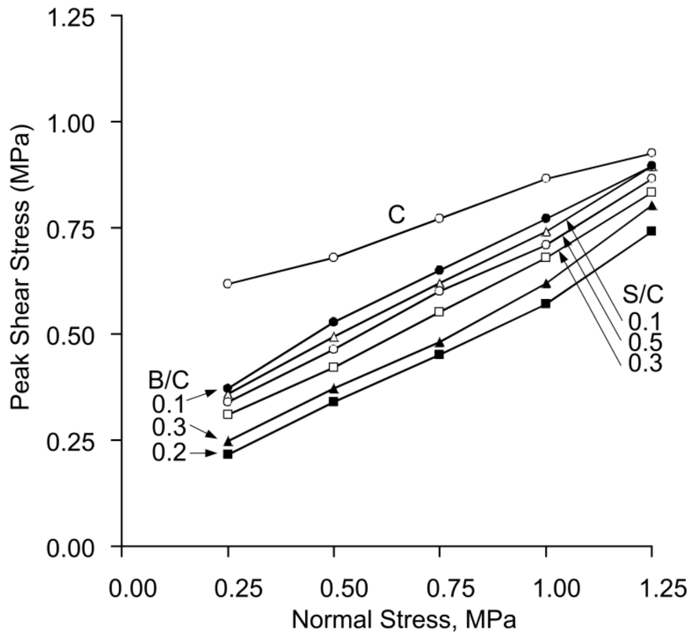

Figure 5.24 Normal stress and peak shear stress.

CHAPTER VI

HYDRAULIC PROPERTIES TESTING

6.1 Introduction

This chapter describes the methods and results of laboratory tests to determinate the permeability of grouting materials in artificial fractures from Phu Kradung sandstone. The permeability of the mixture is an important factor to show the hydraulic potential, otherwise the ability to reduce permeability of fractures in sandstone. Hydraulic properties testing in this chapter is divided into three tasks: 1) grout permeability tests 2) fracture permeability tests, and 3) permeability test of grouting materials in rock fractures. The rock samples are prepared as described in Chapter III.

6.2 Permeability of grouting materials

The objective of the grout permeability tests is to determine the water permeability of grouting material specimen using constant head flow tests. The permeability of grouting material is the a factor to be used to determinate the most suitable mixing ratios for grouting in rock. These tasks describe method for grout permeability testing in the laboratory. Proportions of S:C mixtures are 0:10, 3:10, 5:10 and B:C mixtures are 1:10, 2:10, 3:10 with W:C ratio of 10:10 by weight. Results of both mixtures are compared.

6.2.1 Test methods

The procedure for determining the grout permeability is similar to the ASTM C938 and C39 (ASTM 2010a, 2010c). Proportions of S:C mixtures are 0:10, 3:10, 5:10 and B:C mixtures are 1:10, 2:10, 3:10 with W:C ratio of 10:10 by weight. These tests are conducted at 3, 7, 14 and 28 days of curing. The mold has an inner diameter of 101.6 mm with a length of 152.4 mm. The prepared specimen is sealed between two acrylic platens with the aid of O-ring rubber and epoxy coating (Figures 6.1 and 6.2). Inlet ports is installed at the end of the mold and connected to a water pressure tube. Nitrogen compressed pressure gas about 13.8 kPa. Air bubbles are bled out before measuring the permeability. Outlet ports is installed at another end and connected to a high precision pipette for measuring the outflow (Figures 6.3 and 6.4). The intrinsic permeability (k) is calculated from the flow rate based on the Darcy's law (Freeze and Cherry, 1979; Indraratna and Ranjith 2001).

6.2.2 Test results

The results of comparison of S:C mixtures, B:C mixtures, and C are presented on Figure 6.5. Table 6.1 summarizes the results of permeability testing of grouting material results at 3, 7, 14 and 28 days of curing.

6.3 Permeability of rock fractures

The objective of this task is to assess the permeability of rock fractures under varying normal stresses. The fracture permeability is used to compare with the permeability of grouting materials for both sludge and bentonte mixtures. Constant head flow tests are performed. The normal stresses are different. Five specimens are prepared and tested. The rock samples in 152.4×152.4×152.4 mm^3 prismatic blocks are prepared as described in Chapter III (Figures 6.6 and 6.7).

6.3.1 Test methods

The constant head flow tests are performed. The normal stresses are ranging from 1, 2, 3 and 4 MPa. Five specimens are prepared and tested. The injection hole at the center of the upper block is 12 mm in diameter and 101.6 mm in depth. The tests are conducted by injecting water. Injecting water conducted the tests into the center hole of the rectangular block specimen. The laboratory arrangement of the constant head flow test is shown in Figure 6.8. Water volume and time are recorded that tend to decrease exponentially with the normal stress. The permeability results (k) are plotted as a function of the normal stress (σ_n) in Figure 8. The equivalent hydraulic aperture (e_h) for radial flow, hydraulic conductivity between smooth and parallel plates (K), and intrinsic permeability (k) are calculated by (Tsang, 1992; Indraratna and Ranjith, 2001) :

$$e_h = \{[(6\mu q)/ (\pi\Delta P)] \ln (r/r_0)\}^{1/3} \quad (4.7)$$

$$K = \gamma_w e_h^2/12\mu \quad (4.8)$$

$$k = e_h^2/12 \quad (4.9)$$

where μ is the dynamic viscosity of the water ($N{\cdot}s/cm^2$), q is water flow rate through the specimen (cm^2/s), ΔP is injecting water pressure into the center hole of rectangular blocks of the specimen, r is radius of flow path (m), r_0 is radius of the radius injection hole (m). γ_w is unit weight of water (N/m^2).

6.3.2 Test results

Table 6.2 lists the result of permeability of rock fractures under normal stresses ranging from 1, 2, 3 and 4 MPa. Figure 6.9 is shown relationship of intrinsic permeability (k), hydraulic conductivity (K), and aperture (e_h) as a function of normal stress (σ_n) for fracture in Phu Kradung sandstone. The results show that the intrinsic permeability of the fractures is less than 1.4×10^{-9} m^2.

6.4 Permeability of grouting materials in rock fractures

The objective of permeability test of grouting materials in rock fractures is to determine the permeability of sludge-mixed cement and bentonite-mixed cement in artificial fractures from Phu Kradung sandstone. Six mixture proportions of S:C and B:C selected and prepared are similar Chapter IV. The grouting materials are used to fill the fractures. The constant normal stresses are 0.25, 0.5, 1.0 and 1.25 MPa.

6.4.1 Test methods

The testing method is similar to that described above this task. The grouting materials are injected into the fractures. The fractrue apertures are 2, 10, and 20 mm. The grouting materials are cured for 3 days. Figures 6.10 to 6.11 give the laboratory arrangement. Constant head flow tests is performed. The constant head is ranging between 13.8 and 551.7 kPa. The constant normal stresses are 0.25, 0.5, 1.0 and 1.25 MPa. The results show that the normal stress can reduce the permeability of grouting materials in fractured sandstone. The intrinsic permeability (k) is calculated from the measured flow rate (Q) as follows: (Indraratna and Ranjith, 2001)

$$K = Q \ln(2mL/D)/2\pi LH_c \tag{4.10}$$

$$k = K\mu/\gamma_w \tag{4.11}$$

where K is hydraulic conductivity, Q is flow rate of water flow through the mixture, m is square root of the ratio between the conductivity perpendicular and parallel to the hole (here, m is equal to 1), L is the thickness of grouting material in fracture apertures, D is diameter of the injection hole at the center of the upper block, H_c is the constant head used for the test, μ is dynamic viscosity (891×10^{-6} kg/(m·s)) at temperature of 25°C, γ_w is unit weight of water (997.13 kg/m^3).

6.4.2 Test results

The results of permeability of grouting material in rock fractures aperture 2, 10, and 20 mm are summarized in Tables 6.3 – 6.5. Intrinsic permeability (k), hydraulic conductivity (K), and aperture (e_h) as a function of normal stress (σ_n) for fracture aperture 2, 10, and 20 mm are shown in Figures 6.12 – 6.14.

Table 6.1 Summary of permeability testing of grouting material results at 3, 7, 14 and 28 days of curing.

Curing Time (days)	**Intrinsic Permeability (×10^{-18} m^2)**						
	Pure cement	**S:C = 1:10**	**S:C = 3:10**	**S:C = 5:10**	**B:C = 1:10**	**B:C = 2:10**	**B:C = 3:10**
3	8,930.0	8,250.0	2,930.0	2,210.0	2,370.0	868.0	317.0
7	965.0	3,720.0	643.0	349.0	431.0	265.0	67.6
14	74.1	681.0	115.0	11.6	414.0	228.0	49.0
28	0.441	249.0	62.0	6.8	356.0	208.0	41.3

Table 6.2 Summary of permeability of rock fractures results.

Sample No.	Normal stress (MPa)	K (10^{-3} m/s)	k (10^{-9} m^2)	e_h (μm)
1	1	0.111±0.02	0.099±0.02	34.44±2.53
	2	0.090±0.02	0.080±0.02	30.81±3.91
	3	0.074±0.02	0.074±0.02	27.92±4.12
	4	0.062±0.02	0.062±0.02	25.42±4.36
2	1	0.637±0.02	0.569±0.01	82.64±1.05
	2	0.509±0.05	0.455±0.05	73.82±3.59
	3	0.412±0.01	0.369±0.00	66.50±0.36
	4	0.304±0.00	0.271±0.00	57.06±0.05
3	1	1.167±0.52	1.043±0.47	109.54±25.34
	2	0.914±0.39	0.817±0.35	97.03±21.90
	3	0.733±0.30	0.655±0.26	87.04±18.66
	4	0.607±0.28	0.543±0.25	78.90±18.89
4	1	1.571±0.46	1.403±0.41	128.55±19.88
	2	1.141±0.23	1.019±0.20	110.16±11.03
	3	0.899±0.47	0.803±0.42	95.60±25.01
	4	0.662±0.27	0.592±0.24	82.86±17.06
5	1	0.791±0.11	0.706±0.01	91.90±6.33
	2	0.602±0.14	0.538±0.13	79.91±9.27
	3	0.513±0.08	0.485±0.07	74.00±5.68
	4	0.397±0.05	0.355±0.04	65.20±3.63

Table 6.3 Summary of permeability of grouting material in rock fractures aperture 2 mm.

Binder	Normal stress (MPa)	K (10^{-9} m/s)	k (10^{-15} m^2)	e_h (μm)
C	0.25	11.94±0.48	1.07±0.04	1.24±0.02
	0.50	9.06±0.52	0.81±0.05	1.08±0.03
	0.75	7.06±0.53	0.63±0.05	0.95±0.04
	1.00	5.44±0.39	0.49±0.04	0.84±0.03
	1.25	4.05±0.36	0.36±0.03	0.72±0.03
S:C =1:10	0.25	39.02±5.17	3.49±0.46	2.24±0.15
	0.50	28.98±2.71	2.59±0.24	1.93±0.09
	0.75	22.48±2.51	2.01±0.22	1.70±0.09
	1.00	16.99±1.04	1.52±0.09	1.48±0.05
	1.25	12.60±1.28	1.13±0.11	1.27±0.06
S:C =3:10	0.25	64.44±8.61	5.76±0.77	2.88±0.19
	0.50	45.66±3.64	4.08±0.32	2.42±0.10
	0.75	34.37±1.85	3.07±0.17	2.10±0.06
	1.00	26.05±2.67	2.33±0.24	1.83±0.09
	1.25	19.51±1.55	1.74±0.14	1.58±0.06
S:C =5:10	0.25	16.70±0.90	1.49±0.08	1.47±0.04
	0.50	12.28±0.43	1.10±0.04	1.26±0.02
	0.75	8.70±0.66	0.78±0.06	1.06±0.04
	1.00	6.84±0.90	0.61±0.08	0.94±0.06
	1.25	4.97±0.18	0.44±0.02	0.80±0.01

Table 6.3 Summary of permeability of grouting material in rock fractures aperture 2 mm (continued).

Binder	Normal stress (MPa)	K (10^{-9} m/s)	k (10^{-15} m^2)	e_h (μm)
B:C =1:10	0.25	191.03±23.65	17.07±2.11	4.95±0.30
	0.50	129.69±7.87	11.59±0.70	4.08±0.12
	0.75	88.27±15.57	7.89±1.39	3.36±0.31
	1.00	62.70±4.33	5.60±0.39	2.84±0.10
	1.25	44.08±10.42	3.94±0.93	2.37±0.29
B:C =2:10	0.25	277.04±38.01	24.75±3.40	5.96±0.41
	0.50	191.30±26.97	17.09±2.41	4.95±0.36
	0.75	128.01±15.11	11.44±1.35	4.05±0.24
	1.00	83.42±9.32	7.45±0.83	3.27±0.19
	1.25	51.78±3.82	4.63±0.34	2.58±0.10
B:C =3:10	0.25	141.51±10.42	12.65±0.93	4.27±0.16
	0.50	103.12±11.08	9.21±0.99	3.64±0.20
	0.75	72.68±9.42	6.49±0.84	3.05±0.20
	1.00	52.59±4.72	4.70±0.42	2.60±0.12
	1.25	36.70±2.06	3.28±0.18	2.17±0.06

Table 6.4 Summary of permeability of grouting material in rock fractures aperture 10 mm.

Binder	Normal stress (MPa)	K (10^{-9} m/s)	k (10^{-15} m^2)	e_h (μm)
C	0.25	38.94±1.75	3.48±0.16	2.24±0.05
	0.50	25.08±0.97	2.24±0.09	1.80±0.03
	0.75	16.89±1.61	1.51±0.14	1.47±0.07
	1.00	10.69±1.28	0.95±0.11	1.17±0.07
	1.25	6.79±0.89	0.61±0.08	0.93±0.06
S:C =1:10	0.25	29.45±0.38	2.63±0.03	1.95±0.01
	0.50	19.43±0.75	1.74±0.07	1.58±0.03
	0.75	13.21±1.03	1.18±0.09	1.30±0.05
	1.00	8.87±0.65	0.79±0.06	1.07±0.04
	1.25	5.98±0.49	0.53±0.04	0.88±0.04
S:C =3:10	0.25	3.83±0.46	0.34±0.04	0.70±0.04
	0.50	2.77±0.24	0.25±0.02	0.60±0.03
	0.75	1.89±0.25	0.17±0.02	0.49±0.03
	1.00	1.19±0.09	0.11±0.01	0.39±0.01
	1.25	0.81±0.09	0.07±0.01	0.32±0.02
S:C =5:10	0.25	25.37±0.73	2.27±0.06	1.81±0.03
	0.50	16.81±0.57	1.50±0.05	1.47±0.03
	0.75	10.82±0.45	0.97±0.04	1.18±0.02
	1.00	7.68±0.52	0.69±0.05	0.99±0.03
	1.25	5.24±0.32	0.47±0.03	0.82±0.03

Table 6.4 Summary of permeability of grouting material in rock fractures aperture 10 mm (continued).

Binder	Normal stress (MPa)	K (10^{-9} m/s)	k (10^{-15} m^2)	e_h (μm)
B:C =1:10	0.25	2.12±0.10	0.19±0.01	0.52±0.01
	0.50	1.46±0.04	0.13±0.00	0.43±0.01
	0.75	1.01±0.04	0.09±0.00	0.36±0.01
	1.00	0.69±0.02	0.06±0.00	0.30±0.00
	1.25	0.48±0.01	0.04±0.00	0.25±0.00
B:C =2:10	0.25	9.78±0.27	0.87±0.02	1.12±0.02
	0.50	6.34±0.45	0.57±0.04	0.90±0.03
	0.75	4.31±0.34	0.38±0.03	0.74±0.03
	1.00	2.90±0.14	0.26±0.01	0.61±0.01
	1.25	2.10±0.06	0.19±0.00	0.52±0.01
B:C =3:10	0.25	18.93±0.84	1.69±0.08	1.56±0.03
	0.50	12.69±0.59	1.13±0.05	1.28±0.03
	0.75	8.60±0.14	0.77±0.01	1.05±0.01
	1.00	5.88±0.57	0.53±0.05	0.87±0.04
	1.25	3.91±0.25	0.35±0.02	0.71±0.02

Table 6.5 Summary of permeability of grouting material in rock fractures aperture 20 mm.

Binder	Normal stress (MPa)	K (10^{-9} m/s)	k (10^{-15} m^2)	e_h (μm)
C	0.25	148.68±28.60	13.29±2.56	4.36±0.43
	0.50	90.45±14.07	8.08±1.26	3.40±0.26
	0.75	57.10±9.01	5.10±0.81	2.71±0.21
	1.00	33.09±6.42	2.96±0.57	2.06±0.20
	1.25	20.75±2.34	1.85±0.21	1.63±0.09
S:C =1:10	0.25	108.50±18.42	9.70±1.65	3.73±0.32
	0.50	60.90±5.01	5.44±0.45	2.80±0.11
	0.75	40.20±4.65	3.59±0.42	2.27±0.13
	1.00	23.97±0.72	2.14±0.06	1.76±0.03
	1.25	15.22±1.39	1.36±0.12	1.40±0.06
S:C =3:10	0.25	39.28±1.37	3.51±0.12	2.25±0.04
	0.50	24.16±1.64	2.16±0.15	1.76±0.06
	0.75	16.61±1.02	1.48±0.09	1.46±0.04
	1.00	12.04±1.13	1.08±0.10	1.24±0.06
	1.25	9.00±0.85	0.80±0.08	1.08±0.05
S:C =5:10	0.25	16.60±2.60	1.48±0.23	1.46±0.12
	0.50	11.30±1.65	1.01±0.15	1.20±0.09
	0.75	8.15±1.14	0.73±0.10	1.02±0.07
	1.00	6.50±0.49	0.58±0.04	0.91±0.03
	1.25	4.87±0.04	0.44±0.00	0.79±0.00

Table 6.5 Summary of permeability of grouting material in rock fractures aperture 20 mm (continued).

Binder	Normal stress (MPa)	K (10^{-9} m/s)	k (10^{-15} m^2)	e_h (μm)
B:C =1:10	0.25	9.42±1.18	0.84±0.11	1.10±0.07
	0.50	6.95±0.60	0.62±0.05	0.94±0.04
	0.75	5.33±0.51	0.48±0.05	0.83±0.04
	1.00	4.04±0.38	0.36±0.03	0.72±0.03
	1.25	3.24±0.38	0.29±0.03	0.64±0.04
B:C =2:10	0.25	73.26±11.81	6.55±1.06	3.06±0.25
	0.50	42.97±8.21	3.84±0.73	2.34±0.22
	0.75	28.37±8.14	2.54±0.73	1.90±0.28
	1.00	17.73±2.51	1.58±0.22	1.51±0.11
	1.25	12.34±0.55	1.10±0.05	1.26±0.03
B:C =3:10	0.25	7.05±0.60	0.63±0.05	0.95±0.04
	0.50	4.94±0.31	0.44±0.03	0.80±0.03
	0.75	3.85±0.58	0.34±0.05	0.70±0.05
	1.00	3.10±0.48	0.28±0.04	0.63±0.05
	1.25	2.43±0.23	0.22±0.02	0.56±0.03

Figure 6.1 PVC mold has an inner diameter of 101.6 mm for permeability testing of grouting materials.

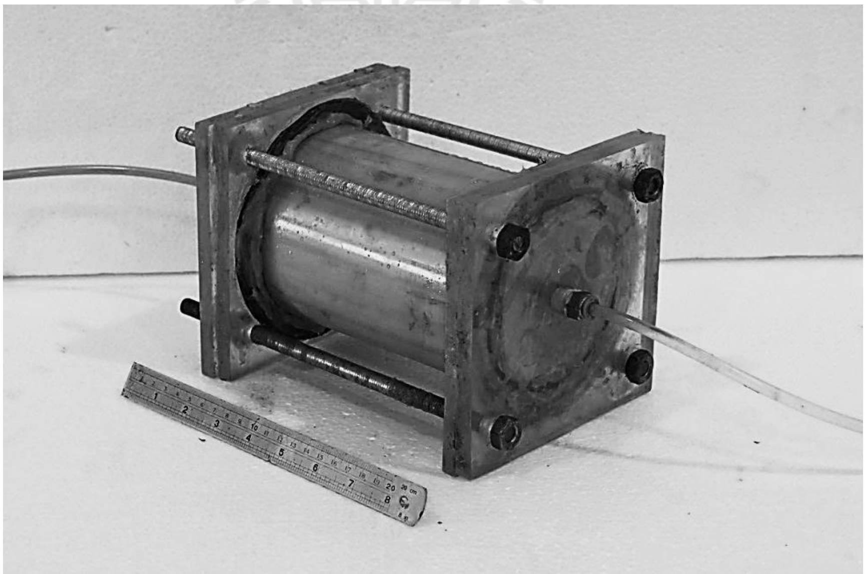

Figure 6.2 PVC mold has sealed between two acrylic platens with the aid of O-ring rubber and epoxy coating for permeability testing of grouting materials.

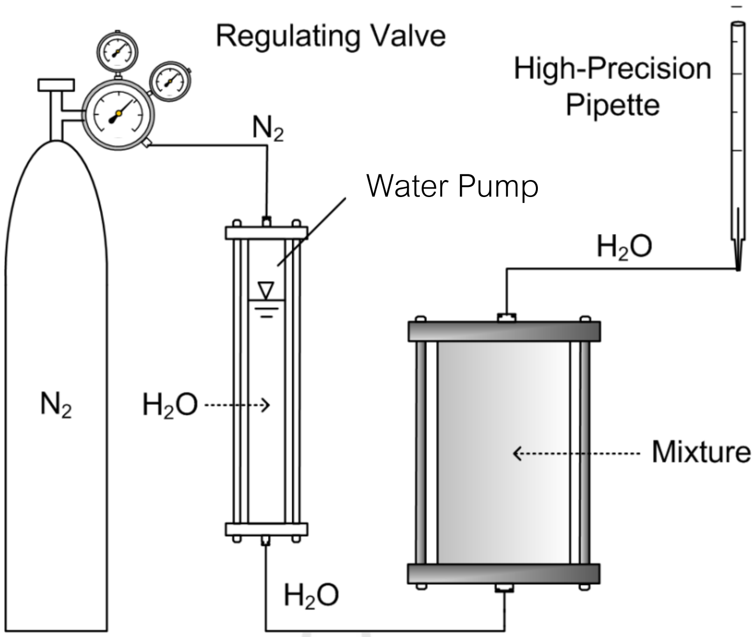

Figure 6.3 Diagram of laboratory arrangement for permeability testing of grouting materials.

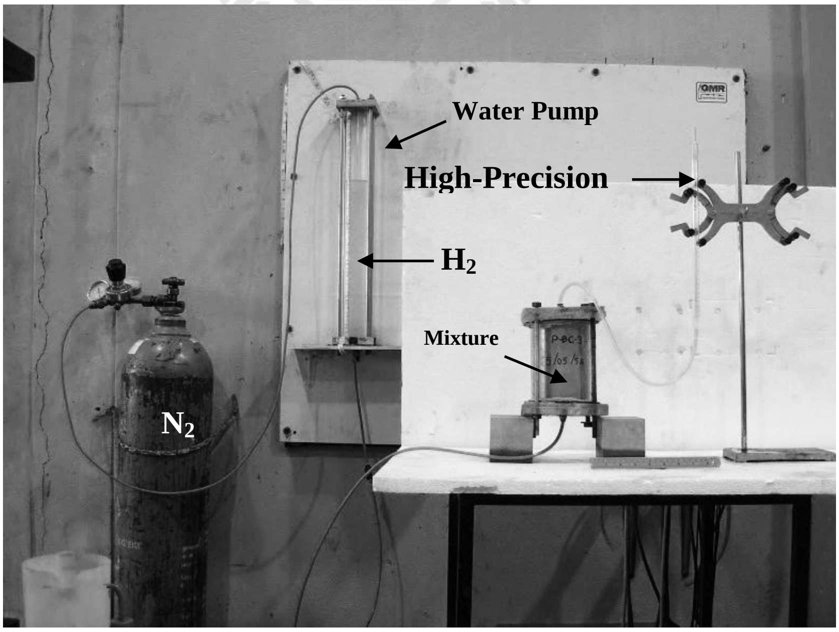

Figure 6.4 Laboratory arrangements for permeability testing of grouting materials.

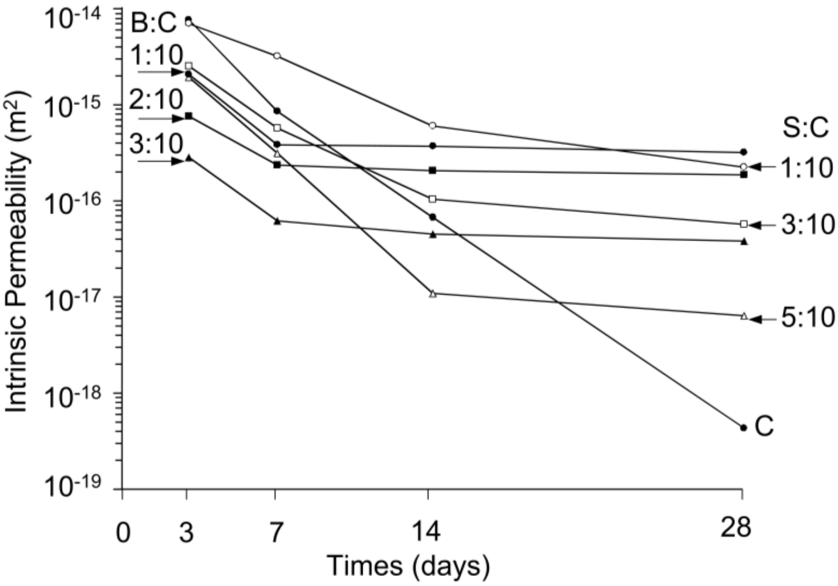

Figure 6.5 Intrinsic permeability as a function of time for pure cement (C), B:C, and S:C with W:C = 1:1.

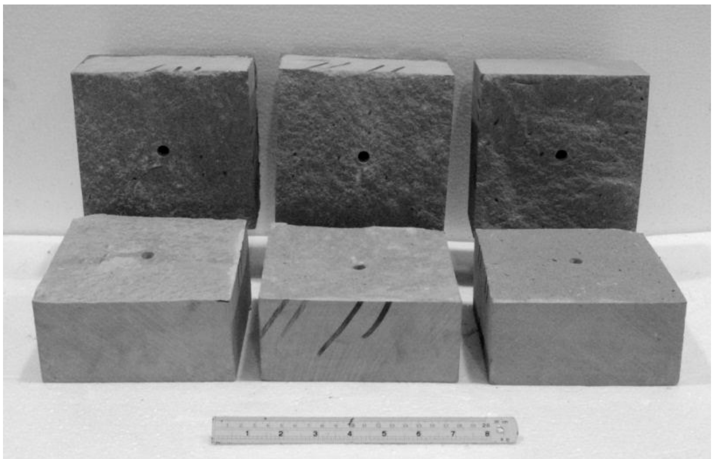

Figure 6.6 Some sandstone specimens of 152.4 × 152.4 × 152.4 mm prepared for permeability testing of rock fractures.

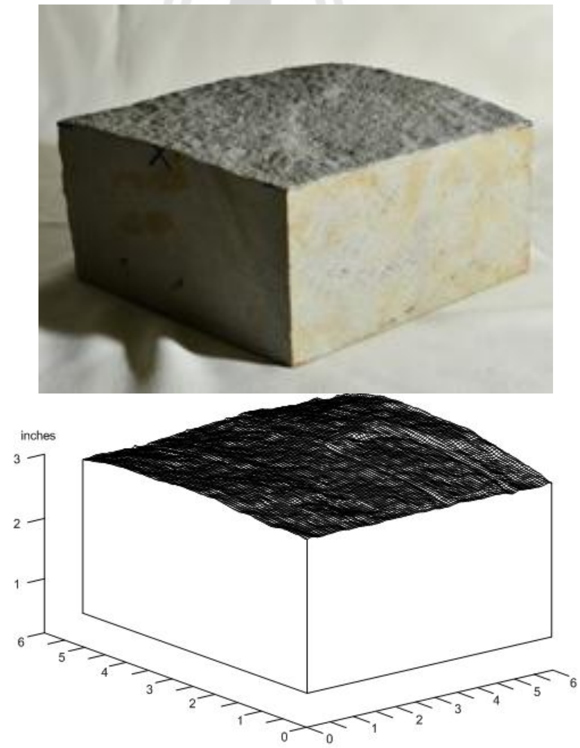

Figure 6.7 Fracture surface in sandstone specimen prepared for permeability testing of rock fractures (left) and surface sandstone model from laser scan (right).

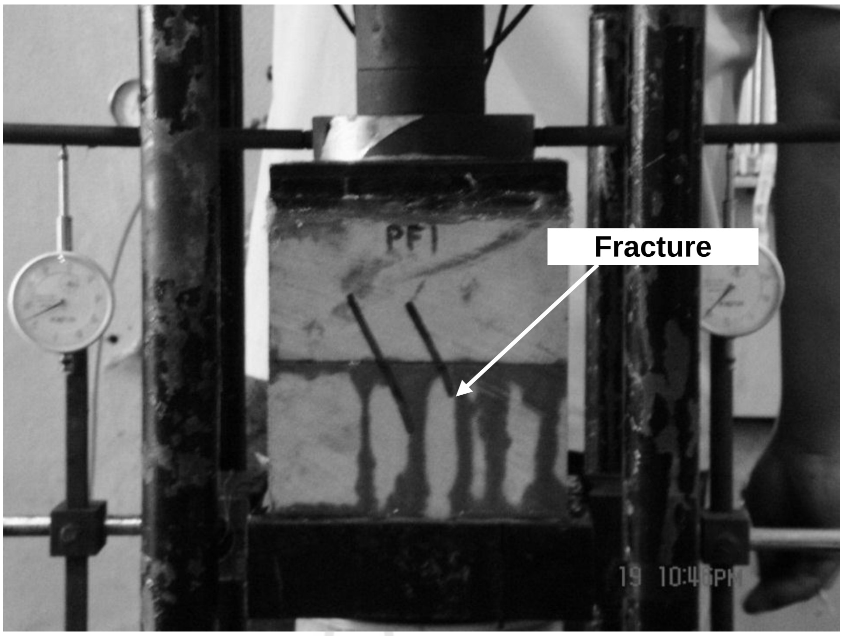

Figure 6.8 Laboratory arrangement for permeability testing of fractures.

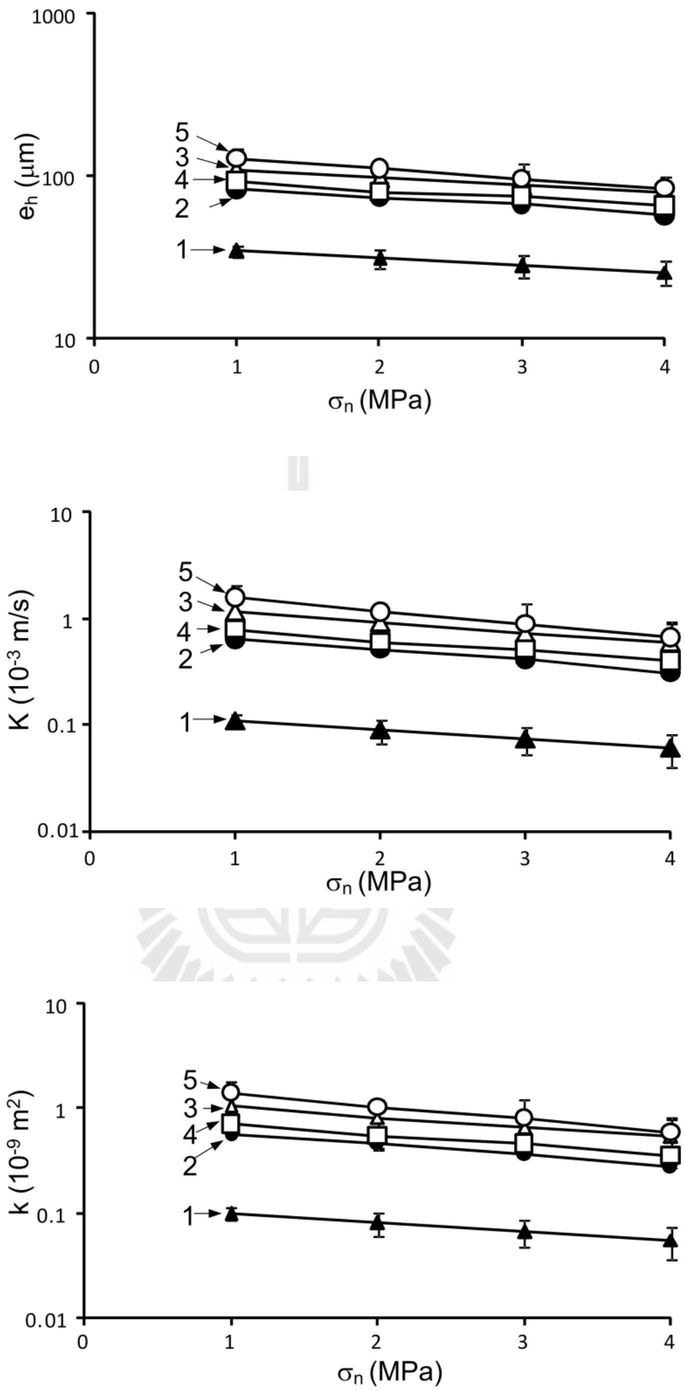

Figure 6.9 Intrinsic permeability (k), hydraulic conductivity (K), and aperture (e_h) as a function of normal stress (σ_n) for fracture in Phu Kradung sandstone.

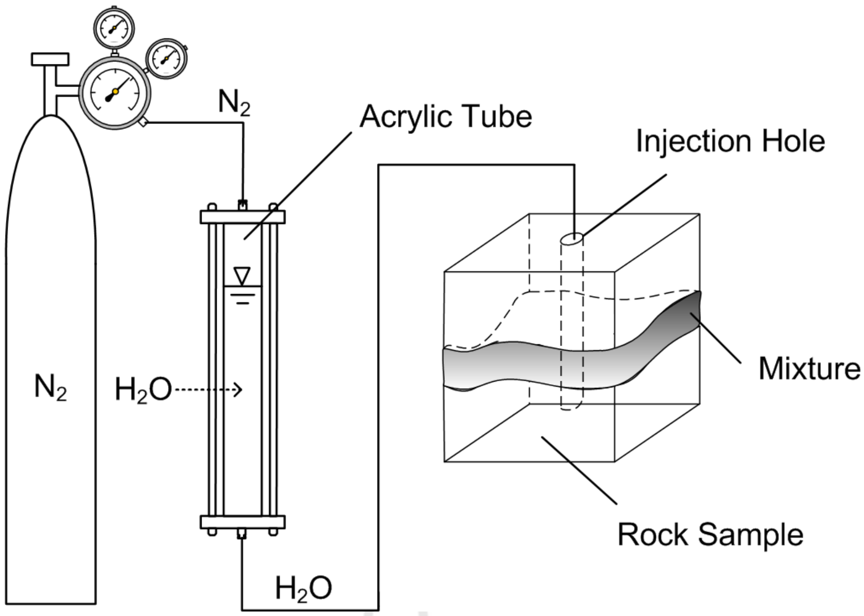

Figure 6.10 Diagram of laboratory arrangement for permeability testing of grouting materials in rock fracture.

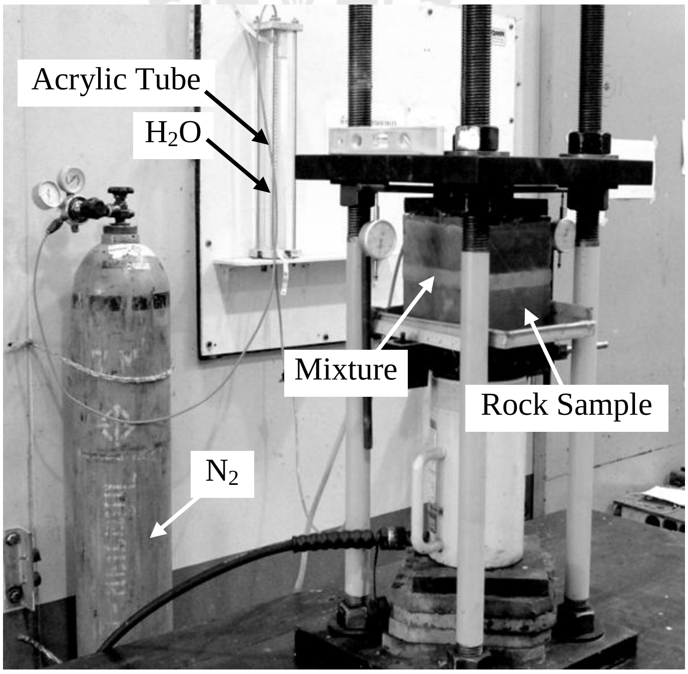

Figure 6.11 Permeability testing of grouting materials in rock fracture.

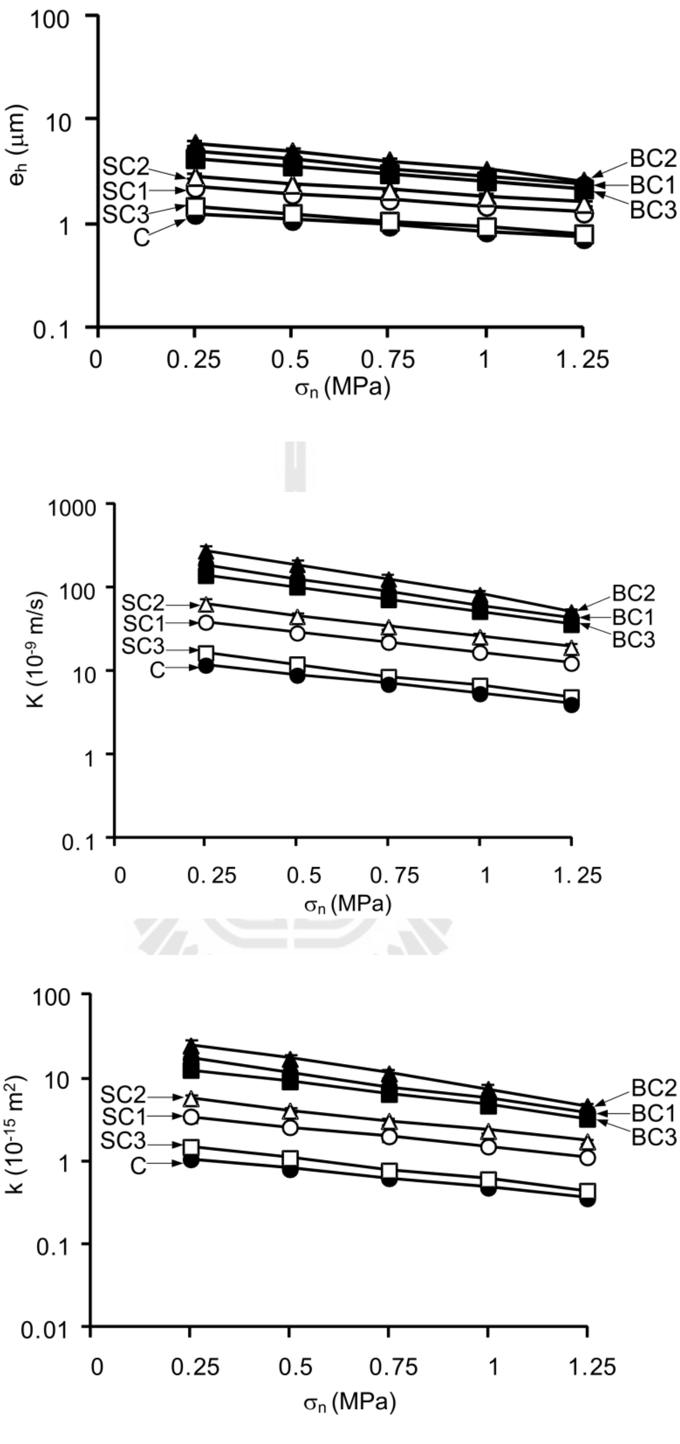

Figure 6.12 Intrinsic permeability (k), hydraulic conductivity (K), and aperture (e_h) as a function of normal stress (σ_n) for fracture aperture 2 mm.

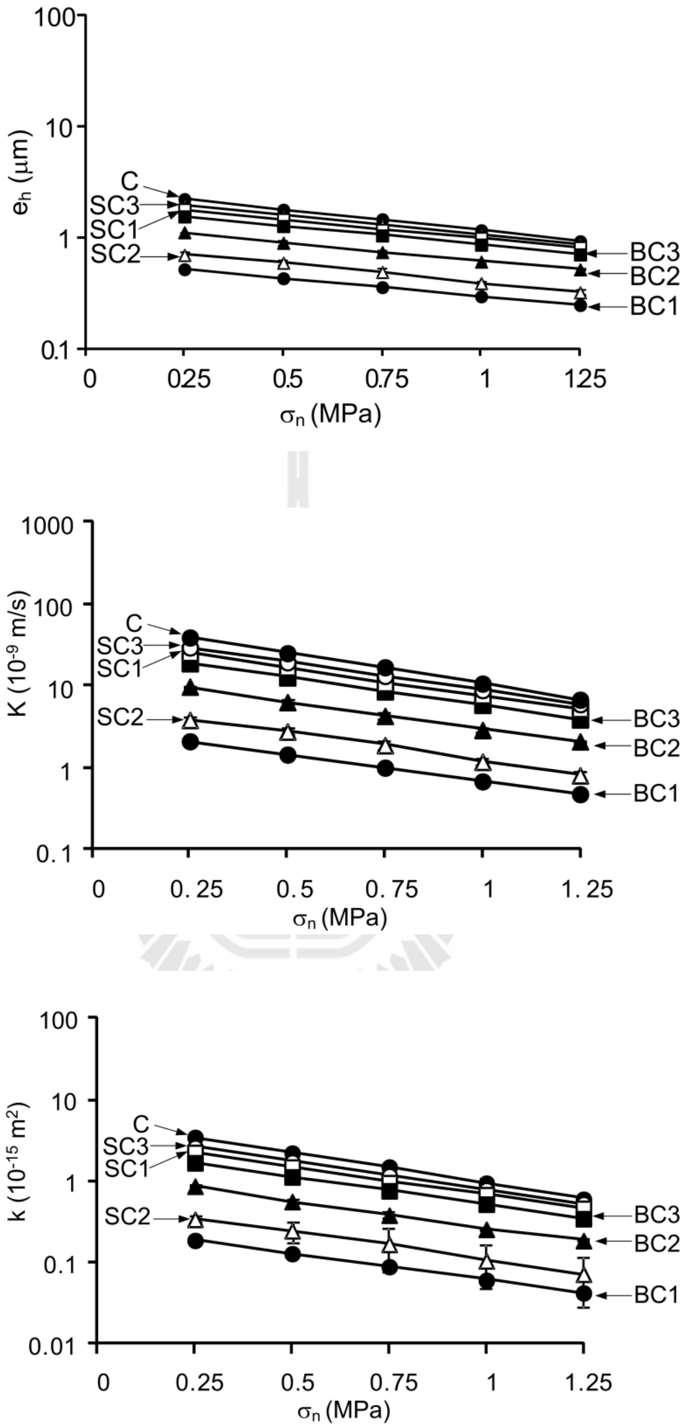

Figure 6.13 Intrinsic permeability (k), hydraulic conductivity (K), and aperture (e_h) as a function of normal stress (σ_n) for fracture aperture 10 mm.

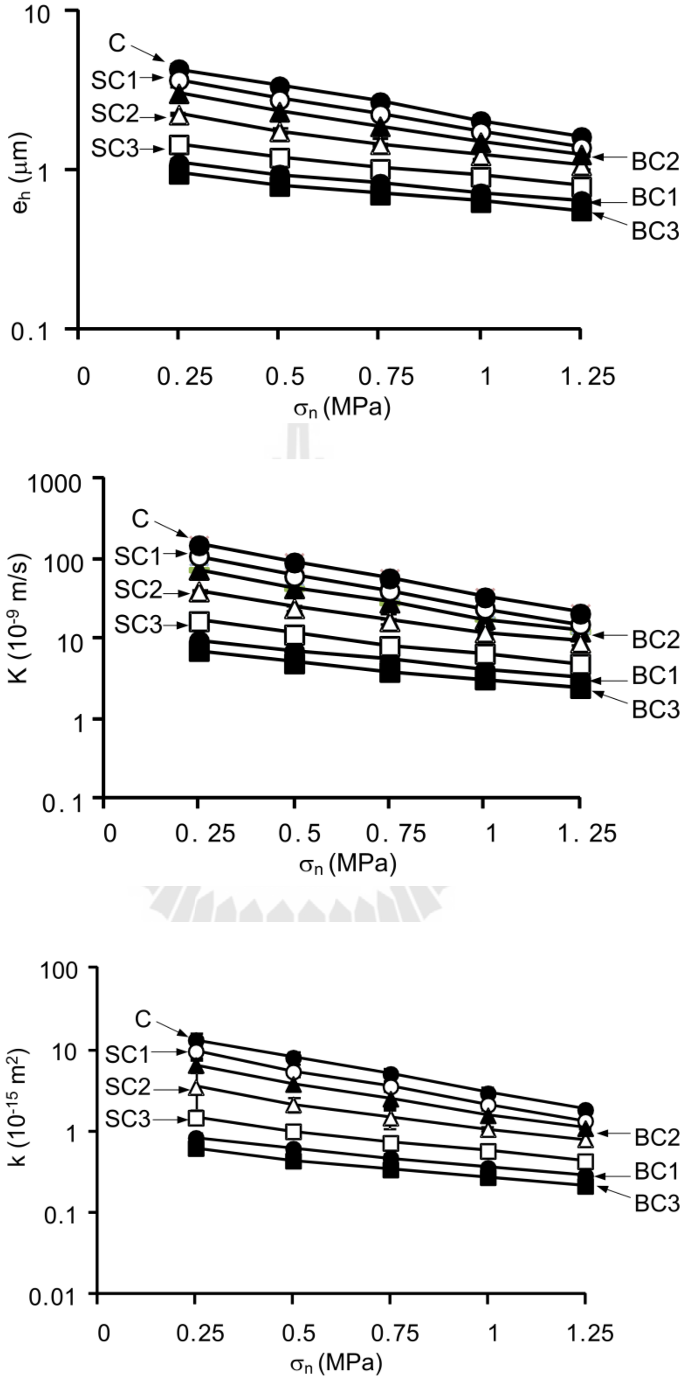

Figure 6.14 Intrinsic permeability (k), hydraulic conductivity (K), and aperture (e_h) as a function of normal stress (σ_n) for fracture aperture 20 mm.

CHAPTER VII

DISCUSSIONS

7.1 Viscosity and density of mixtures

The basic properties of the mixtures slurry are initially designed to select the appropriate proportions of sludge-to-cement ratios. The sludge-mixed cement ratios (S:C) of 0:10, 1:10, 2:10, 3:10, 4:10, 5:10, 6:10, 8:10 and 10:10 by weight are prepared with water-cement ratios (W:C) of 0.8:1, 1:1 and 1.25:1. The bentonite-cement ratios (B:C) are 0:10, 1:10, 2:10, 3:10, 4:10, and 5:10 by weight with W:C of 10:10 and 40:10. Mixing of all grouts is by using a blade paddle mixer as suggested by ASTM C938 (ASTM 2010a). Viscosity measurement follows, as much as practical, the ASTM D2196 (ASTM 2010d). The results are shown in Figure 4.12. The suitable mixing ratios for the S:C are 1:10, 3:10, 5:10 and for the B:C are 1:10, 2:10, 3:10 with the W:C of 1:1 by weight. These proportions yield the lowest slurry viscosity of 5 Pa·s.

Two parameters controlled the workability of mixtures. The first parameter, a constant water to cement ratio (W:C) of 8:10, 10:10 and 12.5:10 are used. The second parameter, the viscosity of mixture is increased by adjusting the quantity of mixing sludge. Table 4.3 shows the test results, the viscosity of the mixture slurry in different proportions. The effect of various ratios of W:C used in the mixture proportions are shown in Figure 4.12. The proportion of cement decreased with slurry viscosity increase exponentially as B:C or S:C more than 0.5. The proportion of water increase with the viscosity of the slurry mixture decreases. Comparing curves of viscosities between S:C and B:C mixtures shows that are corresponding tend. For B:C mixture, the proportion of W:C is not less than 1.0 because the mixtures is sticky and semi-solid condition. Bentonite expands when wet, absorbing as much as several times its dry mass in water. While sludge is used for the S:C mixture, it is largely ranging for increasing and decreasing the quantity of water in proportion. The slurry of S:C mixture can be tested the viscosity with the highest compressive strengths.

Proportion of the mixtures mentioned above, the water to cement ratio of 10:10 is used that does not sticky and can grout in fractures. Mixture of cement proportions (S:C, B:C) be more than 5:10 is used to make the grouting material has high viscosity and can flow in fractures effectively. The proportions of mixtures are comparable to Garvin and Hayles (1999). They are the B:C proportion of 0.33. This study uses the S:C mixtures of 1:10, 2:10 and 3:10, and the B:C mixtures of 1:10, 3:10 and 5:10.

7.2 Mechanical properties testing

7.2.1 Uniaxial compressive strength testing

The uniaxial compressive strength, elastic modulus, and Poisson's ratio of the grouting materials are determined. The results show that the suitable mixing ratios for the S:C are 1:10, 3:10, 5:10 and for the B:C are 1:10, 2:10, 3:10 with the W:C of 1:1 by weight (Tables 5.3 and 5.4). These proportions yield the lowest slurry viscosity of 5 Pa·s and the highest compressive strength. Preparation of these samples follows, as much as practical, the ASTM standards (D7012, C938, C39). All specimens are cured for 3 days before testing. During the test, the axial deformation and lateral deformation are monitored. The maximum loaded at the failure is recorded. The compressive strength (σ_C), Poisson's ratio (ν), elastic modulus (E) are determined. The results of the S:C and B:C indicate that the chemical reaction between cement and water with the large cast are better than the small cast.

Figure 5.10 shows uniaxial compressive strengths for B:C and S:C ratios. The results show that the maximum uniaxial compressive strength of the S:C and B:C are similar to W:C = 10:10. Larger mold allows a better chemical reaction between cement and bentonite or cement and sludge that small mold. Figure 5.11 shows the elasticity modulus of the mixtures selected. The elastic modulus is in the range between 200 MPa to 280 MPa. In particular, water portion tend to decrease with increasing uniaxial compressive strength but is not more than 3 MPa. Then the slurry viscosity is increasing which is not as beneficial as the grouting material used to fill in rock fracture. When water portion tends to increase, W: C > 1:1, with the uniaxial compressive strength is decreasing. The results of this study show that the initial W:C = 1:1 is suitable to apply for this research.

7.2.2 Shearing resistance between grout and fracture

Figure 5.24 shows the relationship between the function of the shear stresses and normal stresses. Table 5.7 lists the shear strength parameters calibrated from direct shear tests using Coulomb's criteria. The results show these friction angles (ϕ_p) from six proportions of mixtures are very similar and cohesions (c_p) are differing only slightly.

7.3 Hydraulic properties testing

7.3.1 Permeability of grouting materials

Figure 6.5 shows the results of S:C mixtures and B:C mixtures for grout permeability tests. The results indicated that intrinsic permeability tends to rapidly decrease at 7 days curing time and it starts gradually decreasing after 14 to 28 days curing time. The intrinsic permeabilities of all mixtures are in the range of 10^{-17} to 10^{-15} m^2. The mixture with the S:C of 5:10 by weight gives the lowest permeability. Table 6.1 summarizes the results of permeability testing of grouting material results at 3, 7, 14 and 28 days of curing.

7.3.2 Permeability of rock fractures

Hydraulic aperture (e_h) and permeability coefficient (K) and the physical permeability (k) are plotted as function of the normal stress of fracture in Figure 6.9. Result shows that permeabilities of five fracture sandstones are comparable. Fracture permeabilites are decreased with the normal stresses on fracture aperture increases. This tested concluded that sandstone surface is close fracture with the aperture and the fracture permeability had very small value (less than value of grouting material in this study). The close fracture does not affect the geo-structural engineering. Therefore, it is not required grouting material to reduce the fracture permeability.

7.3.3 Permeability of grouting materials in rock fractures

Figures 6.12 through 6.14 show fracture permeability and intrinsic permeability for sixty-three samples. Those parameters are similar where the corresponding results in tasks 6.2 and 6.3. It is found that the proportions of S:C mixtures and B:C mixtures used here are similar ranges. This means that the S:C mixtures have hydraulic properties equivalent to those of the B:C mixtures under the most suitable mixing ratios for grouting in rock fracture.

CHAPTER VIII

CONCLUSIONS AND RECOMMENDATIONS FOR FUTURE STUDIES

8.1 Conclusions

The sludge is classified as elastic silt with over 90% of its particles smaller than 0.047 mm. This studied, aim to determine the minimum slurry viscosity and appropriate strength of the grouting materials. Grouting materials in the study are contained sludge (S), cement (C), and water (W) for S:C mixtures and bentonite (B), cement and water for B:C mixtures. The mechanical and hydraulic tests of mixtures are determined to select the appropriate proportions of sludge-to-cement and bentonite-to-cement ratios for grouting material in rock fractures. The results show that the suitable mixing ratios for sludge-to-cement (S:C) are 1:10, 3:10 and 5:10, and for bentonite-to-cement (B:C) are 1:10, 2:10 and 3:10, with water-cement ratio (W:C) of 1:1 by weight that those strengths are about 2 MPa. For the sludge these proportions yield the lowest slurry viscosity of 5 Pa·s and the highest compressive strength. For S:C of 3:10, the compressive strength and elastic modulus are 1.22 MPa and 224 MPa which are similar to those of the B:C. The direct shear tested, results show that the shear strengths at the interface between the grout and sandstone fractures varying from 0.22 to 0.90 MPa under normal stresses ranging from 0.25 to 1.25 MPa (Table 8.1 – 8.2).

Permeability of the grouting materials measured from the one-dimensional flow test with constant head is from 10^{-17} to 10^{-15} m^2 and decreases with curing time. The mixture with the S:C of 5:10 by weight gives the lowest permeability. The permeability of the grouts measured by radial flow test in fractures with apertures of 2, 10 and 20 mm ranges from 10^{-15} to 10^{-14} m^2 under the normal stresses ranging from 0.25 to 1.25 MPa (Table 8.3). The permeability for all grout mixtures decrease by increase normal stresses. The S:C mixtures have the mechanical and hydraulic properties equivalent to those of the B:C mixtures which shows that the sludge can be used as a substituted material to mix with cement for rock fracture grouting purpose. Such applications can also minimize the disposal cost of the sludge and reduce the environmental impact due to the landfill construction.

The sludge can be used as a substitute material for bentonite to be mixed with cement and water to grout in rock fractures. Properties of the liquid mixtures (viscosity and density) and properties of the solid mixtures (mechanical and hydraulic properties) for both sludge and bentonite are closely similar. These studies is conducted to compare the estimated economic cost of the liquid mixture per cubic meter in rock fracture. Result is given in Table 8.4 for economic calculation. Sludge preparation due to the application is uncomplicated process. Therefore, the cost required is only the electric energy for drying and grinding the sludge. The electric power is only about 326 Thai Baht per sludge 1,000 kg. Comparison between S:C proportion and B:C proportion at 1:10 to save costs is equal to 650 - 23 = 627 Thai Baht (per one cubic meter liquid mixture).

The results of laboratory studies aim at determining appropriate grout mixes proportion from sludge-mixed cement for reducing permeability in saturated fractured rock under various stresses in the laboratory and to compare the results with the bentonite-mixed cement in terms of the mechanical and hydraulic properties. Three mixtures of S:C are 1:10, 3:10 and 5:10 that are closely similar in terms of the mechanical and hydraulic properties. Those are some important differences in their viscosity. The minimum and maximum viscosities of S:C are 1:10 and 5:10 by weight. Recommended applications for sludge-mixed cement grout in rock fracture are summarized in Table 8.5.

8.2 Recommendations for future studies

More grout mixtures are needed long-term performance and under in-situ condition. The sludge can be obtained from both Bang Khen and Mahasawat Water Treatment Plants. They should be collected from sludge lagoon in various seasons. Testing time and curing time should be longer (months or years) for long-term testing. The mechanical and hydraulic behavior of the grout in rock fractures is very complicated and is affected by numerous factors. One should investigate the factors affecting such behaviors, such as variations of the mineralogy, admixture content, temperature, humidity and inclusions, etc. Sludge from other plants may be needed to compare the results. The concept of sludge-mixed cement grout in rock fractures may be improved by using cyclic loading test for earthquake.

Table 8.1 Mixture ratios with W:C = 1:1.

Types	Mixing Ratio B:C or S:C	Water (g)	Cement (g)	B or S (g)	Slurry weight (g)	Slurry Volume (cc)	Slurry Density (g/cc)	Kinematic Viscosity (10^{-4} m^2/s)
Cement	-	391	391	0	693.7	470	1.47	0.43
Bentonite	1:10	371	371	37	765.8	560	1.37	2.19
	2:10	352	352	70	729.8	480	1.52	7.31
	3:10	336	336	101	743.5	520	1.42	22.88
Sludge	1:10	367	367	37	772.8	510	1.51	0.56
	3:10	326	326	98	772.7	500	1.53	1.06
	5:10	294	294	147	764.5	490	1.56	2.63

Table 8.2 Summary of mechanical property results of mixture ratios with W:C = 1:1.

Types	Mixing Ratio B:C or S:C	Samples Density (g/cc)	Uniaxial Compressive Strength (MPa)	Elastic Modulus (MPa)	Poisson's Ratio	c_p (MPa)	ϕ_p (degrees)
Cement	-	0.83	0.85 ± 0.0	212	0.18	0.563	14.7
Bentonite	1:10	1.35	1.05 ± 0.1	193	0.17	0.306	23.0
	2:10	1.38	1.83 ± 0.0	275	0.14	0.121	22.3
	3:10	1.33	1.77 ± 0.1	228	0.16	0.143	23.3
Sludge	1:10	1.91	0.79 ± 0.1	190	0.15	0.275	23.6
	3:10	1.81	1.22 ± 0.1	224	0.21	0.213	23.5
	5:10	1.79	1.10 ± 0.3	261	0.16	0.255	23.2

Table 8.3 Summary of hydraulic property results of mixture ratios with W:C = 1:1.

Types	Mixing Ratio B:C or S:C	Cylindrical shape specimen k ($\times10^{-17}$ m^2)	In fracture k ($\times10^{-17}$ m^2) at σ_n = 0.25 MPa		
			Aperture 2 mm	Aperture 10 mm	Aperture 20 mm
Cement	-	893	107	348	1329
Bentonite	1:10	237	1707	19	84
	2:10	86.8	2475	87	655
	3:10	31.7	1265	169	63
Sludge	1:10	825	349	263	970
	3:10	293	576	34	351
	5:10	221	149	227	148

Table 8.4 Estimated quantities of mixture proportions and cost for grout in rock fracture by fractured volume of 1 m^3.

Types	Mixing Ratio B:C or S:C	*Fractured Volume 1 m^3							
		Water weight (kg)	Cement weight (kg)	B or S weight (kg)	Slurry weight (kg)	Slurry Volume (m^3)	Cost (Baht)		
							Cement	Preparation	Purchase
Cement		735	735	0	1470	1	1,838	-	-
Bentonite	1:10	652	652	65	1369	1	1,630	-	650
	2:10	691	691	138	1520	1	1,728	-	1,380
	3:10	617	617	185	1419	1	1,543	-	1,850
Sludge	1:10	719	719	72	1510	1	1,798	23	-
	3:10	665	665	200	1530	1	1,663	65	-
	5:10	624	624	312	1560	1	1,560	102	-

*The preparation cost of 1,000 kg sludge is limit to 326 Baht (exclude shipping charges).

Table 8.5 Recommended applications for sludge-mixed cement grout in rock fracture.

Types	Mixing Ratio	Recommended applications
Sludge	1:10	Suitable for grout in rock fracture that is narrow aperture (less than 5 mm). The mixture slurry is low viscosity that easily flowed in rock fracture.
	3:10	Suitable for grout in rock fracture that moderate aperture (5 mm to 20 mm). This mixture slurry is high compressive strength after curing for enhancement of the strength of the rock mass.
	5:10	Suitable for grout in rock fracture that large aperture (larger than 20 mm). The mixture slurry is high viscosity, but there are advantages to use the highest proportion of sludge.

REFERENCES

Akgün, H. (2010). Geotechnical characterization and performance assessment of bentonite/sand mixtures for underground waste repository sealing. **Applied Clay Science.** 49: 394–399.

Akgün, H., Daemen, J. J. K. (1999). Design implications of analytical and laboratory studies of permanent abandonment plugs. **Canadian Geotechnical.** 36: 21–38.

Akgün, H., Koçkar, M. K., Aktürk, Ö. (2006). Evaluation of a compacted bentonite/sand seal for underground waste repository isolation. **Environmental Geology**. 50, 331–337.

Akgüna, H., and Daemen, J. J. K. (2000). Influence of degree of saturation on the borehole sealing performance of an expansive cement grout. **Cement and Concrete Research.** 30:281–289.

Akkrachattrarat, N., Suanprom, P., Buaboocha J. and Fuenkajorn, K. (2009). Flow testing of sandstone fractures under normal and shear stresses. In **Proceedings of the Second Thailand Symposium on Rock Mechanics**, March 12-13, 2009, Chonburi, Published by Geomechanics Research Unit, Suranaree University of Technology, Nakhon Ratchasima, pp. 319-334.

ASTM C114-11b. Standard Test Methods for Chemical Analysis of Hydraulic Cement. In **Annual Book of ASTM Standards**, 04.01, American Society for Testing and Materials, Philadelphia.

ASTM C150/C150M-09. Standard Specification for Portland Cement. In **Annual Book of ASTM Standards**, 04.01. American Society for Testing and Materials, Philadelphia.

ASTM C192-07. Standard Practice for Making and Curing Concrete Test Specimens in the Laboratory. In **Annual Book of ASTM Standards**, 04.02, American Society for Testing and Materials, Philadelphia.

ASTM C20-00. Standard Test Methods for Apparent Porosity, Water Absorption, Apparent Specific Gravity, and Bulk Density of Burned Refractory Brick and Shapes by Boiling Water. In **Annual Book of ASTM Standards**, 15.01. American Society for Testing and Materials, Philadelphia.

ASTM C33/C33M-11. Standard Specification for Concrete Aggregates. In **Annual Book of ASTM Standards**, 04.02. American Society for Testing and Materials, Philadelphia.

ASTM C39/C39M-10. Standard Test Method for Compressive Strength of Cylindrical Concrete Specimens. In **Annual Book of ASTM Standards**, 04.01, American Society for Testing and Materials, Philadelphia.

ASTM C91-05. Standard Specification for Masonry Cement. In **Annual Book of ASTM Standards**, 04.01, American Society for Testing and Materials, Philadelphia.

ASTM C938-10. Standard Practice for Proportioning Grout Mixtures for Preplaced-Aggregate Concrete. In **Annual Book of ASTM Standards**. 04.02, American Society for Testing and Materials, Philadelphia.

ASTM D2196-10. Standard Test Methods for Rheological Properties of Non-Newtonian Materials by Rotational (Brookfield type) Viscometer. In **Annual Book of ASTM Standards**, 06.01, American Society for Testing and Materials, Philadelphia.

ASTM D2487-11. Standard Practice for Classification of Soils for Engineering Purposes (Unified Soil Classification System). In **Annual Book of ASTM Standards**, 04.08, American Society for Testing and Materials, Philadelphia.

ASTM D422-07. Standard Test Method for Particle-Size Analysis of Soils. Annual Book of ASTM Standards, 04.08, American Society for Testing and Materials, Philadelphia.

ASTM D4221-11. Standard Test Method for Dispersive Characteristics of Clay Soil by Double Hydrometer. In **Annual Book of ASTM Standards**. 04.08, American Society for Testing and Materials, Philadelphia.

ASTM D4318-10. Standard Test Methods for Liquid Limit, Plastic Limit, and Plasticity Index of Soils. In **Annual Book of ASTM Standards**, 04.08, American Society for Testing and Materials, Philadelphia.

ASTM D4543-08. Standard Practices for Preparing Rock Core as Cylindrical Test Specimens and Verifying Conformance to Dimensional and Shape Tolerances. In **Annual Book of ASTM Standards**, 04.01, American Society for Testing and Materials, Philadelphia.

ASTM D4832-10. Standard Test Method for Preparation and Testing of Controlled Low Strength Material (CLSM) Test Cylinders. In **Annual Book of ASTM Standards**, 04.02, American Society for Testing and Materials, Philadelphia.

ASTM D5607-95. Standard test method for performing laboratory direct shear strength test of rock specimens under constant normal force. In **Annual Book of ASTM Standards**, 04.08, American Society for Testing and Materials, Philadelphia.

ASTM D698-07e1. Standard Test Methods for Laboratory Compaction Characteristics of Soil Using Standard Effort (12 400 ft-lbf/ft^3 (600 kN-m/m^3)). In **Annual Book of ASTM Standards**, 04.08, American Society for Testing and Materials, Philadelphia.

ASTM D7012-10. Standard Test Method for Compressive Strength and Elastic Moduli of Intact Rock Core Specimens under Varying States of Stress and Temperatures. In **Annual Book of ASTM Standards**, 04.09, American Society for Testing and Materials, Philadelphia.

ASTM D854-10. Standard Test Methods for Specific Gravity of Soil Solids by Water Pycnometer. In **Annual Book of ASTM Standards**. 04.08, American Society for Testing and Materials, Philadelphia.

Baik, M. H., Cho, W. J., and Hahn, P. S. (2007). Erosion of bentonite particles at the interface of a compacted bentonite and a fractured granite. **Engineering Geology**. 91: 229-239.

Bandis, S. C., Barton, N. R., and Christianson, M. (1985). Application of a New Numerical Model of Joint Behavior to Rock Mechanics Problems. In **Proceeding of the International Symposium on Fundamentals of Rock Joints**, Bjorkliden.

Bandis, S. C., Lumsden, A. C., and Barton, N. R. (1983). Fundamentals of Rock Joint Deformation. **International Journal of Rock Mechanics and Mining Sciences & Geomechanics**. 20: 249-268.

Barton, N. R. (1973). Review of a new shear strength criterion for rock joints. **Engineering Geology** 7: 287-332.

Barton, N., and Bakhtar, K. (1983). **Rock Joint Description and Modeling of the Hydrothermomechanical Design of Nuclear Waste Repositories** (Contact Report, Submitted to CANMET). Mining Research Laboratory, Ottawa.

Barton, N., Bandis, S. and Bakhtar, K. (1985). Strength, Deformation and Conductivity Coupling of Rock Joints. **Int. J. Rock Mech. Min. Sci. Geomech.** 22(3): 121-140.

Bates, R., and Jackson, J. A. (eds.). (1980). **Glossary of Geology (2nd ed.).** Falls Church, Va.: American Geological Institute.

Bishop, A. W. (1995). The use of the slip circle in the stability analysis of earth slope. **Geotechnique**. 5: 7-17.

Bunjongsiri, K. and Bunjongsiri, J. (2005). A study of quantity of heavy metal in bricks produce by clay mix with sludge from community wastewater treatment. In **Proceedings of National Convention on Civil Engineering 2006** (NCCE11), 2 – 4 May 2005, Pattaya, Chonburi.

Butron, C., Axelsson, M. and Gustafson, G. (2009). Silica sol for rock grouting: laboratory testing of strength, fracture behavior and hydraulic conductivity. **Tunnelling and Underground Space Technology.** 24: 603-607.

Butron, C., Gustafson, G., Fransson, A., and Funehag, J. (2010). Drip sealing of tunnels in hard rock: A new concept for the design and evaluation of permeation grouting. **Tunnelling and Underground Space Technology**. 25: 114-121.

Castelbaum, D. and Shackelford, C. D. (2009). Hydraulic Conductivity of Bentonite Slurry Mixed Sands. **Geotechnical and Geoenvironmental Engineering** 135(12): 1941-1956.

Chapius, R.P., 1990. Sand-bentonite liners: predicting permeability from laboratory tests. **Canadian Geotechnical Journal.** 27: 47–57.

Chegbeleh, L. P., Nishigaki, M., Akudago, J. A. and Katayama, T. (2009). Experimental study on ethanol/bentonite slurry injection into synthetic rock fractures: Application to seepage control. **Applied Clay Science.** 45: 232–238.

Coulon, H., Lajudie, A., Debrabant, P., Atabek, R., Jorda, M., Andre-Jehan, R. (1987). Choice of French clays as engineered barrier components for waste disposal. In: Bates, J.K., Seefeldt, W.B. (Eds.), In **Proceedings of Scientific Basis for Nuclear Waste Management X, Materials Research Society Symposium**, Boston, MA, December 1–4, 1986: Materials Research Society, Pittsburgh, PA, 84, pp. 813–824.

Daemen, J.J.K., Ran, C. (1996). **Bentonite as a Waste Isolation Pilot Plant Shaft Sealing Material**. Contractor Report SAND96-1968. Sandia National Laboratories, Albuquerque, NM.

Delaleuxa, F., Pya, X., Olivesa, R. and Dominguezb, A. (2012). Enhancement of geothermal borehole heat exchangers performances by improvement of bentonite grouts conductivity. **Applied Thermal Engineering.** 33-34:92-99.

Detoumay, E. (1980). Hydraulic Conductivity of Closed Rock Fractures: An Experimental and Analytical Study. In **Proceeding of the 13th Canadian Rock Mechanics Symposium.** (pp 168-173). Toronto: (n.p.).

Dixon, D.A., Gray, M.N., Thomas, A.W. (1985). A study of the compaction properties of potential clay–sand buffer mixtures for use in nuclear fuel waste disposal. **Engineering Geology.** 21: 247–255.

Einarson, D.S., Abel, J.F. (1990). Tunnel bulkheads for acid mine drainage. In **Proceedings of International Symposium on Unique Underground Structures**, Denver, Colorado, Vol. II, Chapter 71.

Eriksson, M. (2002). Grouting field experiment at the Äspö hard rock laboratory. . **Tunnelling and Underground Space Technology**. 17: 287-293

Fransson, A. (2001). Characterisation of a fractured rock mass for a grouting field Test. **Tunnelling and Underground Space Technology.** 16: 331-339.

Fransson, A., Tsang, C. F., Rutqvist, J., and Gustafson, G. (2007a). A new parameter to assess hydromechanical effects in single-hole hydraulic testing and grouting. **International Journal of Rock Mechanics and Mining Sciences**. 44:1011-1021.

Fransson, A., Tsang, C. F., Rutqvist, J., and Gustafson, G. (2007b). Effects of the injection grout Silica sol on bentonite. **International Journal of Rock Mechanics and Mining Sciences.** 47: 887-893.

Freeze, R. A., and Cherry, J. A. (1979). **Groundwater**. Prentice Hall, Inc. Upper Saddle River, USA, 604p.

Fuenkajorn, K. (2007). Design process for sealing of boreholes in rock mass. In **Proceedings of the First Thailand Symposium on Rock Mechanics**, September, 13-14, Khao Yai, Thailand, Published by Geomechanics Research Unit, Suranaree University of Technology, Nakhon Ratchasima, Thailand, pp. 245-252.

Fuenkajorn, K., Daemen, J.J.K. (Eds.), 1996. **Sealing of Boreholes and Underground Excavations in Rock**. Chapman and Hall, London.

Funehag, J., and Fransson, A. (2006). Sealing narrow fractures with a Newtonian fluid: Model prediction for grouting verified by field study. **Tunnelling and Underground Space Technology**. 21: 492-498.

Gailing, Z., Kaiyu, Z., Yue, G. and Wenxue, W. (2011). Comparative experimental investigation of chemical grouting into a fracture with flowing and static water. **Mining Science and Technology**. 21: 201-205.

Gangi, A. F. (1978). Variation of Whole and Fractured Porous Rocks Permeability with Confining Pressure. **International Journal of Rock Mechanics and Mining Sciences & Geomechanics.** 15: 249-257.

Garvin, S. L. and Hayles, C. S. (1999). The chemical compatibility of cementbentonite cut-off wall material. **Construction and Building Materials.** 13: 329-341.

Gleason, M. H., Daniel, D. E. and Eykhole, G. R. (1997). Calcium and sodium bentonite for hydraulic containment aplications. **Journal of Geotechnical and Geoenvironmental Engineering**. pp. 438-445.

Gnirk, P., 1988. State-of-the-art evaluation of repository sealing materials and techniques. In: Apted, M.J., Westerman, R.E. (Eds.), Scientific Basis for Nuclear Waste Management XI. In **Proceedings of Materials Research Society Symposium**, Boston, MA, November 30-December 3, 112. Materials Research Society, Pittsburgh, PA, pp. 219–231.

Gothall, R. and Stille, H. (2009). Fracture dilation during grouting. **Tunnelling and Underground Space Technology.** 24: 126-135.

Gothall, R., and Stille. H. (2010). Fracture – fracture interaction during grouting. **Tunnelling and Underground space Technology.** 25: 199-204.

Greer, W. B. and Crouthamel, D. R. (1996). In-situ Hydraulic Performance of Cement Borehole Seals. In Fuenkajorn, K. and Daemen, J. J. K. (eds). **Sealing of Boreholes and Underground Excavations in Rock** (pp. 157-183). Chapman&Hall.

Hadsanan, P., Lertpocasombut, K. and Chatveera, B. (2006). Mechanical properties and durability of cement mortar containing dry sludge ash from Bang Khen water supply plant. In **Proceedings of National Convention on Civil Engineering 2006** (NCCE11), 20-22 April 2006, Phuket.

Hoek, E. and Bray, J. W. (1981). **Rock Slope Engineering**. Revised 3rd ed. IMM, London, 358p.

Hoffman, C., (2004). **Nuclear Waste Repository: Long-term Storage**. Popular Science, Tampa, FL. April.

Holmbee, M., Wold, S. and Petterson, T. (2011). Effects of the injection grout silica sol on bentonite. **Physics and Chemistry of the Earth.** 36: 1580-1589

Hong, C. S., Shackelford, C. D. and Malusis, M. A. (2012). “Consolidation and Hydraulic Conductivity of Zeolite-Amended Soil-Bentonite Backfills” **J. Geotech. Geoenviron. Eng**. 138(1): 15–25.

Huang, W. H. (1997). Properties of cement-fly ash grout admixed with bentonite, silica fume, or organic fiber. **Cement and Concrete Research.** 27(3): 395-406.

Huang, Z., Chen, M. and Chen, X. (2003). A developed technology for wet-ground fine cement slurry with its applications. **Cement and Concrete Research.** 33: 729-732.

Hvorlsev, M. S. (1951). Time lag and soil permeability in groundwater measurements. U.S. Corps of Engineers Waterways Experiment Station, **Bulletin No. 36**, 50p.

IAEA, 1990. Sealing of underground repositories for radioactive wastes. In Gray, M., Gera, F., Wiley, J.R., Dlouhy, Z., Squires, D. (Eds.), **Technical Reports Series No. 319,** International Atomic Energy Agency, Vienna, Unipub, Lanham, MD.

Indraratna, B., and Ranjith, P. (2001). **Hydromechanical aspects and unsaturated flow in joints rock,** A. A. Balkema, Lisse, 83-154.

Jaeger, J. C., and Cook, N. G. W. (1979). **Fundamentals of Rock Mechanics** (3rd ed.). London: Chapman & Hall.

Jaeger, J.C. (1959). The frictional properties of joints in rocks. **Geofis pura appl.** 43: 148-158.

Jones, F. O. (1975). A Laboratory Study of the Effects of Confining Pressure on Fracture Flow and Storage Capacity in Carbonate Rocks. **Journal of Petroleum Technology**. 21: 21-27.

Joshi, K., Kechavarzi, C., Sutherland, K., Albert, M. Y. Soga, K. and Tedd, P. (2010). "Laboratory and In Situ Tests for Long-Term Hydraulic Conductivity of a Cement-Bentonite Cutoff Wall." **J. Geotech. Geoenviron. Eng.** 136(4): 562-572.

Kanchanamai, P. (2003). **The utilization of sludge frome Bang Khen water treatment plant in construction industry.** A thesis submitted in partial fulfilment of the requirements for the degree of master of engineering in the faculty of graduate studies, Kasetsart University.

Karamalidis, A. K. and Voudrias, E. A. (2007). Cement-based stabilization / solidification of oil refinery sludge: Leaching behavior of alkanes and PAHs. **Journal of Hazardous Materials.** 148:122–135.

Kashir, M., and Yanful, E. K. (2000). Compatibility of Slurry Wall Backfill Soils With Acid Mine Dranage. **Advances in Environmental Research.** 4: 251-268.

Katsioti, M., Katsiotis, N., Rouni, G., Bakirtzis, D and Loizidou, M. (2008). The effect of bentonite/cement mortar for the stabilization/solidification of sewage sludge containing heavy metals. **Cement & Concrete Composites.** 30: 1013–1019.

Kenney, T.C., Van Veen, W.A., Swallow, M.A., Sungaila, M.A., 1992. Hydraulic conductivity of compacted bentonite–sand mixtures. **Canadian Geotechnical Journal.** 29: 364–374.

Kjartanson, B.H., Chandler, N.A., Wan, A.W.L., 1996. In situ performance of a clay based barrier. In Fuenkajorn, K., Daemen, J.J.K. (Eds.), **Sealing of Boreholes and Underground Excavations in Rock.** Chapman and Hall, London, pp. 96–125.

Koch, D. (2002). Bentonites as a basic material for technical base liners and site encapsulation cut-off walls. **Applied Clay Science.** 21: 1-11

Komine, H., (2004). Simplified evaluation on hydraulic conductivities of sand–bentonite mixture backfill. **Applied Clay Science.** 26: 13–19.

Kongthong, R. and Lertpocasombut, K. (2006). A study of sludge from water treatment plant on dye adsorption. In **Proceedings of National Convention on Civil Engineering 2006** (NCCE11), 20-22 April 2006, Phuket.

Kuo, W. and Huang J. (2010). Microstructure and properties of cement mortars containing organo-modified reservoir sludge. **Construction and Building Materials.** 24: 2022–2029.

Kuo, W., Huang J. and Tan., T. (2007). Organo-modified reservoir sludge as fine aggregates in cement mortars. **Construction and Building Materials.** 21: 609–615.

Laothong, K. (2003). **The Utilization of Sludge Cake from Water Treatment Processes of Wang Noi Power Plant**. Master of Engineering (Environmental Engineering), Major Field Environmental Engineering, Department of Environmental Engineering, Kasetsart University, 99 pp.

Lee, J.-M. and Shackelford, C. D. (2005). Impact of Bentonite Quality on Hydraulic Conductivity of Geosynthetic Clay Liners. **Journal of Geotechnical and Geoenvironmental Engineering.** 131(1): 64-77.

Malusis, M. A., Barben, E. J. and Evans, J. C. (2009). “Hydraulic conductivity and compressibility of soil-bentonite backfill amended with activated carbon.” **J. Geotech. Geoenviron. Eng.** 135(5): 664–672.

Masumoto, K., Sugita, Y., Fujita, T., Martino, J. B., Kozak, E. T. and Dixon, D. A. (2007). A clay grouting technique for granitic rock adjacent to clay bulkhead. **Physics and Chemistry of the Earth.** 32:691–700.

Metcalfe, R., Walker, C. (2004). **International Workshop on Bentonite Cement Interaction in Repository Environments**. NUMO Technical Report.

National Research Council. (1996). **Rock Fractures and Fluid Flow: Contemporary Understanding and Applications.** Washington, D.C.: National Academy Press.

Navarro, F. C. (2010). Suggested guuidelines for sampling natural stones for laboratorial tests. **Global Stone Congress 2010**, (pp. 1-5).

Nelson, R. (1975). **Fracture Permeability in Porous Reservoirs: Experimental and Field Approach.** Ph.D. dissertation, Department of Geology, Texas A&M University.

Obcheoy, J., Aracheeploha, S. and Fuenkajorn, K. (2011). Fracture permeability under normal and shear stresses. Rock Mechanics, Fuenkajorn & Phien-wej (eds), In **Proceedings of the Third Thailand Symposium on Rock Mechanics**, March, 10-11, Cha-Am, Thailand, Published by Geomechanics Research Unit, Suranaree University of Technology, Nakhon Ratchasima, Thailand, pp. 133-140.

Opdyke, S. M. and Evans, J. C. (2012). Slag-Cement-Bentonite Slurry Walls. **J. Geotech. Geoenviron. Eng.** 131(6): 673–681.

Ouyang, S., Daemen, J.J.K., (1996). Performance of bentonite and bentonite/crushed rock borehole seals. In Fuenkajorn, K., Daemen, J.J.K. (Eds.), **Sealing of Boreholes and Underground Excavations in Rock.** Chapman and Hall, London, (pp. 65–95).

Owaidat, L. M., Andromalos, K. B., and Sisley, J. L. (1999). Construction of a Soil-Cement-Bentonite Slurry Wall for a Levee Strengthening Program. In **Association of State Dam Safety Officials Annual Conference**, 10-12 October 1999, St. Louis, Missouri.

Pettman, E.R., (1984). Tunnel plugs in recent H.E.C. Practice. In **5th Australian Tunnelling Conference**, Sydney. (pp. 207–212)

Philip, L. K. (2001). An investigation into contaminant transport processes through single-phase cement-bentonite slurry walls. **Engineering Geology.** 60: 209-221.

Picandet, V., Rangeard, D., Perrot, A. and Lecompte, T. (2011). Permeability measurement of fresh cement paste. **Cement and Concrete Research.** 41:330–338.

Poonsawat, C. and Lertpocasombut, K. (2006). Study on the properties of sludge from water supply plant as raw material for clay plan roofing tile. In **National Convention on Civil Engineering 2006** (NCCE11), 20-22 April 2006, Phuket.

Pusch, R. (1978). **Small-scale bentonite injection test on rock.** KBS Report 75, Stockholm.

Pusch, R. (1983). Borehole sealing for underground waste storage. **ASCE Journal of Geotechnical Engineering**. 109: 113–119.

Pusch, R. (1994). Waste disposal in rock. **Developments in Geotechnical Engineering 76,** Elsevier, Amsterdam.

Rahmani, H. (2004). **Estimation of grout distribution in a fractured rock by numerical modeling.** A thesis submitted in partial fulfilment of the requirements for the degree of master of applied science in the faculty of graduate studies (Civil Engineering), University of Tehran.

Ranjith, P. G. and Viete, D. R. (2011). Applicability of the 'cubic law' for non-Darcian fracture flow. **Petroleum Science and Engineering.** In Press, Accepted Manuscript, Available online 7 August 2011.

Rutqvist, J. (1995). Determination of Hydraulic Normal Stiffness of Fractures in Hard Rock from Well Testing. **Rock Mech. Min. Sci. & Geomech.** 32(5): 513-523.

Ryan, C. R., and Day, S. R. (2002). **Soil-Cement-Bentonite Slurry Wall. International Deep Foundation Congress**, GSP No. 116, American Society of Civil Engineers, Orlando, FL.

Şahmaran, M. Özkan, N. Keskin, S. B., Uzal, B., Yaman, İ. Ö. and Erdem, T. K. (2008). Evaluation of natural zeolite as a viscosity-modifying agent for cement-based grouts. **Cement and Concrete Research.** 38:930–937.

Saiyouri, N., Bouasker, M. and Khelidj,. A. (2008). Gas permeability measurement on injected soils with cement grout. **Cement and Concrete Research.** 38:95–103.

Sa-ngiumsak, N. and Cheerarot, R. (2008). The study of properties of artificial aggregates made from water supply sludge. In **National Convention on Civil Engineering 2006** (NCCE11), 14-16 Mayl 2008, Pattaya, Chonburi.

Saric-Coric, M. Khayat, K. H. and Tagnit-Hamou, A. (2003). Performance characteristics of cement grouts made with various combinations of high-range water reducer and cellulose-based viscosity modifier. **Cement and Concrete Research.** 33:1999–2008.

Sivapullaiah, P.V., Sridharan, A., Stalin, V.K. (2000). Hydraulic conductivity of bentonite–sand mixtures. **Canadian Geotechnical Journal.** 37, 406–413.

Smith, L. C., Mase, C. W. and Schwartz, F. W. (1987). Estimation of Fracture Using Hydraulic and Tracer Tests. 28th U.S. In **Symposium on Rock Mechanics**, University of Arizona, Tucson, June 29th to July 1st, (pp. 453-463).

Snow, D. T. (1968). Anisotropic Permeability of Fractured Media. **Water Resources Research.** 5(6): 1273-1289.

Sonsakul, P., Fuenkajorn, K. (2013). evelopment of Three-Ring Compaction and Direct Shear Test Mold for Soils with Oversized Particles. **Research and Development Journal of The Engineering institute of Thailand**. 24(2): 1-7.

Stampinoa, P. G., Zamporia, L., Dotelli, G., Melonib, P., Sorac, I. N. and Pelosatoc, R. (2009). Use of admixtures in organic-contaminated cement–clay pastes. **Journal of Hazardous Materials.** 161:862–870. 120

Suanprom, P. Obcheoy, J. and Fuenkajorn, K. (2009). Permeability of Rock Fractures under Shear Stresses. **EIT-JSCE Joint International Symposium Geotechnical Infrastructure Asset Management**, Bangkok, Thailand.

Suriyachat, D., Vichitamornpun, P. and Ruengsumrej, W. (2004). Water treatment sludge utilization. **Technical Report No. 16/2547**. department of primary industries and mines, Bangkok.

Svermova, L. Sonebi, M. and Barto, P. J. M. (2003). Influence of mix proportions on rheology of cement grouts containing limestone powder. **Cement & Concrete Composites.** 25:737–749.

Svermova, L., Sonebi, M., Bartos, P.J.M., 2003. Influence of mix proportions on rheology of cement grouts containing limestone powder. **Cement & Concrete Composites.** 25, 737–749.

Terzaghi, K. (1936). The Shearing Resistance of Saturated Soils. (pp.402-407). In **Proceedings of the International Conference on Foundation Engineering**, Graduate School of Engineering, Harvard University. Boston: Spaulding Moss.

Trakoolngam, K. (2009). Determination of the mechanical-hydraulic coupled behavior of the Phu Thok sandstone: A dual-porosity approach. Rock Mechanics, Fuenkajorn & Phien-wej (eds), In **Proceedings of the Second Thailand Symposium on Rock Mechanics**, March 12-13, 2009, Chonburi, Published by Geomechanics Research Unit, Suranaree University of Technology, Nakhon Ratchasima, Thailand (pp. 219-234).

Tsang, Y. W. (1992). Usage of equivalent apertures for rock fractures as derived from hydraulic and tracer tests. **J. Water Resour. Res.** 28(5): 1451-1455.

US Nuclear Regulatory Commission. (1983). Disposal of high-level radioactive wastes in geologic repositories. **Final rule 10 CFR 60**. Federal Register, Vol. 48, No. 120, June 30, Washington, D.C.

US Nuclear Regulatory Commission. (1985). Disposal of high-level radioactive wastes in geologic repositories, **Final rule, unsaturated zone amendment**. Federal Register, Vol. 50, No. 140, July 22, Washington, D.C.

USDOE/WIPP. (1995). **Waste isolation pilot plant sealing system design report.** DOE/WIPP-95-3117. U.S. Department of Energy,Waste Isolation Pilot Plant, Carlsbad, NM.

USEPA. (1995). **Environmental radiation protection standards for management and disposal of spent nuclear fuel, high-level and transuranic radioactive wastes**. CFR 40, Part 191, Washington, D.C.

Varol, A., and Dalgic, S. (2006). Grouting applications in the Istanbul metro, Turkey. **Tunnelling and Underground Space Technology**. 21: 602-612

Vitipanit, S. and Rianbupa, S. (2004). **A Study for Development an Appropriate Material in Construction by Using Sand Mixed with Bentonite**. Research and Development Institute, Royal Irrigation Department.

Wang, M. C. and Tseng, W. (1993). Permeability behavior of a water treatment sludge. **J Geotech. Engrg.** 119: 1672-1677.

Wang, M. C., Hull, J. Q., Jao, M., Dempsey, B. A. and Cornwell, D. A. (1992). Engineering behavior of water treatment sludge. **J. Environ. Eng.** 118: 848-864.

Witherspoon, P. A., Wang, J. S. Y., Iwai, K., and Gale, J. E. (1980). Validity of cubic law for fluid flow in a deformable rock fracture. **Water Resour. Res.** 16(6): 1016-1024.

Xinghua, W. and Quqing, G. (1997). Study of a New Cheap Grouting Material: Clay-Hardening Grout. **Tunnelling and Underground Space Technology**. 12(4): 497-502.

Yan, S., Sagoe-Crentsil, K. and Shapiro, G. (2011). Reuse of de-inking sludge from wastepaper recycling in cement mortar products. **Journal of Environmental Management.** 92: 2085-2090.

Yong, R. N., Boonsinsuk, P., Wong, G. (1986). Formulation of backfill material for a nuclear fuel waste disposal vault. **Canadian Geotechnical Journal.** 23: 216–228.

APPENDIX A

PUBLICATION

List of Publications

Wetchasat, K., and Fuenkajorn, K., (2012). **Mechanical and Hydraulic Performance of Sludge-Mixed Cement Grout in Rock Fractures.** In Proceedings of the seventh Asian Rock Mechanics Symposium, 15-19 October 2012, Seoul, Korea, pp. 1477-1485.

Wetchasat, K. and Fuenkajorn, K., (2013). **Laboratory Assessment of Mechanical and Hydraulic Performance of Sludge-Mixed Cement Grout in Rock Fractures.** In Proceedings of the Fourth Thailand Symposium on Rock Mechanics, January 24-25, 2013, Wang Nam Keaw, Nakhon Ratchasima, Thailand, Published by Geomechanics Research Unit, Suranaree University of Technology, Nakhon Ratchasima, pp. 259-268.

Wetchasat, K. and Fuenkajorn, K. **Mechanical and Hydraulic Performance of Sludge-Mixed Cement Grout in Rock Fractures.** Research and Development J. EIT. (Accepted 20 December 2013).

Wetchasat, K. and Fuenkajorn, K., **Mechanical and Hydraulic Performance of Sludge-Mixed Cement Grout in Rock Fractures. Songklanakarin**. J. Sci. Technol. (Accepted 24 March 2014).

Mechanical and Hydraulic Performance of Sludge-Mixed Cement Grout in Rock Fractures

K. Wetchasat[a*] and K. Fuenkajorn, Ph.D., P.E.[b]

[a] *Engineer level 6, Metropolitan Waterworks Authority, Bangkok, Thailand*
[b] *Associate Professor, Suranaree University of Technology, Nakhon Ratchasima, Thailand*
[*] *Corresponding Author's E-mail:* aek@mwa.co.th

ABSTRACT

The objective of this study is to assess the performance of sludge mixed with the commercial grade Portland cement type I for use in minimizing permeability of fractures in rock. The fractures are artificially made in 3 rectangular blocks of sandstone by applying a line load to induce a splitting tensile crack. The water treatment sludge tested comprises over 80% of quartz with grain sizes less than 75 μm. The results indicate that the mixing ratios of sludge:cement (S:C) of 1:10, 3:10, 5:10 are suitable with water:cement ratio (W:C) of 1:1 by weight. For S:C = 3:10, the compressive strength and elastic modulus are 1.22 MPa and 224 MPa which are similar to those of bentonite mixed with cement. The shear strengths between the grouts and fractures surfaces are from 0.22 to 0.90 MPa under normal stresses from 0.25 to 1.25 MPa. The S:C ratio of 5:10 gives the lowest permeability. The permeability of grouted fractures with apertures of 2, 10 and 20 mm range from 10^{-16} to 10^{-14} m^2 and decrease with curing time.

Keywords: Rock fracture, Grouting, Permeability, Sludge, Cement

1. INTRODUCTION

The increasing amount of the water treatment sludge from the Metropolitan Waterworks Authority of Thailand (MWA) has called for a permanent solution to dispose of the sludge from the Bang khen Water Treatment Plants. The MWA report (2007-2009) indicates that the plant produces sludge with the maximum capacity of 3.2×10^6 m^3 per day. The sludge has been collected from the water treatment process. The increasing rate of the sludge is about 247×10^3 kg per day. One of the solutions is to apply the sludge to minimizing groundwater circulation in rock mass. Groundwater in rock mass is one of the key factors governing the mechanical stability of slope embankments, underground mines, tunnels, and dam foundation. A common solution practiced internationally in the construction industry is to use bentonite mixed with cement as a grouting material to reduce permeability in fractured rock mass (Akgün and Daemen, 1999; Fuenkajorn and Daemen, 1996). Knowledge and experimental evidences about the permeability of the sludge-mixed cement in fractured rock under varied stress conditions have been rare. The objectives of this study are to assess the performance of sludge mixed with the commercial grade Portland cement for reducing permeability in saturated fractured rock under various stresses in the laboratory and to compare the results with those of the bentonite-mixed cement in terms of the mechanical and hydraulic performance.

2. GROUTS PREPARATION

The grouting materials used in this study are (1) sludge with particle sizes less than 75 μm, (2) commercial grade bentonite, and (3) commercial grade Portland cement type I for mixing with the sludge and bentonite. The fractures in sandstone collcted from Phu Kradung formation are artificially made by applying a line load to induce a splitting tensile crack. Two shapes of the sandstone samples are $152.4\times152.4\times152.4$ mm^3 blocks and 100 mm diameter cylinder with 100 mm in length. Bentonite is from America colloid company.

Sludge and bentonite are tested for the Atterberg's limits, specific gravity, and particle size distribution. The equipment and test procedure follow the ASTM standards (D422, D854). The results are summarized in Table 1. Figure 1 shows the particle size distributions of the sludge used here.

3. BASIC MECHANICAL PROPERTIES OF GROUTING MATERIALS

The basic mechanical properties of the mixtures are determined to select the appropriate proportions of sludge-to-cement ratios. The sludge-mixed cement ratios (S:C) of 0:10, 1:10, 2:10, 3:10, 4:10, 5:10, 6:10, 8:10 and 10:10 by weight are prepared with water-cement ratios (W:C) of 0.8:1, 1:1 and 1.25:1. The bentonite-mixes cement ratios (B:C) are 0:10, 1:10, 2:10, 3:10, 4:10, and 5:10 by weight with water-cement ratios (W:C) of 1:1, 4:1. Mixing of all grouts is accomplished using a blade paddle mixer as suggested by ASTM C938. The mixtures are placed in a 54 mm PVC mold. They are cured under water at room temperature (ASTM C192). Viscosity measurement follows, as much as practical, the ASTM D2196. The results are shown in Figure 2.

The procedure for determining the grout permeability is similar to the ASTM standards (C938, C39). The water flow tests are conducted at 3, 7, 14 and 28 days of curing. The mold has an inner diameter of 101.6 mm with a length of 152.4 mm. The prepared specimen is sealed between two acrylic platens with the aid of O-ring rubber and epoxy coating. Inlet port is installed at the end of the mold and connected to a water pressure tube compressed by nitrogen gas at about 13.8 kPa. Air bubbles are bled out before measuring the permeability. Outlet port is installed at the other end and connected to a high precision pipet for measuring the outflow. The coefficient of permeability is computed from the flow rate based on the Darcy's law. The results are presented in Figure 3.

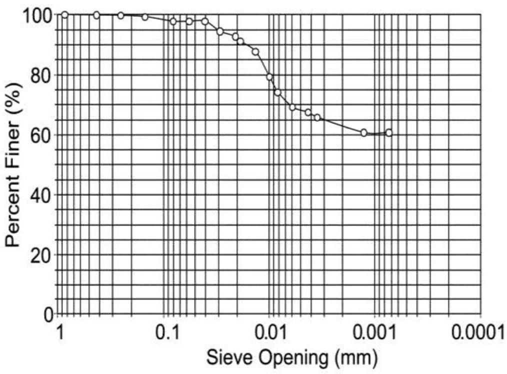

Figure 1. Grain size distribution of water treatment sludge

Table 1. Atterberg's limits and specific gravity of sludge and bentonite

Atterberg Limits	Bentonite (%)		Sludge (%)	
	SUT [1]	ACC [2]	SUT [1]	TU [3]
Liquid limit	357	478	55	69
Plastic limit	44	28	22	42
Plasticity index	313	449	23	28
Specific gravity	-	-	2.56	-

[1] SUT = Suranaree University of Technology Laboratory,
[2] ACC = American Colloid Company Technical Data,
[3] TU = Tummasart University Laboratory (after Hadsanan et al., 2006)

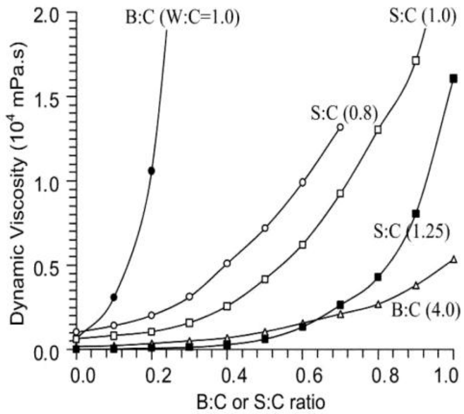

Figure 2. Dynamic viscosity of S:C and B:C for different W:C ratio

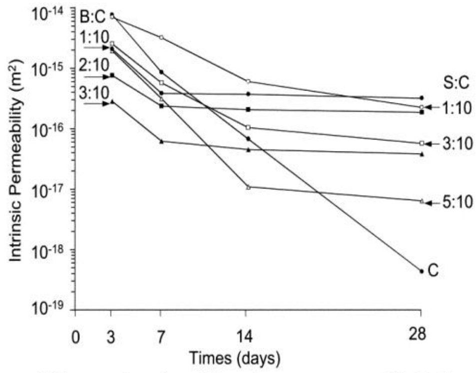

Figure 3. Intrinsic permeability as a function of time for pure cement (C), B:C, and S:C with W:C = 1:1

Table 2. Mechanical properties of grouting materials

Type	Mix ratio	Number of Samples	Average density (g/cm^3)	Poisson Ratio ν	σ_c (MPa)	E (MPa)
C	0:10	5	0.83 ± 0.01	0.18	1.40 ± 0.27	212
B:C	1:10	5	1.35 ± 0.04	0.17	1.59 ± 0.28	193
B:C	2:10	5	1.38 ± 0.04	0.14	2.09 ± 0.26	275
B:C	3:10	5	1.33 ± 0.02	0.16	1.92 ± 0.05	228
S:C	1:10	5	1.91 ± 0.06	0.15	1.35 ± 0.06	190
S:C	3:10	5	1.81 ± 0.07	0.21	1.77 ± 0.21	224
S:C	5:10	5	1.79 ± 0.06	0.16	1.52 ± 0.19	261

4. UNIAXIAL COMPRESSIVE STRENGTH OF GROUTING MATERIALS

The uniaxial compressive strength, elastic modulus, and Poisson's ratio of the grouting materials are determined. The results indicate that the suitable mixing ratios for the S:C are 1:10, 3:10, 5:10 and for the B:C are 1:10, 2:10, 3:10 with the W:C of 1:1 by weight. These proportions yield the lowest slurry viscosity of 5 Pa·s and the highest compressive strength. Preparation of these samples follows, as much as practical, the ASTM standards (D7012, C938, C39). All specimens are cured for 3 days before testing. During the test, the axial deformation and lateral deformation are monitored. The maximum load at the failure is recorded. The compressive strength (σ_C), Poisson's ratio (ν), elastic modulus (E) are determined. The results of the S:C and B:C indicate that the chemical reaction between cement and water with the large cast are better than the small cast. Figure 4 shows the uniaxial compressive strength for the S:C and B:C with W:C = 1:1. The uniaxial compressive strength and elastic modulus for the specimens with the diameter of 101.6 mm are summarized in Table 2. The maximum compressive strengths for the S:C and B:C are similar.

5. SHEARING RESISTANCE BETWEEN GROUT AND FRACTURE

The maximum shear strength of grouting material in sandstone fracture are determined by direct shear testing. The test procedure is similar to the ASTM standard (D5607). Three-ring shear test equipment is used. All specimens are cured for three days before testing. Laboratory arrangement for the three-ring shear test equipment is shown in Figure 5. The constant normal stresses used are 0.25, 0.5, 0.75, 1.0 and 1.25 MPa. The shear stress is applied while the shear displacement and dilation are monitored for every 0.2 mm of shear displacement. The failure modes are recorded. The test results are presented in forms of the shear strength as a function of normal stress (Figure 6). The angles of internal friction and cohesion for all mixtures are similar.

6. PERMEABILITY TESTING OF FRACTURES

The objective of this task is to assess the permeability of rock fractures under varying normal stresses. The fracture permeability is used to compare with the permeability of grouting materials for both sludge and bentonte mixtures. Constant head flow tests are performed. The normal stresses are ranging from 1 to 4 MPa. The experimental procedure is similar to Obcheoy et al. (2011). Five specimens are preapred and tested. The injection hole at the center of the upper block is 12 mm in diameter and 101.6 mm in depth. The tests are conducted by injecting water into the center hole of the rectangular block specimen. The laboratory arrangement of the constant head flow test is shown in Figure 7. Water volume and time are recorded. Both tend to decrease exponentially with the normal stress. The permeability results (k) are plotted as a function of the normal stress (σ_n) in Figure 8. The equivalent hydraulic aperture (e_h) for radial flow, hydraulic conductivity between smooth and parallel plates (K), and intrinsic permeability (k) are calculated by (Tsang, 1992; Indraratna and Ranjith, 2001) :

$$e_h = \{[(6\mu q)/ (\pi\Delta P)] \ln (r/r_0)\}^{1/3} \tag{1}$$

$$K = \gamma_w e_h^2/12\mu \tag{2}$$

$$k = e_h^2/12 \tag{3}$$

where μ is the dynamic viscosity of the water (N·s/cm^2), q is water flow rate through the specimen (cm^2/s), ΔP is injecting water pressure into the center hole of rectangular blocks of the specimen, r is radius of flow path (m), r_0 is radius of the radius injection hole (m). γ_w is unit weight of water (N/m^2). The results indicate that the intrinsic permeability of the fractures is less than 1.4×10^{-9} m^2.

7. PERMEABILITY OF GROUTING MATERIALS IN ROCK FRACTURES

The permeability of sludge- and bentonite-mixed cement in artificial fractures is experimentally determined. The testing method is similar to that described above. The grouting materials are injected into the fractures. The fractrue apertures are 2, 10, and 20 mm. The grouting materials are cured for 3 days. Figure 9 gives the laboratory arrangement. Constant head flow tests is performed. The constant head is ranging between 13.8 and 551.7 kPa. The constant normal stresses are 0.25, 0.5, 1.0 and 1.25 MPa. The results indicate that the normal stress can reduce the permeability of grouting materials in fractured sandstone. The intrinsic permeability (k) is calculated from the measured flow rate (Q) as follows: (Indraratna and Ranjith, 2001)

$$K = Q \ln(2mL/D)/2\pi L H_c \quad (4)$$

$$k = K\mu/\gamma_w \quad (5)$$

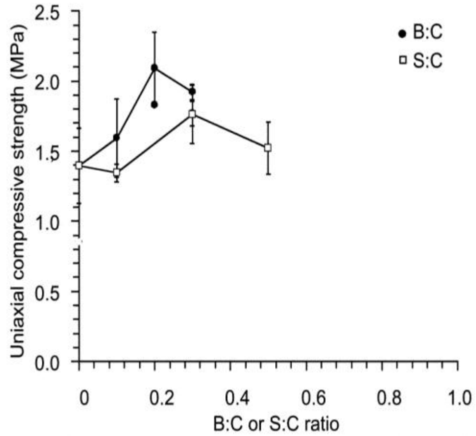

Figure 4. Uniaxial compressive strengths for B:C and S:C with W:C = 1:1

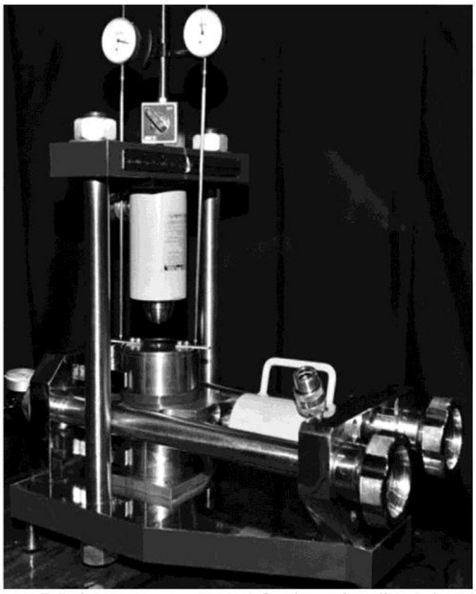

Figure 5. Laboratory arrangement for three-ring direct shear test

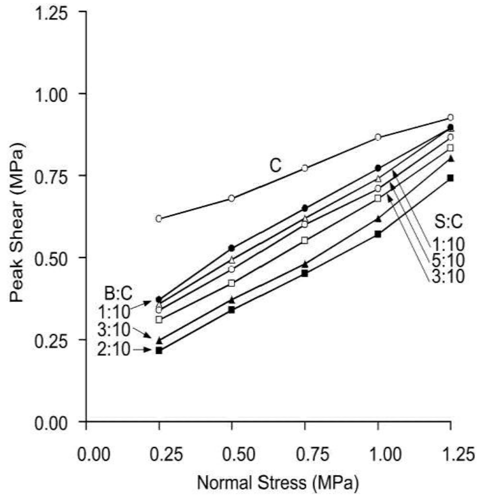

Figure 6. Normal stress and peak shear stress

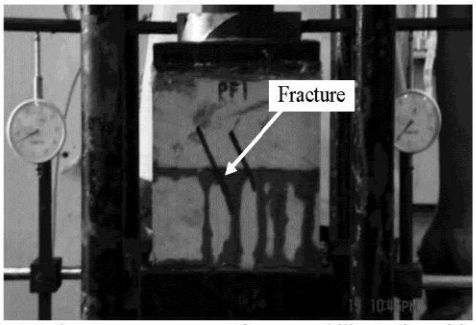

Figure 7. Laboratory arrangement for permeability testing of fractures

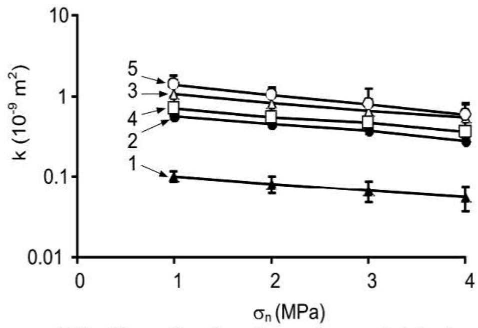

Figure 8. Intrinsic permeability (k) as a function of normal stress (σ_n) for fracture in Phu Kradung sandstone

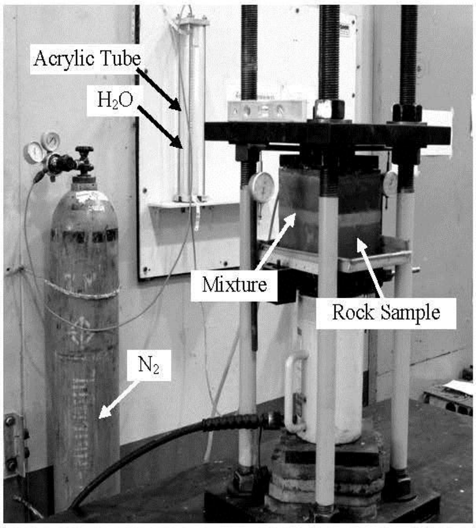

Figure 9. Permeability testing of grouting materials in rock fracture aperture 20 mm

where K is hydraulic conductivit, Q is flow rate of water flow through the mixture, m is square root of the ratio between the conduuctivity perpendicular and parallel to the hole (in this case, m is equal to 1), L is the thickness of grouting material in fracture apertures, D is diameter of the injection hole at the center of the upper block, H_c is the constant head used for the test, μ is dynamic viscosity (891×10^{-6} kg/(m·s)) at temperature of 25°C, γ_w is unit weight of water (997.13 kg/m^3). Figure 10 shows the intrinsic permeability of grouting materials in fracture apertures in twenty-one samples.

8. DISCUSSIONS AND CONCLUSIONS

The sludge is classified as elastic silt with over 90% of its particles smaller than 0.047 mm. This study aims to determine the minimum slurry viscosity and appropriate strength of the grouting materials. The results indicate that the suitable mixing ratios for sludge-to-cement (S:C) are 1:10, 3:10 and 5:10, and for bentonite-to-cement (B:C) are 1:10, 2:10 and 3:10, with water-cement ratio (W:C) of 1:1 by weight. For the sludge these proportions yield the lowest slurry viscosity of 5 Pa·s and the highest compressive strength. For S:C of 3:10, the compressive strength and elastic modulus are 1.22 MPa and 224 MPa which are similar to those of the B:C. The direct shear test results indicate that the shear strengths at the interface between the grout and sandstone fractures varying from 0.22 to 0.90 MPa under normal stresses ranging from 0.25 to 1.25 MPa. Permeability of the grouting materials measured from the one-dimensional flow test with constant head is from 10^{-17} to 10^{-15} m^2 and decreases with curing time. The mixture with the S:C of 5:10 by weight gives the lowest permeability. The permeability of the grouts measured by radial flow test in fractures with apertures of 2, 10 and 20 mm ranges from 10^{-16} to 10^{-14} m^2. The S:C mixtures have the mechanical and hydraulic properties equivalent to those of the B:C mixtures which indicates that the sludge can be used as a substituted material to mix with cement for rock fracture grouting purpose. Such applications can also minimize the disposal cost of the sludge and reduce the environmental impact due to the landfill construction.

ACKNOWLEDGEMENT

This research is funded by Metropolitan Waterworks Authority of Thailand for fiscal year 2011. Permission to publish this paper is gratefully acknowledged.

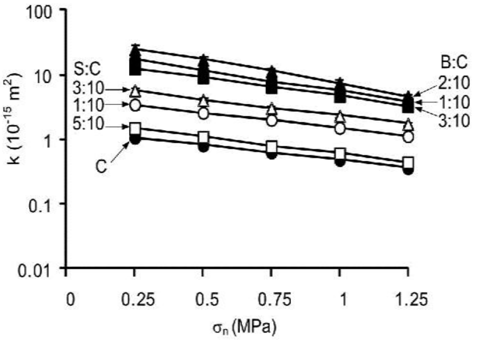

(a)

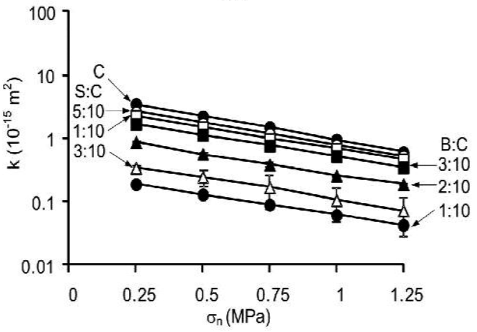

(b)

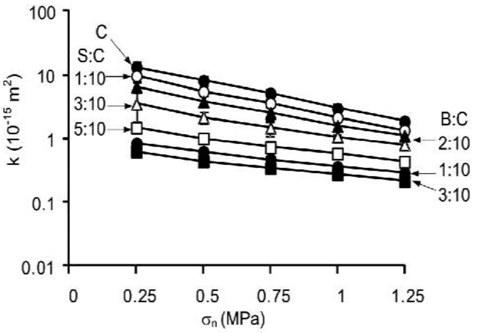

(c)

Figure 10. Intrinsic permeability (k) as a function of normal stress (σ_n) for fracture apertures (a) 2 mm (b) 10 mm and (c) 20 mm in Phu Kradung sandstones

REFERENCES

Akgün, H., Daemen, J.J.K., 1999, Design implications of analytical and laboratory studies of permanent abandonment plugs, *Canadian Geotechnical Journal*, 36: 21–38.

ASTM, 2007, Standard Practice for Making and Curing Concrete Test Specimens in the Laboratory, C192, *Annual Book of ASTM Standards 04.02*, American Society for Testing and Materials, Philadelphia.

ASTM, 2010, Standard Test Method for Compressive Strength of Cylindrical Concrete Specimens, C39, *Annual Book of ASTM Standards 04.01*, American Society for Testing and Materials, Philadelphia.

ASTM, 2010, Standard Practice for Proportioning Grout Mixtures for Preplaced-Aggregate Concrete, C938, *Annual Book of ASTM Standards 04.02*, American Society for Testing and Materials, Philadelphia.

ASTM, 2010, Standard Test Methods for Rheological Properties of Non-Newtonian Materials by Rotational (Brookfield type) Viscometer, D2196, *Annual Book of ASTM Standard, 06.01*, American Society for Testing and Materials, Philadelphia.

ASTM, 2007, Standard Test Method for Particle-Size Analysis of Soils, D422, *Annual Book of ASTM Standards 04.08*, American Society for Testing and Materials, Philadelphia.

ASTM, 2008, Standard Test Method for Performing Laboratory Direct Shear Strength Tests of Rock Specimens Under Constant Normal Force, D5607, *Annual Book of ASTM Standards 04.08*, American Society for Testing and Materials, Philadelphia.

ASTM, 2010, Standard Test Method for Compressive Strength and Elastic Moduli of Intact Rock Core Specimens under Varying States of Stress and Temperatures, D7012, *Annual Book of ASTM Standard 04.09*, American Society for Testing and Materials, Philadelphia.

ASTM, 2010, Standard Test Methods for Specific Gravity of Soil Solids by Water Pycnometer, D854, *Annual Book of ASTM Standards 04.08*, American Society for Testing and Materials, Philadelphia.

Fuenkajorn, K., Daemen, J.J.K. (Eds.), 1996, *Sealing of Boreholes and Underground Excavations in Rock*, Chapman and Hall, London.

Hadsanan, P., Lertpocasombut, K., Chatveera, B., 2006, Mechanical properties and durability of cement mortar containing dry sludge ash from Bang Khen water supply plant, *National Convention on Civil Engineering 2006 (NCCE11)*, 20-22 April 2006, Phuket.

Indraratna, B., Ranjith, P., 2001, *Hydromechanical Aspects and Unsaturated Flow in Joints Rock*, Lisse: A. A. Balkema.

Obcheoy, J., Aracheeploha, S., Fuenkajorn, K., 2011, Fracture permeability under normal and shear stresses, *Rock Mechanics*, Fuenkajorn & Phien-wej (eds), Geomechanics Research Unit, Suranaree University of Technology, Thailand, 133-140.

Tsang, Y. W., 1992, Usage of Equivalent Apertures for Rock Fractures as Derived From Hydraulic and Tracer Tests, *Water Resour. Res.*, 28(5): 1451-1455.

Rock Mechanics, Fuenkajorn & Phien-wej (eds) © 2013

Laboratory assessment of mechanical and hydraulic performance of sludge-mixed cement grout in rock fractures

K. Wetchasat & K. Fuenkajorn
Geomechanics Research Unit, Suranaree University of Technology, Thailand

Keywords: Fracture, grouting, permeability, sludge

ABSTRACT: The objective of this study is to assess the performance of sludge mixed with the commercial grade Portland cement type I for use in reducing permeability of fractures in sandstone. The fractures are artificially made in Phu Kradung sandstone by applying a line load to induce a splitting tensile crack in 0.15×0.15×0.15 m prismatic blocks. The Bang Khen water treatment sludge is used. More than 80% of the sludge is quartz with grain size less than 75 μm. This study aims at determining the minimum slurry viscosity and appropriate strength of the grouting materials. The results indicate that the suitable mixing ratios for sludge:cement (S:C) are 1:10, 3:10, 5:10 with water-cement ratio (W:C) of 1:1 by weight. These proportions yield the lowest slurry viscosity of 5 Pa·s. For S:C = 3:10, the compressive strength and elastic modulus are 1.22 MPa and 224 MPa which are similar to those of bentonite mixed with cement. The shear strength of grouted fractures varies from 0.22 to 0.90 MPa under normal stresses ranging from 0.25 to 1.25 MPa. Permeability of grouting materials is from 10^{-17} to 10^{-15} m^2 and decreases with curing time. The S:C ratio of 5:10 gives the lowest permeability. Permeabilities of grouted fractures with apertures of 2, 10 and 20 mm range from 10^{-16} to 10^{-14} m^2.

1 INTRODUCTION

The increasing amount of the water treatment sludge from the Metropolitan Waterworks Authority of Thailand (MWA) has called for a permanent solution to dispose of the sludge from the Bang khen Water Treatment Plants. The MWA report (2007-2009) indicates that the plant produces sludge with the maximum capacity of 3.2×10^6 m^3 per day. The sludge has been collected from the water treatment process. The increasing rate of the sludge is about 247×10^3 kg per day. One of the solutions is to apply the sludge to minimizing groundwater circulation in rock mass. Groundwater in rock mass is one of the key factors governing the mechanical stability of slope embankments, underground mines, tunnels, and dam foundation. A common solution practiced internationally in the construction industry is to use bentonite mixed with cement as a grouting material to reduce permeability in fractured rock mass (Akgün & Daemen, 1999; Fuenkajorn & Daemen, 1996). Knowledge and experimental evidences about the permeability of the sludge-mixed cement in fractured rock under varied stress conditions have been rare. The objectives of this study are to assess the performance of sludge mixed with the commercial grade Portland cement for reducing permeability in saturated fractured rock under various stresses in the laboratory and to compare the results with those of the bentonite-mixed cement in terms of the mechanical and hydraulic performance.

2 GROUTS PREPARATION

The grouting materials used in this study are (1) sludge with particle sizes less than 75 µm, (2) commercial grade bentonite, and (3) commercial grade Portland cement type I for mixing with the sludge and bentonite. The fractures in sandstone collected from Phu Kradung formation are artificially made by applying a line load to induce a splitting tensile crack. Two shapes of the sandstone samples are 152.4×152.4×152.4 mm^3 blocks and 100 mm diameter cylinder with 100 mm in length. Bentonite is from America colloid company.

Sludge and bentonite are tested for the Atterberg's limits, specific gravity, and particle size distribution. The equipment and test procedure follow the ASTM standards (D422, D854). The results are summarized in Table 1. Figure 1 shows the particle size distributions of the sludge used here.

Table 1. Atterberg's limits and specific gravity of sludge and bentonite.

Atterberg Limits	Bentonite (%)		Sludge (%)	
	SUT [1]	ACC [2]	SUT [1]	TU [3]
Liquid limit	357	478	55	69
Plastic limit	44	28	22	42
Plasticity index	313	449	23	28
Specific gravity	-	-	2.56	-

[1] SUT = Suranaree University of Technology Laboratory,
[2] ACC = American Colloid Company Technical Data,
[3] TU = Tummasart University Laboratory (after Hadsanan et al., 2006)

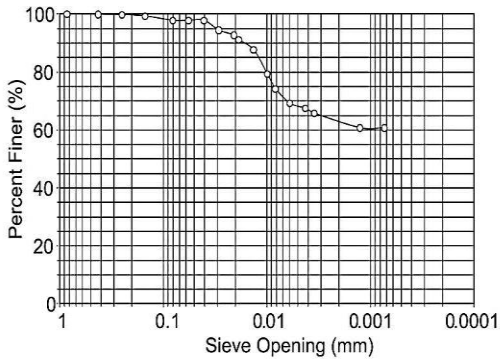

Figure 1. Grain size distribution of water treatment sludge.

3 BASIC MECHANICAL PROPERTIES OF GROUTING MATERIALS

The basic mechanical properties of the mixtures are determined to select the appropriate proportions of sludge-to-cement ratios. The sludge-mixed cement ratios (S:C) of 0:10, 1:10, 2:10, 3:10, 4:10, 5:10, 6:10, 8:10 and 10:10 by weight are prepared with water-cement ratios (W:C) of 0.8:1, 1:1 and 1.25:1. The bentonite-mixes cement ratios (B:C) are 0:10, 1:10, 2:10, 3:10, 4:10, and 5:10 by weight with water-cement ratios (W:C) of 1:1, 4:1. Mixing of all grouts is accomplished using a blade paddle mixer as suggested by ASTM C938. The mixtures are placed in a 54 mm PVC mold. They are cured under water at room temperature (ASTM C192). Viscosity measurement follows, as much as practical, the ASTM D2196. The results are shown in Figure 2.

The procedure for determining the grout permeability is similar to the ASTM standards (C938, C39). The water flow tests are conducted at 3, 7, 14 and 28 days of curing. The mold has an inner diameter of 101.6 mm with a length of 152.4 mm. The prepared specimen is sealed between two acrylic platens with the aid of O-ring rubber and epoxy coating. Inlet port is installed at the end of the mold and connected to a water pressure tube compressed by nitrogen gas at about 13.8 kPa. Air bubbles are bled out before measuring the permeability. Outlet port is installed at the other end and connected to a high precision pipet for measuring the outflow. The coefficient of permeability is computed from the flow rate based on the Darcy's law. The results are presented in Figure 3.

4 UNIAXIAL COMPRESSIVE STRENGTH OF GROUTING MATERIALS

The uniaxial compressive strength, elastic modulus, and Poisson's ratio of the grouting materials are determined. The results indicate that the suitable mixing ratios for the S:C are 1:10, 3:10, 5:10 and for the B:C are 1:10, 2:10, 3:10 with the W:C of 1:1 by weight. These proportions yield the lowest slurry viscosity of 5 Pa·s and the highest compressive strength. Preparation of these samples follows, as much as practical, the ASTM standards (D7012, C938, C39). All specimens are cured for 3 days before testing. During the test, the axial deformation and lateral deformation are monitored. The maximum load at the failure is recorded. The compressive strength (σ_C), Poisson's ratio (ν), elastic modulus (E) are determined. The results of the S:C and B:C indicate that the chemical reaction between cement and water with the large cast are better than the small cast. Figure 4 shows the uniaxial compressive strength for the S:C and B:C with W:C = 1:1. The uniaxial compressive strength and elastic modulus for the specimens with the diameter of 101.6 mm are summarized in Table 2. The maximum compressive strengths for the S:C and B:C are similar.

5 SHEARING RESISTANCE BETWEEN GROUT AND FRACTURE

The maximum shear strength of grouting material in sandstone fracture are determined by direct shear testing. The test procedure is similar to the ASTM standard (D5607). Three-ring shear test equipment is used. All specimens are cured for three days before testing. Laboratory arrangement for the three-ring shear test equipment is shown in Figure 5. The constant normal stresses used are 0.25, 0.5, 0.75, 1.0 and 1.25 MPa. The shear stress is applied while the shear displacement and dilation are monitored for every 0.2 mm of shear displacement. The failure modes are recorded. The test results are presented in forms of the shear strength as a function of normal stress (Figure 6). The angles of internal friction and cohesion for all mixtures are similar.

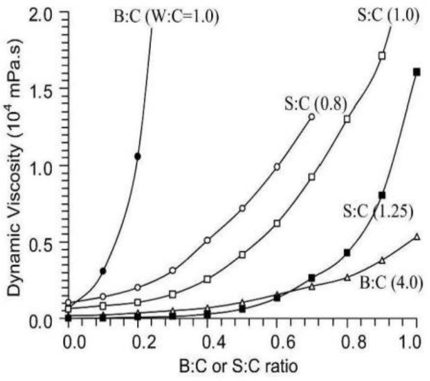

Figure 2. Dynamic viscosity of S:C and B:C for different W:C ratio.

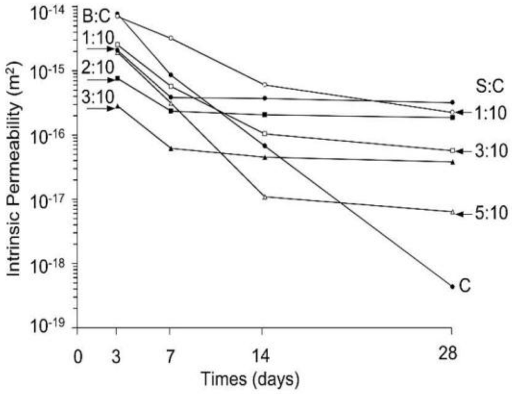

Figure 3. Intrinsic permeability as a function of time for pure cement (C), B:C and S:C with W:C = 1:1.

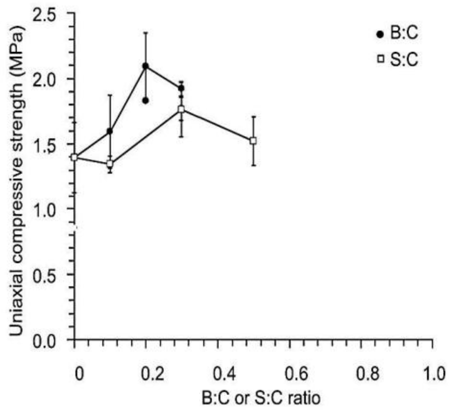

Figure 4. Uniaxial compressive strengths for B:C and S:C with W:C = 1:1.

Table 2. Mechanical properties of grouting materials.

Type	Mix ratio	Number of Samples	Average density (g/cm^3)	Poisson Ratio ν	σ_c (MPa)	E (MPa)
C	0:10	5	0.83 ± 0.01	0.18	1.40 ± 0.27	212
B:C	1:10	5	1.35 ± 0.04	0.17	1.59 ± 0.28	193
B:C	2:10	5	1.38 ± 0.04	0.14	2.09 ± 0.26	275
B:C	3:10	5	1.33 ± 0.02	0.16	1.92 ± 0.05	228
S:C	1:10	5	1.91 ± 0.06	0.15	1.35 ± 0.06	190
S:C	3:10	5	1.81 ± 0.07	0.21	1.77 ± 0.21	224
S:C	5:10	5	1.79 ± 0.06	0.16	1.52 ± 0.19	261

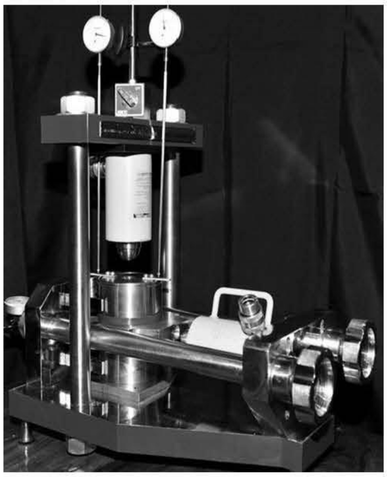

Figure 5. Laboratory arrangement for three-ring direct shear test.

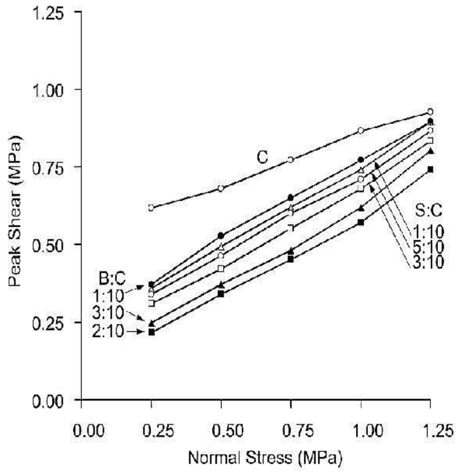

Figure 6. Normal stress and peak shear stress.

6 PERMEABILITY TESTING OF FRACTURES

The objective of this task is to assess the permeability of rock fractures under varying normal stresses. The fracture permeability is used to compare with the permeability of grouting materials for both sludge and bentonte mixtures. Constant head flow tests are performed. The normal stresses are ranging from 1 to 4 MPa. The experimental procedure is similar to Obcheoy et al. (2011). Five specimens are prepared and tested. The injection hole at the center of the upper block is 12 mm in diameter and 101.6 mm in depth. The tests are conducted by injecting water into the center hole of the rectangular block specimen. The laboratory arrangement of the constant head flow test is shown in Figure 7. Water volume and time are recorded. Both tend to decrease exponentially with the normal stress. The permeability results (k) are plotted as a function of the normal stress (σ_n) in Figure 8. The equivalent hydraulic aperture (e_h) for radial flow, hydraulic conductivity between smooth and parallel plates (K), and intrinsic permeability (k) are calculated by (Tsang, 1992; Indraratna & Ranjith, 2001):

$$e_h = \{[(6\mu q)/(\pi\Delta P)] \ln (r/r_0)\}^{1/3} \quad (1)$$

$$K = \gamma_w e_h^2/12\mu \quad (2)$$

$$k = e_h^2/12 \quad (3)$$

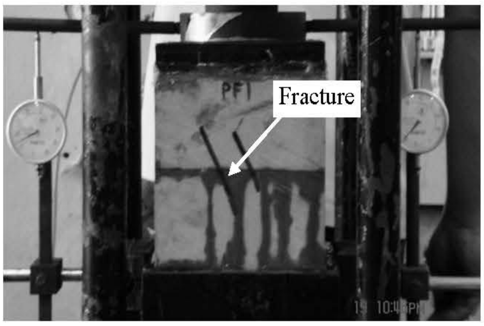

Figure 7. Laboratory arrangement for permeability testing of fractures.

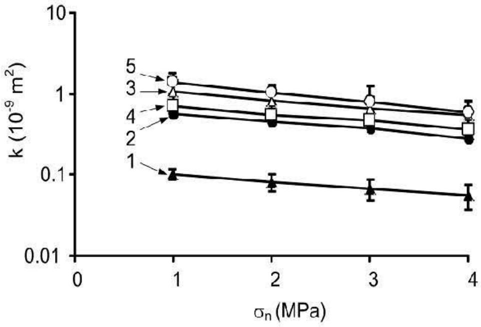

Figure 8. Intrinsic permeability (k) as a function of normal stress (σ_n) for fracture in Phu Kradung sandstone.

where μ is the dynamic viscosity of the water ($N \cdot s/cm^2$), q is water flow rate through the specimen (cm^2/s), ΔP is injecting water pressure into the center hole of rectangular blocks of the specimen, r is radius of flow path (m), r_0 is radius of the radius injection hole (m). γ_w is unit weight of water (N/m^2). The results indicate that the intrinsic permeability of the fractures is less than 1.4×10^{-9} m^2.

7 PERMEABILITY OF GROUTING MATERIALS IN ROCK FRACTURES

The permeability of sludge- and bentonite-mixed cements in artificial fractures is experimentally determined. The testing method is similar to that described above. The grouting materials are injected into the fractures. The fracture apertures are 2, 10, and 20 mm. The grouting materials are cured for 3 days. Figure 9 gives the laboratory arrangement. Constant head flow tests is performed. The constant head is ranging between 13.8 and 551.7 kPa. The constant normal stresses are 0.25, 0.5, 1.0 and 1.25 MPa. The results indicate that the normal stress can reduce the permeability of grouting materials in fractured sandstone. The intrinsic permeability (k) is calculated from the measured flow rate (Q) as follows: (Indraratna & Ranjith, 2001)

$$K = Q \ln(2mL/D)/2\pi LH_c \tag{4}$$

$$k = K\mu/\gamma_w \tag{5}$$

where K is hydraulic conductivity, Q is flow rate of water flow through the mixture, m is square root of the ratio between the conductivity perpendicular and parallel to the hole (in this case, m is equal to 1), L is the thickness of grouting material in fracture apertures, D is diameter of the injection hole at the center of the upper block, H_c is the constant head used for the test, μ is dynamic viscosity (891×10^{-6} kg/(m·s)) at temperature of 25°C, γ_w is unit weight of water (997.13 kg/m^3). Figure 10 shows the intrinsic permeability of grouting materials in fracture apertures in twenty-one samples.

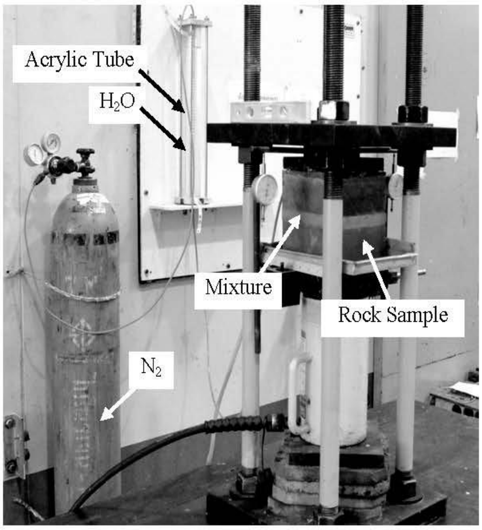

Figure 9. Permeability testing of grouting materials in rock fracture aperture 20 mm.

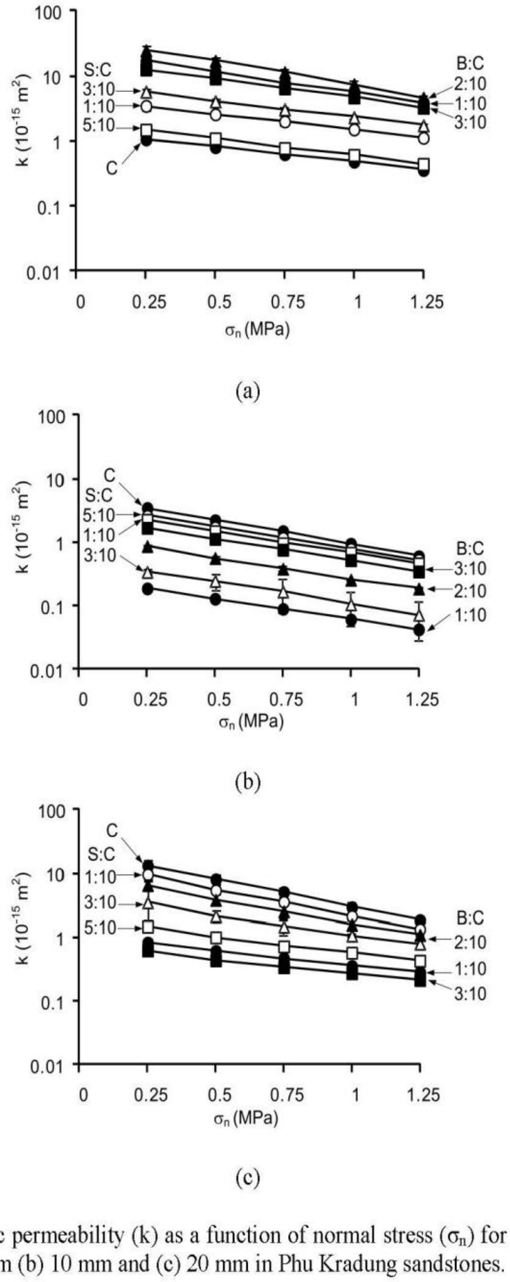

Figure 10. Intrinsic permeability (k) as a function of normal stress (σ_n) for fracture apertures (a) 2 mm (b) 10 mm and (c) 20 mm in Phu Kradung sandstones.

8 DISCUSSIONS AND CONCLUSIONS

The sludge is classified as elastic silt with over 90% of its particles smaller than 0.047 mm. This study aims to determine the minimum slurry viscosity and appropriate strength of the grouting materials. The results indicate that the suitable mixing ratios for sludge-to-cement (S:C) are 1:10, 3:10 and 5:10, and for bentonite-to-cement (B:C) are 1:10, 2:10 and 3:10, with water-cement ratio (W:C) of 1:1 by weight. For the sludge these proportions yield the lowest slurry viscosity of 5 Pa·s and the highest compressive strength. For S:C of 3:10, the compressive strength and elastic modulus are 1.22 MPa and 224 MPa which are similar to those of the B:C. The direct shear test results indicate that the shear strengths at the interface between the grout and sandstone fractures varying from 0.22 to 0.90 MPa under normal stresses ranging from 0.25 to 1.25 MPa. Permeability of the grouting materials measured from the one-dimensional flow test with constant head is from 10^{-17} to 10^{-15} m^2 and decreases with curing time. The mixture with the S:C of 5:10 by weight gives the lowest permeability. The permeability of the grouts measured by radial flow test in fractures with apertures of 2, 10 and 20 mm ranges from 10^{-16} to 10^{-14} m^2. The S:C mixtures have the mechanical and hydraulic properties equivalent to those of the B:C mixtures which indicates that the sludge can be used as a substituted material to mix with cement for rock fracture grouting purpose. Such applications can also minimize the disposal cost of the sludge and reduce the environmental impact due to the landfill construction.

ACKNOWLEDGEMENT

This research is funded by Metropolitan Waterworks Authority of Thailand for fiscal year 2011. Permission to publish this paper is gratefully acknowledged.

REFERENCES

Akgün, H. & Daemen, J.J.K. 1999. Design implications of analytical and laboratory studies of permanent abandonment plugs. *Canadian Geotechnical Journal*. 36: 21–38.

ASTM Standard C192-07. 2007. Standard Practice for Making and Curing Concrete Test Specimens in the Laboratory. *Annual Book of ASTM Standards*, American Society for Testing and Materials, Weat Conshohocken, PA.

ASTM Standard C39-10. 2010. Standard Test Method for Compressive Strength of Cylindrical Concrete Specimens. *Annual Book of ASTM Standards*, American Society for Testing and Materials, Weat Conshohocken, PA.

ASTM Standard C938-10. 2010. Standard Practice for Proportioning Grout Mixtures for Preplaced-Aggregate Concrete. *Annual Book of ASTM Standards*, American Society for Testing and Materials, Weat Conshohocken, PA.

ASTM Standard D2196-10. 2010. Standard Test Methods for Rheological Properties of Non-Newtonian Materials by Rotational (Brookfield type) Viscometer. *Annual Book of ASTM Standard*, American Society for Testing and Materials, Weat Conshohocken, PA.

ASTM Standard D422-07. 2007. Standard Test Method for Particle-Size Analysis of Soils. *Annual Book of ASTM Standards,* American Society for Testing and Materials, Weat Conshohocken, PA.

ASTM Standard D5607-08. 2008. Standard Test Method for Performing Laboratory Direct Shear Strength Tests of Rock Specimens Under Constant Normal Force. *Annual Book of ASTM Standards*, American Society for Testing and Materials, Weat Conshohocken, PA.

ASTM Standard D7012-10. 2010. Standard Test Method for Compressive Strength and Elastic Moduli of Intact Rock Core Specimens under Varying States of Stress and Temperatures. *Annual Book of ASTM Standard*, American Society for Testing and Materials, Weat Conshohocken, PA.

ASTM Standard D854-10. 2010. Standard Test Methods for Specific Gravity of Soil Solids by Water Pycnometer. *Annual Book of ASTM Standards*, American Society for Testing and Materials, Weat Conshohocken, PA.

Fuenkajorn, K. & Daemen, J.J.K. 1996. *Sealing of Boreholes and Underground Excavations in Rock*. Chapman and Hall, London.

Hadsanan, P., Lertpocasombut, K. & Chatveera, B. 2006. Mechanical properties and durability of cement mortar containing dry sludge ash from Bang Khen water supply plant. In *Proceedings of National Convention on Civil Engineering 2006 (NCCE11)*. April 20-22, Phuket.

Indraratna, B., & Ranjith, P. 2001. *Hydromechanical Aspects and Unsaturated Flow in Joints Rock*. A. A. Balkema, Lisse.

Obcheoy, J., Aracheeploha, S. & Fuenkajorn, K. 2011. Fracture permeability under normal and shear stresses. *Rock Mechanics*. Fuenkajorn & Phien-wej (eds), Geomechanics Research Unit, Suranaree University of Technology, Thailand, pp. 133-140.

Tsang, Y. W. 1992. Usage of Equivalent Apertures for Rock Fractures as Derived From Hydraulic and Tracer Tests. *Water Resour. Res.* 28(5): 1451-1455.

70th Anniversary
วิศวกรรมสถานแห่งประเทศไทย ในพระบรมราชูปถัมภ์ (วสท.)

70th Anniversary
THE ENGINEERING INSTITUTE OF THAILAND
UNDER H.M. THE KING'S PATRONAGE · EIT

ที่ R&D 142/2556

20 ธันวาคม 2556

เรื่อง ผลการพิจารณาบทความลงตีพิมพ์ในวิศวกรรมสารฉบับวิจัยและพัฒนา

เรียน นายคมกริช เวชสัสถ์

ตามที่ท่านได้จัดส่งบทความเรื่อง **“ศักยภาพเชิงกลศาสตร์และเชิงชลศาสตร์ของส่วนผสมตะกอนดินกับซีเมนต์ในรอยแตกของหิน”** เพื่อพิจารณาลงตีพิมพ์ในวิศวกรรมสารฉบับวิจัยและพัฒนานั้น

กองบรรณาธิการขอแจ้งให้ทราบว่า บทความที่ท่านเสนอมาได้รับการพิจารณาประเมินจากผู้ทรงคุณวุฒิเรียบร้อยแล้วโดยไม่มีการแก้ไข และให้ลงตีพิมพ์ได้ในวิศวกรรมสารฉบับวิจัยและพัฒนา

จึงเรียนมาเพื่อโปรดทราบ

ขอแสดงความนับถือ

(ผู้ช่วยศาสตราจารย์ถาวร อมตกิตติ์)
ประธานคณะอนุกรรมการวิศวกรรมสารฉบับวิจัยและพัฒนา

ฝ่ายประสานงาน : คุณอัจราภรณ์ รอดเกลี้ยง โทรศัพท์ 0-2319-2410-3 ต่อ 516 E-mail: ach_eit@eit.or.th

วิศวกรรมสถานแห่งประเทศไทย ในพระบรมราชูปถัมภ์ (วสท.)
The Engineering Institute of Thailand under H.M. The King's Patronage
487 ซอยรามคำแหง 39 (เทพลีลา 1) ถนนรามคำแหง แขวงพลับพลา เขตวังทองหลาง กรุงเทพมหานคร 10310
487 Ramkhamhaeng 39, Phlabphla, Wangthonglang Bangkok 10310
Tel. (662) 184 4600-9, Fax (662) 319-2710-1, (662) 184 4597-8 www.eit.or.th E-mail : eit@eit.or.th

ศักยภาพเชิงกลศาสตร์และเชิงชลศาสตร์ของส่วนผสมตะกอนดินกับซีเมนต์ในรอยแตกของหิน

MECHANICAL AND HYDRAULIC PERFORMANCE OF SLUDGE-MIXED CEMENT GROUT IN ROCK FRACTURES

คมกริช เวชสัสถ์[1] และ กิตติเทพ เฟื่องขจร

Khomkrit Wetchasat[1] and Kittitep Fuenkajorn

สาขาวิชาเทคโนโลยีธรณี สำนักวิชาวิศวกรรมศาสตร์ มหาวิทยาลัยเทคโนโลยีสุรนารี

อำเภอเมืองนครราชสีมา จังหวัดนครราชสีมา 30000

โทร: 0-4422-4758, โทรสาร: 0-4422-4448

E-Mail: [1]d5340248@g.sut.ac.th

บทคัดย่อ

วัตถุประสงค์ของการศึกษานี้คือเพื่อประเมินศักยภาพของตะกอนดินผสมกับปูนซีเมนต์ปอร์ตแลนด์ประเภท 1 เพื่อใช้ลดความซึมผ่านของน้ำในรอยแตกของหินทราย รอยแตกถูกทำขึ้นโดยแรงกดในแนวเส้นบนตัวอย่างหินทรายชุดภูกระดึงเพื่อให้หินแตกออกจากกันด้วยแรงดึง ตัวอย่างหินมีขนาด 15×15×15 ซม. ตะกอนจากโรงงานกำจัดตะกอนบางเขนถูกนำมาทดสอบคุณสมบัติเชิงกายภาพและเชิงเคมี มีการหาค่าความหนืดของส่วนผสมเหลวที่น้อยที่สุดแต่ให้ค่ากำลังกดในแกนเดียวที่เหมาะสม ผลทดสอบระบุว่าสัดส่วนที่เหมาะสมของตะกอนต่อซีเมนต์ (S:C) เท่ากับ 1:10, 3:10, 5:10 และเบนทอไนต์ต่อซีเมนต์ (B:C) เท่ากับ 1:10, 2:10, 3:10 ใช้ปริมาณน้ำต่อซีเมนต์เท่ากับ 1:1 เนื่องจากให้ค่าความหนืดของส่วนผสมเหลวไม่เกิน 5 Pa·s และให้ค่ากำลังกดสูงสุด สัดส่วนของ S:C เท่ากับ 3:10 จะให้ค่ากำลังกดเท่ากับ 1.77 MPa และค่าสัมประสิทธิ์ความยืดหยุ่นเท่ากับ 224 MPa ซึ่งต่ำกว่าค่าจาก B:C เล็กน้อย ค่ากำลังเฉือนระหว่างผิวรอยแตกกับส่วนผสมทั้ง 6 สัดส่วน มีค่าใกล้เคียงกันคืออยู่ในช่วง 0.36 ถึง 0.90 MPa ภายใต้ความเค้นตั้งฉากจาก 0.25 ถึง 1.25 MPa ค่าความซึมผ่านของทุกส่วนผสมจะลดลงในเชิงเวลาซึ่งให้ค่าอยู่ในช่วง 10^{-17} ถึง 10^{-15} ตร.ม. สัดส่วนของ S:C เท่ากับ 5:10 ให้ค่าความซึมผ่านต่ำสุด ค่าความซึมผ่านของรอยแตกประชิดภายใต้ความเค้นตั้งฉากที่ผันแปรจาก 1 ถึง 4 MPa อยู่ในช่วง 10^{-8} ถึง 10^{-10} ตร.ม. และของส่วนผสมที่อยู่ในรอยแตกมีระยะการเปิดเผยอเท่ากับ 0.2, 1.0 และ 2.0 ซม. มีค่าใกล้เคียงกันคือประมาณ 10^{-15} ตร.ม.

Abstract

The objective of this study is to assess the performance of sludge mixed with the commercial grade Portland cement type I for use in reducing permeability of fractures in sandstone. The fractures are artificially made in Phu Kradueng sandstone by applying a line load to induce a splitting tensile crack in 15×15×15 cm prismatic blocks. The Bang Khen water treatment sludge is used. The physical and chemical properties of the sludge are examined. This research emphasizes on determining the minimum slurry viscosity and appropriate strength of the grouting materials. The results indicate that the suitable mixing ratios for sludge:cement (S:C) are 1:10, 3:10, 5:10 and for bentonite:cement (B:C) are 1:10, 2:10, 3:10 with water-cement ratio of 1:1 by weight. These proportions yield the lowest slurry viscosity of 5 Pa·s and the highest compressive strength. For S:C = 3:10, the compressive strength and elastic modulus are 1.77 MPa and 224 MPa which are similar to those of bentonite mixed with cement. The shear strength of grouted fractures varies from 0.36 to 0.90 MPa under normal stresses ranging from 0.25 to 1.25 MPa. Permeability of grouting materials are from 10^{-17} to 10^{-15} m^2 and decrease with curing time. S:C of 5:10 give the lowest permeability. Fracture permeability under normal stress of 1 to 4 MPa ranges from 10^{-8} to 10^{-10} m^2. Permeabilities of grouted fractures with aperture of 0.2, 1.0 and 2.0 cm are about 10^{-15} m^2.

1. บทนำ

ปัจจุบันโรงงานผลิตน้ำบางเขนมีการผลิตและจ่ายน้ำในปริมาณที่สูงขึ้นวันละประมาณ 3.6 ล้าน ลบ.ม. มีตะกอนที่ต้องทำการกำจัดเฉลี่ย 247 ตันต่อวัน [1] และยังไม่สามารถนำตะกอนไปประยุกต์ใช้ประโยชน์ได้เท่าที่ควร ซึ่งในแต่ละปีจะต้องเสียค่าใช้จ่ายในการกำจัดตะกอนเป็นจำนวน 38 ล้านบาท และด้วยพื้นที่ที่ใช้เป็นบ่อกักตะกอนและบ่อตากตะกอนมีอยู่อย่างจำกัด ไม่สามารถขยายออกไปได้ การประปานครหลวงจึงได้ก่อสร้างโรงงานกำจัดตะกอนบางเขน โดยใช้วิธีรีดกรองเพื่อแยกกากตะกอนหมาด และน้ำที่ผ่านการบำบัดแล้วกลับมาใช้ประโยชน์ใหม่ ดังนั้นผู้วิจัยจึงมีแนวคิดที่จะนำตะกอนดินจากระบบผลิตน้ำประปามาใช้เป็นวัสดุทดแทนในภาคอุตสาหกรรมก่อสร้างด้วยการใช้เป็นวัสดุอุด (Grouting Material) โดยผสมกับซีเมนต์เพื่อลดความซึมผ่านของรอยแตกในมวลหินบริเวณรอบๆ โครงสร้างวิศวกรรม เช่น อุโมงค์ที่อยู่ใต้ระดับน้ำบาดาล ฐานรากของเขื่อนที่ตั้งอยู่บนมวลหินที่มีรอยแตกและการรุกล้ำของน้ำเค็มเข้าสู่ชั้นน้ำบาดาลบริเวณชายฝั่งทะเล อีกทั้งยังช่วยลดการใช้วัสดุอุดที่ผลิตจากทรัพยากรธรรมชาติและยังเป็นการลดวัสดุเหลือทิ้งที่ระบายออกสู่สิ่งแวดล้อม

วัตถุประสงค์ของการศึกษานี้คือเพื่อทำการศึกษาศักยภาพของตะกอนดินประปาผสมกับปูนซีเมนต์ปอร์ตแลนด์ในห้องปฏิบัติการ เพื่อนำมาประยุกต์ใช้อุดรอยแตกในมวลหินเพื่อลดค่าความซึมผ่าน

2. งานวิจัยที่เกี่ยวข้อง

มีผู้วิจัยหลายท่าน [2] ได้ศึกษาคุณสมบัติเบื้องต้นขององค์ประกอบเชิงเคมีและเชิงกลศาสตร์ของตะกอนดินจากโรงงานผลิตน้ำบางเขน โดยเสนอแนะให้ใช้ตะกอนดินประปาเป็นวัตถุดิบในอุตสาหกรรมเซรามิก เช่น ถ้วยชาม เครื่องประดับ มวลรวมประดิษฐ์ กระเบื้อง อิฐมอญ และบล็อกประสานดิน เป็นต้น นอกจากนี้ยังมีผู้วิจัยท่านอื่นอีกหลายท่าน [3] ได้ศึกษาคุณสมบัติการดูดซับตะกอนประปาเพื่อลดสีของน้ำเสียที่ผ่านการบำบัดแล้วจากอุตสาหกรรมฟอกย้อม

การศึกษาความซึมผ่านในรอยแตกเดี่ยว [4] มีปัจจัยหลักที่ควบคุมการไหลและค่าความซึมผ่าน คือ ความเปิดเผยอ ความขรุขระของผิวรอยแตก ทิศทางการวางตัว ความเค้นตั้งฉากและความเค้นเฉือน นอกจากนี้มีการทดสอบการไหลเพื่อคำนวณค่าเหนี่ยวนำชลศาสตร์ในรอยแตกหินภายใต้ความเค้นตั้งฉากและแนวเฉือนโดยใช้ตัวอย่างหินทราย [5-7]

ส่วนการศึกษาการลดค่าความซึมผ่านของรอยแตกในหิน เช่น งานขุดเจาะอุโมงค์ งานเหมืองแร่ งานกำแพงทึบน้ำใต้ดิน งานทิ้งกากกัมมันตรังสี ผู้วิจัยหลายท่านได้ศึกษาทดสอบในห้องปฏิบัติการและภาคสนามโดยใช้ซีเมนต์ ดินเบนทอไนต์ ดิน หรือขี้เถ้าลอยมาเป็นส่วนผสมวัสดุอุดในสัดส่วนที่เหมาะสมเพื่อให้คุณสมบัติเชิงกลศาสตร์และชลศาสตร์อยู่ในเกณฑ์ดีและมีความหนืดน้อย ผลวิจัยระบุว่าสามารถลดความซึมผ่านได้ [8-13]

3. ระเบียบวิธีวิจัยและผลการศึกษา

วัสดุหลักที่ใช้ในการศึกษานี้คือ 1) ตะกอนดินจากโรงกำจัดตะกอนบางเขนที่ถูกคัดขนาดเม็ดดินเล็กกว่า 0.075 มม. 2) ดินเบนทอไนต์ 3) ซีเมนต์ปอร์ตแลนด์ และ 4) หินที่มีรอยแตกโดยมีพื้นที่ของรอยแตกไม่ต่ำกว่า 152.4×152.4 มม. จำนวน 60 ตัวอย่างสำหรับการทดสอบความซึมผ่านและเส้นผ่านศูนย์กลาง 10 ซม. ยาว 10 ซม. ประมาณ 40 ตัวอย่างสำหรับการทดสอบกำลังเฉือนของวัสดุอุดกับรอยแตกหิน ในการศึกษานี้เลือกใช้หินทรายชุดภูกระดึง ซึ่งเป็นหินที่มีความซึมผ่านต่ำ เป็นเนื้อเดียวกัน และจัดเตรียมรอยแตกได้ง่าย

3.1 การทดสอบคุณสมบัติกายภาพ

ตะกอนดินประปาและดินเบนทอไนต์ถูกทดสอบคุณสมบัติกายภาพเกี่ยวกับค่าขีดจำกัดของ Atterberg ค่าความถ่วงจำเพาะ การกระจายอนุภาค ตามมาตรฐาน ASTM (D422, D854) เพื่อใช้เป็นข้อมูลพื้นฐาน

ผลการทดสอบคุณสมบัติกายภาพของตะกอนและเบนทอไนต์สามารถสรุปในตารางที่ 1 และผลการทดสอบการกระจายอนุภาคของตะกอนดินประปาเปรียบเทียบกับผลการทดสอบของกรมอุตสาหกรรมและการเหมืองแร่แสดงในรูปที่ 1

ตารางที่ 1 ค่าขีดจำกัดของ Atterberg และค่าความถ่วงจำเพาะของตะกอนดินประปาและดินเบนทอไนต์

Atterberg Limits	Bentonite content (%)		Sludge content (%)	
	SUT*	US [14]	SUT*	KU [15]
Liquid limit	357	478	55	69
Plastic limit	44	28	22	42
Plasticity index	313	449	23	28
Specific gravity	-	-	2.56	-

* Suranaree University of Technology Laboratory

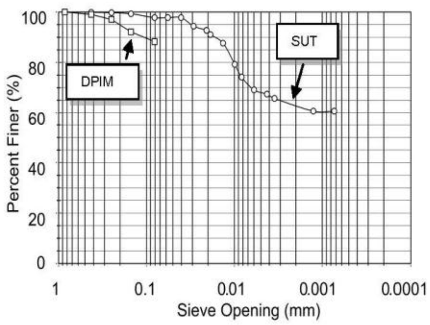

รูปที่ 1 การกระจายขนาดอนุภาคของตะกอนดินประปา

3.2 การทดสอบคุณสมบัติพื้นฐานของส่วนผสม

การทดสอบคุณสมบัติพื้นฐานของส่วนผสมเพื่อกำหนดวิธีและสัดส่วนที่เหมาะสมเพื่อนำไปใช้ในการทดสอบเชิงกลศาสตร์และเชิงชลศาสตร์ โดยใช้เกณฑ์ความหนืด กำลังกดสูงสุดและความซึมผ่าน ประกอบด้วย 3 กลุ่ม คือ 1) การทดสอบความหนืด 2) การทดสอบกำลังกดในแกนเดียวเบื้องต้น และ 3) การทดสอบความซึมผ่านของส่วนผสม

การจัดเตรียมส่วนผสมตะกอนดินประปากับซีเมนต์ (S:C) และส่วนผสมของดินเบนทอไนต์กับซีเมนต์ (B:C) มีค่าตั้งแต่ 0:10, 1:10, 2:10, 3:10, 4:10, 5:10, 6:10, 7:10, 8:10, 9:10 ถึง 10:10 แปรผันกับสัดส่วนน้ำต่อซีเมนต์ (W:C) ตั้งแต่ 4:10, 8:10, 10:10 ถึง 12.5:10 ชั่งวัสดุทั้งสี่ชนิดตามสัดส่วนที่กำหนดผสมให้เข้ากันด้วยเครื่องผสม โดยใช้ความเร็วไม่เกิน 275 รอบต่อนาที

การทดสอบความหนืดเริ่มจากนำส่วนผสมที่ได้จัดเตรียมไปทดสอบด้วยเครื่องวัดความหนืดพร้อมหาค่าความหนาแน่นและความถ่วงจำเพาะ (ASTM D2196) ของส่วนผสมเหลวขณะที่ยังไม่แข็งตัว

ผลการทดสอบความหนืดของส่วนผสมในสัดส่วนที่ต่างกันแสดงในรูปที่ 2 ซึ่งระบุว่า เมื่อสัดส่วนของซีเมนต์ลดลงส่วนผสมจะมีความหนืดเพิ่มขึ้นเป็นทวีคูณ โดยเฉพาะอย่างยิ่งเมื่อ B:C หรือ S:C มากกว่า 0.5 นอกจากนั้นเมื่อเพิ่มปริมาณน้ำจะทำให้ความหนืดของส่วนผสมมีค่าลดลง ซึ่งสอดคล้องกันทั้งส่วนผสมที่ใช้กับเบนทอไนต์และตะกอนดินประปา สำหรับส่วนผสมที่ใช้ดินเบนทอไนต์ สัดส่วนของน้ำต่อซีเมนต์ (W:C) ต้องไม่น้อยกว่า 1.0 เนื่องจากจะทำให้ส่วนผสมเหนียว เกาะตัวกันแน่น และหมดสภาพความเป็นของเหลว ทั้งนี้เกิดจากดินเบนทอไนต์มีความสามารถในการดูดซึมน้ำได้มาก และจับตัวกันเป็นก้อน ในขณะที่ส่วนผสมที่ใช้ตะกอนดินประปาสามารถเพิ่มและลดปริมาณของน้ำได้ในสัดส่วนที่กว้างกว่า และยังคงตัวเป็นของเหลวที่สามารถนำมาทดสอบความหนืดและค่ากำลังกดสูงสุดได้

การทดสอบกำลังกดในแกนเดียวเบื้องต้นส่วนผสมของตัวอย่างแท่งรูปทรงกระบอกขนาดเส้นผ่านศูนย์กลาง 5.08 ซม. สัดส่วนความยาวต่อเส้นผ่านศูนย์กลาง (L/D ratio) ประมาณ 2.0-2.5 ที่ถูกบ่มมาแล้ว 3 วัน ตัวอย่างแท่งถูกกดในแนวแกนด้วยโครงกดทดสอบที่อัตรา 1 MPa/s จนกระทั่งตัวอย่างวิบัติ

ผลการทดสอบกำลังกดในแกนเดียวเบื้องต้นแสดงในรูปที่ 3 ซึ่งระบุว่าค่ากำลังกดสูงสุดมีค่าใกล้เคียงกัน โดยเฉพาะเมื่อใช้ W:C = 1:1 เมื่อลดสัดส่วนของน้ำลงจะทำให้ค่ากำลังกดสูงขึ้น แต่ไม่เกิน 3 MPa และจะทำให้ส่วนผสมเหลวมีความหนืดเพิ่มมากขึ้น ซึ่งอาจจะไม่เป็นผลดีต่อการนำไปเป็นวัสดุอุดในรอยแตกของหิน แต่เมื่อเพิ่มปริมาณน้ำมากขึ้นที่ W:C > 1:1 ค่ากำลังกดจะลดลงอย่างมาก ดังนั้นผลการทดสอบนี้สามารถสรุปในเบื้องต้นได้ว่า W:C = 1:1 จะมีความเหมาะสมที่สุด

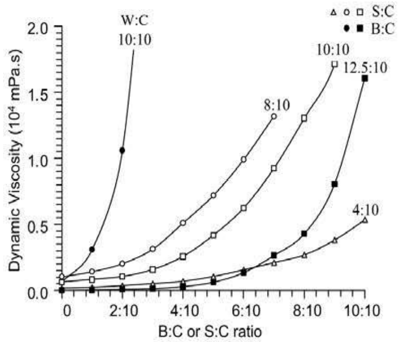

รูปที่ 2 ค่า Dynamic viscosity ของ ส่วนผสมเหลว

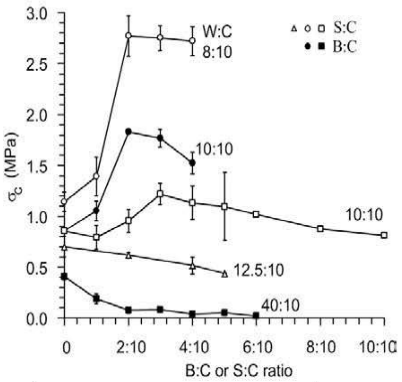

รูปที่ 3 ค่ากำลังกดสูงสุดของ B:C และ S:C ที่อัตราส่วนต่างๆ

การทดสอบความซึมผ่านของส่วนผสมทำหลังจากนำส่วนผสมที่ได้จัดเตรียมหล่อลงในท่อ PVC ขนาดเส้นผ่านศูนย์กลาง 10.16 ซม. สูง 15.24 ซม. ในการทดสอบนี้ได้ทำการทดสอบตามมาตรฐาน ASTM (C938, C39) ซึ่งมีการหาค่าความซึมผ่านในช่วงเวลาของการบ่มที่ต่างกัน คือ 3, 7, 14 และ 28 วันการทดสอบเริ่มจากการติดตั้งชุดประกอบแผ่นอะคริลิกหนา 1.5 ซม. ที่ปลายบนและล่างของแบบหล่อ PVC ที่จุดกึ่งกลางของแผ่นอะคริลิกมีรูที่ต่อกับหมุดยึดท่อแรงดันสูงเส้นผ่านศูนย์กลาง 6.35 มม. แผ่นด้านล่างต่อเข้ากับปั๊มน้ำ และแผ่นด้านบนจะต่อเข้ากับหลอดวัดปริมาตรน้ำปิเปตต์ ในขณะทดสอบจะทำการอัดน้ำ ด้วยความดันคงที่เท่ากับ 13.8 kPa โดยใช้วาล์วปรับความดันที่ส่วนบนของถังก๊าซไนโตรเจนและไล่ฟองอากาศออกให้ก่อนการตรวจวัดความซึมผ่านสามารถทำได้โดยจับเวลาการไหลของน้ำในเชิงปริมาตรที่หลอดวัดปริมาตรน้ำปิเปตต์ ความซึมผ่านของตัวอย่างส่วนผสมสามารถคำนวณได้จากสมการ (2) [4]

$$K = \frac{Q}{iA} \tag{1}$$

$$k = \frac{K \cdot \mu}{\gamma_w} \tag{2}$$

โดยที่ K คือ ค่าเหนี่ยวนำชลศาสตร์ของน้ำ (Hydraulic conductivity) Q คือ ปริมาตรของน้ำที่ไหลต่อช่วงเวลาที่ตรวจวัดจากหลอดวัดปริมาตรน้ำปิเปตต์ i คือ Hydraulic gradient A คือ พื้นที่หน้าตัดของตัวอย่าง k คือค่าความซึมผ่านทางกายภาพ (Intrinsic permeability) γ_w คือความหนาแน่นโดยมวลของน้ำ และ μ คือความหนืดของน้ำ (ใช้ที่อุณหภูมิ 25°C)

ผลการทดสอบค่าความซึมผ่านของทุกส่วนผสมจะลดลงในเชิงเวลาแสดงในรูปที่ 4

3.3 การทดสอบกำลังกดในแกนเดียว

การทดสอบกำลังกดในแกนเดียวมีวัตถุประสงค์เพื่อหาค่ากำลังกดสูงสุด ค่าสัมประสิทธิ์ความยืดหยุ่น และอัตราส่วน Poisson ของส่วนผสมที่ได้คัดสรรมาจากการทดสอบเบื้องต้นในหัวข้อ 3.2 ดังนี้ S:C เท่ากับ 1:10, 3:10, 5:10, B:C เท่ากับ 1:10, 2:10, 3:10 และซีเมนต์ล้วน ทุกส่วนผสมกำหนด W:C เท่ากับ 1:1 การจัดเตรียมตัวอย่างและการทดสอบได้ดำเนินการตามมาตรฐาน ASTM (D7012, C938, C39) และทำการบ่มเป็นเวลา 3 วันก่อนนำมาทดสอบ โดยตัวอย่างถูกกดในแนวแกนด้วยเครื่องกดทดสอบที่อัตรา 1 MPa/s ในขณะเดียวกันได้มีการตรวจวัดการเปลี่ยนรูปร่างในแนวแกนและแนวเส้นผ่านศูนย์กลาง ด้วยมาตรวัดที่มีความละเอียด ±0.01 มม. ซึ่งดำเนินการจนกระทั่งตัวอย่างเกิดการวิบัติ ผลที่ได้นำเสนอในความสัมพันธ์ระหว่างค่าความเค้นกับความเครียดในแนวแกนและแนวเส้นผ่านศูนย์กลาง

รูปที่ 5 แสดงกราฟเปรียบเทียบค่ากำลังกดที่ได้จากตัวอย่างส่วนผสมที่มีเส้นผ่านศูนย์กลาง 10.16 ซม. และ 5.08 ซม. ซึ่งระบุว่าส่วนผสมที่มีแบบหล่อขนาดใหญ่สามารถทำปฏิกิริยาทางเคมีระหว่างซีเมนต์กับดินเบนทอไนต์ หรือซีเมนต์กับตะกอนดินประปาได้ดีกว่าส่วนผสมที่ได้จากแบบหล่อขนาดเล็ก

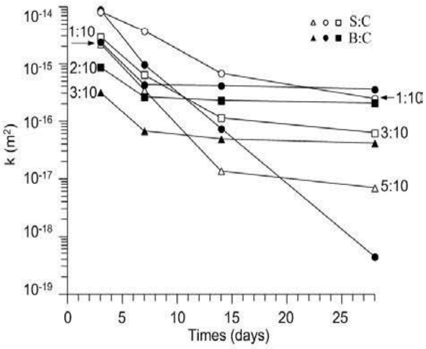

รูปที่ 4 ผลการทดสอบความซึมผ่านของส่วนผสม

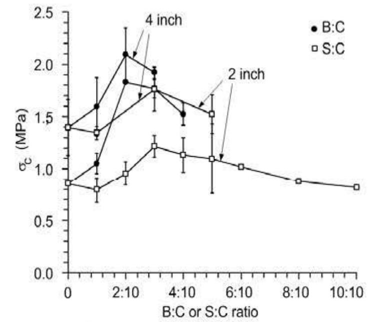

รูปที่ 5 ผลการทดสอบแรงกดในแกนเดียว

ค่ากำลังกดในแกนเดียว (σ_c) และคุณสมบัติความยืดหยุ่น (E) ของส่วนผสมที่มีเส้นผ่านศูนย์กลาง 101.6 มม. ได้แสดงไว้ในตารางที่ 2 ซึ่งผลการทดสอบแสดงให้เห็นว่าค่ากำลังกดสูงสุดของส่วนผสมที่ใช้ดินเบนทอไนต์และที่ใช้ตะกอนดินประปามีค่าใกล้เคียงกัน โดยส่วนผสมทั้งสองชนิดมีค่ากำลังกดสูงสุดอยู่ที่ประมาณ 2 MPa

3.4 การทดสอบกำลังเฉือนของส่วนผสมกับรอยแตกหิน

วัตถุประสงค์ของการทดสอบกำลังเฉือนของส่วนผสมกับรอยแตกหินเพื่อหาค่ากำลังเฉือนสูงสุดที่เกิดขึ้นบริเวณรอยต่อระหว่างผิวของส่วนผสมกับผิวของรอยแตกในหิน ซึ่งเป็นปัจจัยกำหนดความสามารถในการต้านแรงเฉือนของส่วนผสมที่สัดส่วนต่างๆ ต่อแรงที่มากระทำในแนวขนานกับรอยแตก การทดสอบได้ใช้สัดส่วนของส่วนผสมที่คัดเลือกมาจากผลการทดสอบ วิธีการผสมและการบ่มได้ดำเนินการตามหัวข้อ 3.2

การทดสอบกำลังเฉือนของส่วนผสมกับรอยแตกของหินจะใช้อุปกรณ์ทดสอบกำลังเฉือนแบบสามวงแหวน โดยนำตัวอย่างหินที่มีวัสดุอุดในรอยแตกที่บ่มมาแล้ว 3 วัน ประกอบเข้ากับชุดทดสอบในรูปที่ 6 [16] การทดสอบได้ใช้ความเค้นในแนวตั้งฉาก 5 ระดับตั้งแต่ 0.25, 0.50, 0.75, 1.00 ถึง 1.25 MPa ระหว่างทำการทดสอบจะมีการบันทึกค่าแรงเฉือนและปริมาณการเคลื่อนตัวในแนวเฉือนอย่างต่อเนื่อง พร้อมทั้งสังเกตลักษณะการวิบัติของตัวอย่าง ผลการทดสอบได้นำเสนอในรูปของความสัมพันธ์ระหว่างค่าความเค้นในแนวตั้งและแนวเฉือน

ผลการคำนวณค่าคงที่ของกฎ Coulomb แสดงในตารางที่ 3 ความสัมพันธ์ระหว่างค่ากำลังเฉือนในฟังก์ชันของความเค้นในแนวตั้งฉาก (รูปที่ 7) ซึ่งผลที่ได้ระบุว่าส่วนผสมที่เลือกมาทั้ง 6 สัดส่วน มีค่ามุมเสียดทาน (ϕ_p) ใกล้เคียงกันมากและมีค่าความเค้นยึดติด (c_p) ต่างกันเพียงเล็กน้อย

3.5 การทดสอบความซึมผ่านในรอยแตกของหิน

ค่าความซึมผ่านในรอยแตกของหินเพื่อใช้เป็นข้อมูลพื้นฐานในการเปรียบเทียบขีดความสามารถของส่วนผสมในระดับต่างๆ ทดสอบความซึมผ่านในรอยแตกภายใต้ความเค้นกดที่ตั้งฉากกับรอยแตกในระดับต่างๆ กัน คือ 1, 2, 3 และ 4 MPa จำนวน 5 ตัวอย่าง ตัวอย่างหินส่วนบนถูกเจาะเป็นรูกลมในทิศทางตั้งฉากกับระนาบการวางตัวของชั้นหิน มีเส้นผ่านศูนย์กลาง 12 มม. ลึก 10.16 ซม. อยู่ที่จุดกึ่งกลางเพื่อใช้เป็นทางส่งแรงดันน้ำเข้าสู่รอยแตก ตัวอย่างถูกกดทดสอบโดยใช้เครื่องทดสอบ รูปที่ 8 ระหว่างการทดสอบได้มีการบันทึกค่าปริมาตรน้ำและเวลา ผลที่ได้นำเสนอในรูปแผนภูมิระหว่างค่าความเค้นตั้งฉาก (σ_n) กับค่าความเปิดเผยอชลศาสตร์ (e_h) ค่าเหนี่ยวนำชลศาสตร์ (K) และค่าความซึมผ่านในรอยแตกเดี่ยว (k) เป็นตามสมการ (3) ถึง (5) [6]

$$e_h = \left(\frac{1}{3}\right)\left\{\frac{(6\mu q)}{\pi \Delta P}\ln\left(\frac{r}{r_0}\right)\right\} \qquad (3)$$

ตารางที่ 2 ผลการทดสอบแรงกดในแกนเดียว

Type	Mix ratio	σ_c (MPa)	ν	E (MPa)
C	0:10	1.40	0.18	212
B:C	1:10	1.59	0.17	193
B:C	2:10	2.09	0.14	275
B:C	3:10	1.92	0.16	228
S:C	1:10	1.35	0.15	190
S:C	3:10	1.77	0.21	224
S:C	5:10	1.52	0.16	261

ตารางที่ 3 ค่าคงที่ตามกฎการแตกของ Coulomb

Sample No.	c_p (MPa)	$\tan\phi_p$	ϕ_p (°)	R^2
C	0.563	0.263	14.7	0.962
S:C=1:10	0.275	0.436	23.6	0.985
S:C=3:10	0.213	0.435	23.5	0.988
S:C=5:10	0.255	0.428	23.2	0.985
B:C=1:10	0.306	0.424	23.0	0.968
B:C=2:10	0.121	0.410	22.3	0.998
B:C=3:10	0.143	0.430	23.3	0.996

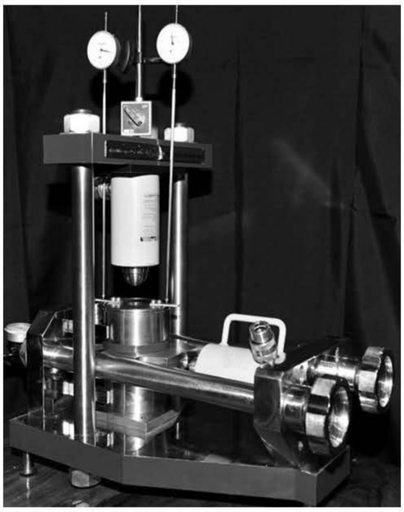

รูปที่ 6 เครื่องทดสอบกำลังเฉือนแบบสามวงแหวน [16]

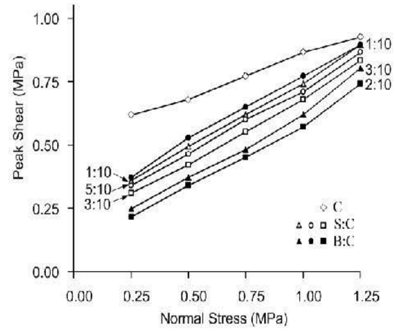

รูปที่ 7 ผลการทดสอบค่ากำลังเฉือนของส่วนผสม

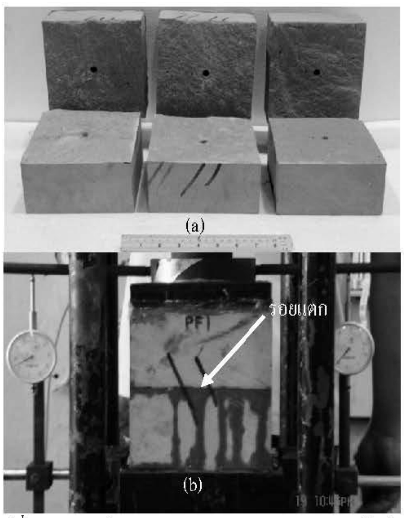

รูปที่ 8 (a) ตัวอย่างรอยแตกหิน (b) การทดสอบความซึมผ่านของรอยแตก

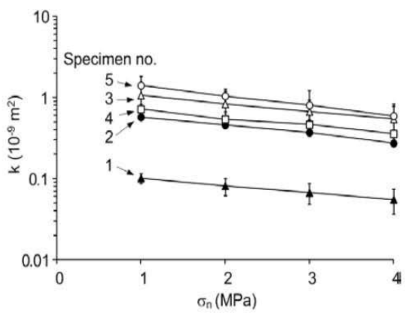

รูปที่ 9 ค่าความซึมผ่านที่สัมพันธ์กับ σ_n

$$K = \gamma_w \frac{e_h^{\ 2}}{12\mu} \tag{4}$$

$$k = \frac{e_h^{\ 2}}{12} \tag{5}$$

โดยที่ e_h คือระยะเปิดเผยอเชิงไฮดรอลิกของรอยแตก γ_w คือความหนาแน่นโดยมวลของน้ำ μ คือความหนืดเชิงพลศาสตร์ r0 คือรัศมีของรูที่จุดกึ่งกลางของตัวอย่างรอยแตก r คือระยะจากจุดกึ่งกลางของรอยแตกถึงขอบนอก q คืออัตราไหลเชิงปริมาตรที่วัดได้จากการทดสอบ และ ΔP คือค่าความดันของน้ำที่อัดเข้าไปที่รูกลางของตัวอย่างหิน

ผลที่ได้จากการทดสอบความซึมผ่านในรอยแตกของหินตัวอย่างที่ 1 ถึง 5 ที่ระดับความเค้นตั้งฉากตั้งแต่ 1 ถึง 4 MPa แสดงในรูปที่ 9 ระบุว่ามีค่าความซึมผ่านในรอยแตกเดี่ยวน้อยกว่า 1.4×10^{-9} ตร.ม.

3.6 การทดสอบความซึมผ่านของส่วนผสมในรอยแตกหิน

ค่าความซึมผ่านของส่วนผสมเป็นปัจจัยสำคัญที่จะบ่งบอกถึงการไหลซึมของน้ำในรอยแตกของหินได้มากหรือน้อย การทดสอบความซึมผ่านจะมีวัสดุอุดอยู่ภายในรอยแตกที่มีการเปิดเผยอ 0.2, 1.0 และ 2.0 ซม. ที่เวลาบ่ม 3 วัน ตัวอย่างหินและวิธีทดสอบจะมีลักษณะตามหัวข้อ 3.2 แผนภูมิแสดงลักษณะการทดสอบและการจัดเตรียมอุปกรณ์แสดงตามรูปที่ 11 และ 12

ตัวอย่างหินทั้ง 21 ตัวอย่างถูกให้แรงดันน้ำคงที่ในขณะทดสอบ ซึ่งอยู่ในช่วง 13.8 ถึง 551.7 kPa โดยการทดสอบเริ่มจากความเค้นกดส่วนผสมในรอยแตกจากน้อยไปมาก กล่าวคือ จาก 0.25 ,0.50 ,0.75, 1.00 และ 1.25 MPa ในแต่ละระดับความเค้นกดบนส่วนผสมในรอยแตก ค่าเหนี่ยวนำชลศาสตร์และค่าความซึมผ่านของส่วนผสมในรอยแตกสามารถคำนวณได้จากสมการ (6) และ (7) [4] ดังนี้

$$K = \frac{Q}{2\pi L H_c} \ln\left(\frac{2mL}{D}\right) \tag{6}$$

$$k = \frac{K\mu}{\gamma_w} \tag{7}$$

โดยที่ Q คืออัตราการไหลเชิงปริมาตรของน้ำที่ไหลผ่านส่วนผสม (หลังจากหักลบน้ำที่ไหลผ่านรอยต่อระหว่างส่วนผสมกับผิวหินแล้ว) m คือรากที่สองของสัดส่วนระหว่างค่าเหนี่ยวนำการไหลในแนวขนานกับรอยแตกกับแนวตั้งฉากกับรอยแตก กรณีนี้มีค่าคงที่เท่ากับ 1 ส่วน L คือความหนาของส่วนผสมในรอยแตก (0.2, 1.0 และ 2.0 ซม.) D คือเส้นผ่านศูนย์กลางของรูเจาะที่จุดกึ่งกลางของตัวอย่าง H_c คือแรงดันเมื่อเทียบกับความสูงของน้ำ ซึ่งมีค่าคงที่

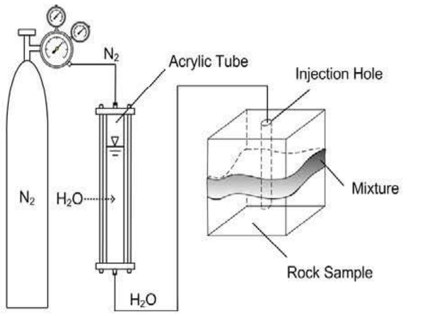

รูปที่ 10 แผนภูมิแสดงลักษณะการทดสอบความซึมผ่านของส่วนผสมในรอยแตกในหินที่มีการเปิดเผยอ

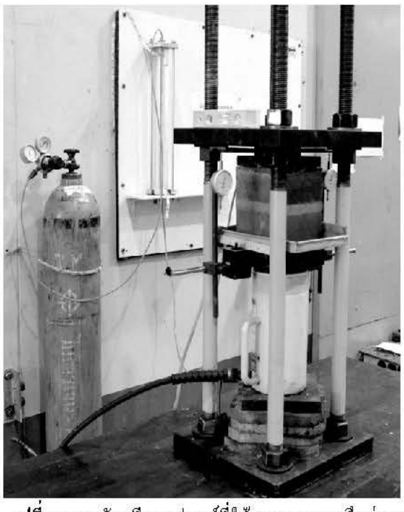

รูปที่ 12 การจัดเตรียมอุปกรณ์ที่ใช้ทดสอบความซึมผ่านของส่วนผสมในรอยแตกที่เปิดเผยอ

รูปที่ 12 ระบุว่าค่าความซึมผ่านเชิงกายภาพของส่วนผสมในรอยแตกหินทั้ง 21 ตัวอย่างมีค่าสอดคล้องกับผลที่ทดสอบได้ในหัวข้อ 3.5

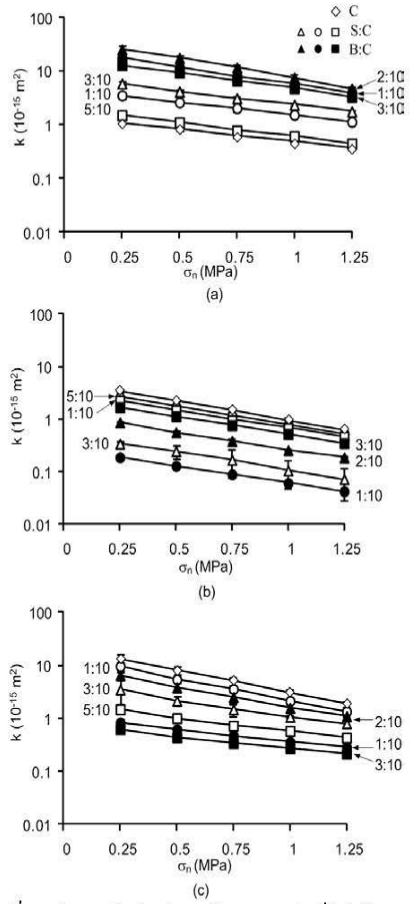

รูปที่ 12 ค่าความซึมผ่านวัสดุอุดในรอยแตกหินที่มีค่าเปิดเผยอ (a) 0.2 ซม. (b) 1.0 ซม. และ (c) 2.0 ซม.

7. สรุปผลการศึกษา

ตะกอนดินประปาผสมกับปูนซีเมนต์ปอร์ตแลนด์มีศักยภาพเพื่อนำมาประยุกต์ใช้อุดรอยแตกในมวลหินเพื่อลดค่าความซึมผ่านแทนวัสดุอุดเบนทอไนต์กับซีเมนต์ โดยกำหนดชนิดของวัสดุอุดที่นำมาใช้ในการศึกษาประกอบด้วย ตะกอนดินประปาจากโรงกำจัดตะกอนบางเขน ปูนซีเมนต์ตรานกอินทรีย์จากบริษัทปูนซีเมนต์นครหลวง จำกัด และดินเบนทอไนต์ของบริษัท American Colloid Company

การทดสอบส่วนผสมที่หลากหลายระหว่างตะกอนดิน ซีเมนต์ และน้ำ และระหว่างดินเบนทอไนต์ ซีเมนต์ และน้ำ เพื่อให้ได้มาซึ่งสัดส่วนที่เหมาะสมและเลือกใช้อุดรอยแตกในหิน กล่าวคือ จะต้องมีคุณสมบัติเชิงกลศาสตร์และชลศาสตร์อยู่ในเกณฑ์ดีและมีความหนืดน้อย ในขั้นตอนนี้ได้มีการคัดเลือกสัดส่วน S:C เท่ากับ 1:10, 3:10 และ 5:10 และสัดส่วน B:C เท่ากับ 1:10, 2:10 และ 3:10 โดยทั้ง 6 สัดส่วนจะใช้ปริมาณน้ำต่อซีเมนต์เท่ากับ 1:1 เนื่องจากจะให้ค่ากำลังกดสูงประมาณ 2 MPa ในขณะที่มีค่าความหนืดของส่วนผสมเหลวไม่เกิน 5 Pa·s ผลการทดสอบสมบัติเชิงกลศาสตร์ระบุว่าส่วนผสมตะกอนดินกับซีเมนต์ที่อัตราส่วน 3:10 จะให้ค่ากำลังกดสูงสุดเท่ากับ 1.77 MPa และค่าสัมประสิทธิ์ความยืดหยุ่นเท่ากับ 224 MPa ซึ่งจะต่ำกว่าค่าที่ได้จากส่วนผสมระหว่างดินเบนทอไนต์กับซีเมนต์เพียงร้อยละ 10 ค่ากำลังเฉือนระหว่างผิวรอยแตกกับส่วนผสมทั้ง 6 สัดส่วน มีค่าใกล้เคียงกันคืออยู่ในช่วง 0.36 ถึง 0.90 MPa ซึ่งขึ้นกับค่าความเค้นกดที่ให้บนตัวอย่างหิน

ผลการทดสอบความซึมผ่านของส่วนผสมระบุว่าค่าความซึมผ่านของทุกส่วนผสมจะลดลงในเชิงเวลา โดยเฉพาะอย่างยิ่งในช่วง 7 วันแรก จากนั้นค่าความซึมผ่านจะมีค่าค่อนข้างคงที่หลังจากบ่มได้ 14 ถึง 28 วัน หลังจากถูกบ่มมาแล้วส่วนผสมทุกสัดส่วนจะมีค่าความซึมผ่านเชิงกายภาพผันแปรอยู่ในช่วง 10^{-17} ถึง 10^{-15} ตร.ม. ผลการทดสอบความซึมผ่านของรอยแตกประชิดระบุว่าที่ภายใต้ความเค้นตั้งฉากที่ผันแปรจาก 1 ถึง 4 MPa มีค่าความซึมผ่านอยู่ในช่วง 10^{-8} ถึง 10^{-10} ตร.ม. ผลการทดสอบความซึมผ่านของส่วนผสมที่อยู่ในรอยแตกมีระยะการเปิดเผยอเท่ากับ 0.2, 1.0 และ 2.0 ซม. มีค่าความซึมผ่านใกล้เคียงกันคือประมาณ 10^{-15} ตร.ม. ซึ่งหมายถึงภายใต้การผสมในสัดส่วนที่เหมาะสมส่งผลให้ ตะกอนดินประปามีศักยภาพเชิงชลศาสตร์ทัดเทียมกับส่วนผสมที่ใช้ดินเบนทอไนต์

8. กิตติกรรมประกาศ

การศึกษาครั้งนี้ได้รับทุนสนับสนุนจากมหาวิทยาลัยเทคโนโลยีสุรนารี จากการส่งเสริมการศึกษาระดับอุดมศึกษา และมหาวิทยาลัยวิจัยแห่งชาติ จึงขอขอบพระคุณอย่างสูงซึ่งที่อนุญาตให้เผยแพร่บทความนี้

เอกสารอ้างอิง

[1] คมกริช เวชสัสถ์, สุทธิรักษ์ บูชากุล, ปาริฉัตร ปั้นทอง และ สุรเดช เหรัมพกุล, "การออกแบบและก่อสร้างระบบกำจัดตะกอนโดยใช้วิธีรีดกรองโรงงานผลิตน้ำบางเขน" การประชุมวิชาการวิศวกรรมโยธาแห่งชาติ ครั้งที่ 15, อุบลราชธานี, 2553.

[2] นพปฎล เสงี่ยมศักดิ์ และเรืองรุชดิ์ ชีรโรจน์, "การศึกษาคุณสมบัติมวลรวมประดิษฐ์ที่ทำจากตะกอนน้ำประปา" การประชุมวิชาการวิศวกรรมโยธาแห่งชาติ ครั้งที่ 13, พัทยา, 2551.

[3] ฤชากร คงทอง และกฤติยากร เลิศโภคะสมบัติ, "การศึกษาตะกอนสลัดจ์จากโรงผลิตน้ำประปาในการดูดซับสีย้อม" การประชุมวิชาการวิศวกรรมโยธาแห่งชาติ ครั้งที่ 11, ภูเก็ต, 2549.

[4] B. Indraratna, and P. Ranjith, "Hydromechanical Aspects and Unsaturated Flow in Joints Rock" Lisse: A.A. Balkema, 2001.

[5] J. Obcheoy, S. Aracheeploha, and K. Fuenkajorn, "Fracture permeability under normal and shear stresses" Rock Mechanics, Fuenkajorn & Phien-wej (eds), Geomechanics Research Unit, Suranaree University of Technology, Thailand, 2011, pp. 133-140.

[6] N. Akkrachattrarat, P. Suanprom, J. Buaboocha, and K. Fuenkajorn, "Flow testing of sandstone fractures under normal and shear stresses" Rock Mechanics, Fuenkajorn & Phien-wej (eds), Geomechanics Research Unit, Suranaree University of Technology, Thailand, 2009, pp. 319-334.

[7] P. Suanprom, J. Obcheoy, and K. Fuenkajorn, "Permeability of Rock Fractures under Shear Stresses" EIT-JSCE Joint International Symposium Geotechnical Infrastructure Asset Management, Bangkok, Thailand, 2009.

[8] A. Fransson, "Characterisation of a fractured rock mass for a grouting field Test" Tunnelling and Underground Space Technology, 2001, Vol. 16, pp. 331-339.

[9] R. Gothall, and H. Stille, "Fracture – fracture interaction during grouting" Tunnelling and Underground space Technology, 2001, Vol 25, pp. 199-204.

[10] A. Fransson, C.F. Tsang, J. Rutqvist, and G. Gustafson, "Effects of the injection grout Silica sol on bentonite" International Journal of Rock Mechanics and Mining Sciences, 2007, Vol. 47, pp. 887-893.

[11] K. Fuenkajorn, "Design process for sealing of boreholes in rock mass" Rock Mechanics, Fuenkajorn & Phien-wej (eds), Geomechanics Research Unit, Suranaree University of Technology, Thailand, 2007, pp. 245-252.

[12] J. Funehag, and A. Fransson, "Sealing narrow fractures with a Newtonian fluid: Model prediction for grouting verified by field study" Tunnelling and Underground Space Technology, 2006, Vol. 21, pp. 492-498.

[13] A. Varol, and S. Dalgic, "Grouting applications in the Istanbul metro, Turkey" Tunnelling and Underground Space Technology, 2006, Vol. 21, pp. 602-612.

[14] D. Castelbaum, and C.D. Shackelford, "Hydraulic Conductivity of Bentonite Slurry Mixed Sands" Geotechnical and Geoenvironmental Engineering, 2009, Vol. 135, No. 12, pp. 1941-1956.

[15] P. Kanchanamai, "The utilization of sludge from Bang Khen water treatment plant in construction industry" A thesis submitted in partial fulfilment of the requirements for the degree of master of engineering in the faculty of graduate studies, Kasetsart University, 2003.

[16] กิตติเทพ เฟื่องขจร, "การประดิษฐ์แบบหล่อทดสอบการบดอัดและกำลังเฉือนแบบสามวงแหวน" รายงานวิจัย รหัสโครงการ 3-1/54 กองทุนนวัตกรรมและสิ่งประดิษฐ์ สมเด็จพระเทพรัตนราชสุดาฯ สยามบรมราชกุมารี, มหาวิทยาลัยเทคโนโลยีสุรนารี, นครราชสีมา, 2554, 53 หน้า.

[17] J.C. Jaeger, "The frictional properties of joints in rocks" Geofis pura appl., 1959, Vol. 43, pp. 148-158.

Decision Letter (SJST-2013-0170.R1)

From: proespichaya.k@psu.ac.th

To: aek@live.in, d5340248@g.sut.ac.th

CC:

Subject: Songklanakarin Journal of Science and Technology - Decision on Manuscript ID SJST-2013-0170.R1

Body: 24-Mar-2014

Dear Mr. Wetchasat:

It is a pleasure to accept your manuscript entitled "Mechanical and Hydraulic Performance of Sludge-Mixed Cement Grout in Rock Fractures" in its current form for publication in the Songklanakarin Journal of Science and Technology.

Thank you for your fine contribution. On behalf of the Editors of the Songklanakarin Journal of Science and Technology, we look forward to your continued contributions to the Journal.

Sincerely,
Prof. Proespichaya Kanatharana
Editor in Chief, Songklanakarin Journal of Science and Technology
proespichaya.k@psu.ac.th

Reviewer(s)' Comments to Author:

Date Sent: 24-Mar-2014

Close Window

Songklanakarin Journal of Science and Technology SJST-2013-0170.R1 Wetchasat

Mechanical and Hydraulic Performance of Sludge-Mixed Cement Grout in Rock Fractures

Journal:	*Songklanakarin Journal of Science and Technology*
Manuscript ID:	SJST-2013-0170.R1
Manuscript Type:	Original Article
Date Submitted by the Author:	23-Mar-2014
Complete List of Authors:	Wetchasat, Khomkrit; Maintenance Division, Phaya Thai Branch Office, Metropolitan Waterworks Authority; Institute of Engineering, School of Geotechnology
Keyword:	Engineering and Industrial Research

Reviewer: 1

Q1. Page 6 line 8: "conductivit" should be "conductivity"

A1. Corrected.

Q2. The English word describing activities in the past should be in past tense.

A2. Corrected.

Reviewer: 2

Comments to the Author

None

Mechanical and Hydraulic Performance of Sludge-Mixed Cement Grout in Rock Fractures

Khomkrit Wetchasat*

Kittitep Fuenkajorn

School of Geotechnology, Institute of Engineering, Suranaree University of Technology

University Avenue, Muang District, Nakhon Ratchasima 30000, THAILAND

*Tel.: 66-44-224-443, Fax.: 66-44-224-448, *E-mail: d5340248@g.sut.ac.th*

ABSTRACT: The objective is to assess the performance of sludge mixed with the commercial grade Portland cement type I for use in minimizing permeability of fractures in rock. The fractures were artificially made by applying a line load to sandstone block specimens. The sludge comprises over 80% of quartz with grain sizes less than 75 μm. The results indicate that the mixing ratios of sludge:cement (S:C) of 1:10, 3:10, 5:10 with water:cement ratio of 1:1 by weight are suitable for fracture grouting. For S:C = 3:10, the compressive strength and elastic modulus are 1.22 MPa and 224 MPa which are comparable to those of bentonite mixed with cement. The shear strengths between the grouts and fractures surfaces are from 0.22 to 0.90 MPa. The S:C ratio of 5:10 gives the lowest permeability. The permeability of grouted fractures with apertures of 2, 10 and 20 mm range from 10^{-16} to 10^{-14} m^2 and decrease with curing time.

Keywords: rock fracture, grouting, permeability, sludge, cement

1 INTRODUCTION

The increasing amount of the water treatment sludge from the Metropolitan Waterworks Authority of Thailand (MWA) has called for a permanent solution to dispose of the sludge from the Bang khen Water Treatment Plants. The MWA report (2007-2009) indicates that the plant produces sludge with the maximum capacity of 3.2×10^{6} m^3 per day. The sludge has been collected from the water treatment process. The increasing rate of the sludge is about 247×10^{3} kg per day. One of the solutions is to apply the sludge to minimize groundwater circulation in rock mass. Groundwater in rock mass is one of the key factors governing the mechanical stability of slope embankments, underground mines, tunnels, and dam foundation. A common solution practiced internationally in the construction industry is to use bentonite mixed with cement as a grouting material to reduce permeability in fractured rock mass (Akgün and Daemen, 1999; Papp, 1996). Knowledge and experimental evidences about the permeability of the sludge-mixed cement in fractured rock under varied stress conditions have been rare. The objectives of this study are to assess the performance of sludge mixed with the commercial grade Portland cement for reducing permeability in saturated fractured rock under various stresses in the laboratory and to compare the results with those of the bentonite-mixed cement in terms of the mechanical and hydraulic performance.

2 GROUTS PREPARATION

The grouting materials used in this study are (1) sludge with particle sizes less than 75 μm, (2) commercial grade bentonite, and (3) commercial grade Portland cement type I for mixing with the sludge and bentonite. The fractures in sandstone collected from Phu Kradung formation were artificially made by applying a line load to induce a splitting tensile crack. Two shapes of the sandstone samples are 152.4×152.4×152.4 mm^3 blocks and 100 mm diameter cylinder with 100 mm in length. Bentonite is from American Colloid Company.

Sludge and bentonite were tested for the Atterberg's limits, specific gravity, and particle size distribution. The equipment and test procedure follow the ASTM standards (D422, D854). The results are summarized in Table 1. Figure 1 shows the particle size distributions of the sludge used here.

3 BASIC MECHANICAL PROPERTIES OF GROUTING MATERIALS

The basic mechanical properties of the mixtures were determined to select the appropriate proportions of sludge-to-cement ratios. The sludge-mixed cement ratios (S:C) of 0:10, 1:10, 2:10, 3:10, 4:10, 5:10, 6:10, 8:10 and 10:10 by weight were prepared with water-cement ratios (W:C) of 0.8:1, 1:1 and 1.25:1. The bentonite-mixes cement ratios (B:C) are 0:10, 1:10, 2:10, 3:10, 4:10, and 5:10 by weight with water-cement ratios (W:C) of 1:1, 4:1. Mixing of all grouts was accomplished using a blade paddle mixer as suggested by ASTM standard (C938). The mixtures were placed in a 54 mm PVC mold. They were cured under water at room temperature (ASTM C192). Viscosity measurement follows, as much as practical, the ASTM standard (D2196). The results are shown in Figure 2.

The procedure for determining the grout permeability is similar to the ASTM standard (C938, C39). The water flow tests were conducted at 3, 7, 14 and 28 days of curing. The mold has an inner diameter of 101.6 mm with a length of 152.4 mm. The prepared specimen was sealed between two acrylic platens with the aid of O-ring rubber and epoxy coating. Inlet port was installed at the end of the mold and connected to a water pressure tube compressed by nitrogen gas at about 13.8 kPa. Air bubbles were bled out before measuring the permeability. Outlet port was installed at the other end and connected to a high precision pipette for measuring the outflow. The coefficient of permeability is computed from the flow rate based on the Darcy's law. The results are presented in Figure 3.

4 UNIAXIAL COMPRESSIVE STRENGTH OF GROUTING MATERIALS

The uniaxial compressive strength, elastic modulus, and Poisson's ratio of the grouting materials were determined. The results indicate that the suitable mixing ratios for the S:C are 1:10, 3:10, 5:10 and for the B:C are 1:10, 2:10, 3:10 with the W:C of 1:1 by weight. These proportions yield the lowest slurry viscosity of 5 Pa·s and the highest compressive strength. Preparation of these samples follows, as much as practical, the ASTM standard (C938, C39, D7012). All specimens were cured for 3 days before testing. During the test, the axial deformation and lateral deformation were monitored. The maximum load at the failure was recorded. The compressive strength (σ_C), Poisson's ratio (ν), and elastic modulus (E) are determined. The results of the S:C and B:C mixtures indicate that the chemical reaction between cement and water with the large casts were better than the small ones. Figure 4 shows the uniaxial compressive strength for the S:C and B:C with W:C = 1:1. The uniaxial compressive strength and elastic modulus for the specimens with the diameter of 101.6 mm are summarized in Table 2. The maximum compressive strengths for the S:C and B:C are similar.

5 SHEARING RESISTANCE BETWEEN GROUT AND FRACTURE

The maximum shear strengths of grouting material in sandstone fractures were determined by direct shear testing. The test procedure is similar to the ASTM standard (D5607). Three-ring shear test equipment was used. All specimens were cured for three days before testing. Laboratory arrangement for the three-ring shear test equipment is shown in Figure 5. The constant normal stresses used were 0.25, 0.5, 0.75, 1.0 and 1.25 MPa. The shear stress was applied while the shear displacement and dilation were monitored for every 0.2 mm of shear displacement. The failure modes were recorded. The test results are presented in the forms of the shear strength as a function of normal stress in Figure 6. The angles of internal friction and cohesion for all mixtures are similar.

6 PERMEABILITY TESTING OF FRACTURES

The objective of this task is to assess the permeability of rock fractures under varying normal stresses. The fracture permeability is used to compare with the permeability of grouting materials for both sludge and bentonte mixtures. Constant head flow tests were performed. The normal stresses are from 1 to 4 MPa. The experimental procedure is similar to Obcheoy et al. (2011). Five specimens were prepared and tested. The injection hole at the center of the upper block is 12 mm in diameter and 101.6 mm in depth. The tests were conducted by injecting water into the center hole of the rectangular block specimen. The laboratory arrangement of the constant head flow test is shown in Figure 7. Water volume and time were recorded. Both tend to decrease exponentially with the normal stress. The permeability results (k) are plotted as a function of the normal stress (σ_n) in Figure 8. The equivalent hydraulic aperture (e_h) for the radial flow, hydraulic conductivity between smooth and parallel plates (K), and intrinsic permeability (k) are calculated by (Tsang, 1992; Indraratna and Ranjith, 2001) :

$$e_h = \left\{ \frac{6\mu q}{\pi \Delta P} \ln\left(\frac{r}{r_0}\right) \right\}^{\frac{1}{3}} \quad (1)$$

$$K = \gamma_w \frac{{e_h}^2}{12\mu} \quad (2)$$

$$k = \frac{{e_h}^2}{12} \quad (3)$$

where μ is the dynamic viscosity of the water ($N \cdot s/cm^2$), q is water flow rate through the specimen (cm^2/s), ΔP is injecting water pressure into the center hole of rectangular blocks of the specimen, r is radius of flow path (m), r_0 is radius of the radius injection hole (m). γ_w is unit weight of water (N/m^2). The results indicate that the intrinsic permeability of the fractures is less than 1.4×10^{-9} m^2.

7 PERMEABILITY OF GROUTING MATERIALS IN ROCK FRACTURES

The permeability of sludge- and bentonite-mixed cement in artificial fractures was determined. The testing method is similar to that described above. The grouting materials were injected into the fractures. The fracture apertures are 2, 10, and 20 mm. The grouting materials were cured for 3 days. Figure 9 shows the laboratory arrangement. Constant head flow tests was performed. The constant head ranges between 13.8 and 551.7 kPa. The constant normal stresses are 0.25, 0.5, 1.0 and 1.25 MPa. The results indicate that the normal stress could reduce the permeability of grouting materials in sandstone fractures. The intrinsic permeability (k) is calculated from the measured flow rate (Q) as follows (Indraratna and Ranjith, 2001) :

$$K = \frac{Q}{2\pi LH_c} \ln\left(\frac{2mL}{D}\right) \tag{4}$$

$$k = \frac{K\mu}{\gamma_w} \tag{5}$$

where K is hydraulic conductivity, Q is flow rate of water flow through the mixture, m is square root of the ratio between the conductivity perpendicular and parallel to the hole (in this case, m is equal to 1), L is the thickness of grouting material in fracture apertures, D is diameter of the injection hole at the center of the upper block, H_c is the constant head used for the test, μ is dynamic viscosity (891×10^{-6} kg/(m·s)) at temperature of 25 °C, γ_w is unit weight of water (997.13 kg/m^3). Figure 10 shows the intrinsic permeability of grouting materials in fracture apertures for twenty-one samples.

8 DISCUSSIONS AND CONCLUSIONS

The sludge is classified as elastic silt with over 90% of its particles smaller than 0.047 mm. This study aims to determine the minimum slurry viscosity and appropriate strength of the grouting materials. The results indicate that the suitable mixing ratios for sludge-to-cement (S:C) are 1:10, 3:10 and 5:10, and for bentonite-to-cement (B:C) are 1:10, 2:10 and 3:10, with water-cement ratio (W:C) of 1:1 by weight. For the sludge these proportions yield the lowest slurry viscosity of 5 Pa·s and the highest compressive strength. For S:C of 3:10, the compressive strength and elastic modulus are 1.22 MPa and 224 MPa which are similar to those of the B:C. The direct shear test results indicate that the shear strengths at the interface between the grout and sandstone fractures varying from 0.22 to 0.90 MPa under normal stresses ranging from 0.25 to 1.25 MPa. Permeability of the grouting materials measured from the one-dimensional flow test with constant head is from 10^{-17} to 10^{-15} m^2 and decreases with curing time. The mixture with the S:C of 5:10 by weight gives the lowest permeability. The permeability of the grouts measured by radial flow test in fractures with apertures of 2, 10 and 20 mm ranges from 10^{-16} to 10^{-14} m^2. The S:C mixtures have the mechanical and hydraulic properties equivalent to those of the B:C mixtures which indicates that the sludge can be used as a substituted material to mix with cement for rock fracture grouting purpose. Such applications can also minimize the disposal cost of the sludge and reduce the environmental impact due to the landfill construction.

ACKNOWLEDGEMENTS

This study is funded by Suranaree University of Technology and by the Higher Education Promotion and National Research University of Thailand. Permission to publish this paper is gratefully acknowledged.

REFERENCES

Akgün H. and Daemen J.J.K. 1999. Design implications of analytical and laboratory studies of permanent abandonment plugs. Canadian Geotechnical J. 36, 21–38.

ASTM standard C192 2013. Practice for Making and Curing Concrete Test Specimens in the Laboratory, Section four, Vol. 04.02, ASTM International, West Conshohocken, PA, DOI: 10.1520/C0192_C0192M, www.astm.org.

ASTM standard C39 2012. Test Method for Compressive Strength of Cylindrical Concrete Specimens, Section four, Vol. 04.01, ASTM International, West Conshohocken, PA, DOI: 10.1520/C0039_C0039M-12A, www.astm.org.

ASTM standard C938 2010. Practice for Proportioning Grout Mixtures for Preplaced-Aggregate Concrete, Section four, Vol. 04.02, ASTM International, West Conshohocken, PA, DOI: 10.1520/C0938-10, www.astm.org.

ASTM standard D2196 2010. Test Methods for Rheological Properties of Non-Newtonian Materials by Rotational (Brookfield type) Viscometer, Section Six, Vol. 06.01, ASTM International, West Conshohocken, PA, DOI: 10.1520/D2196-10, www.astm.org.

ASTM standard D422 2007. Test Method for Particle-Size Analysis of Soils, Section four, Vol. 04.08, ASTM International, West Conshohocken, PA, DOI: 10.1520/D0422-63R07, www.astm.org.

ASTM standard D5607 2008. Test Method for Performing Laboratory Direct Shear Strength Tests of Rock Specimens Under Constant Normal Force, Section four, Vol. 04.08, ASTM International, West Conshohocken, PA, DOI: 10.1520/D5607-08, www.astm.org.

ASTM standard D7012 2010. Test Method for Compressive Strength and Elastic Moduli of Intact Rock Core Specimens under Varying States of Stress and Temperatures, Section four, Vol. 04.09, ASTM International, West Conshohocken, PA, DOI: 10.1520/D7012-10, www.astm.org.

ASTM standard D854 2010. Test Methods for Specific Gravity of Soil Solids by Water Pycnometer, Section four, Vol. 04.08, ASTM International, West Conshohocken, PA, DOI: 10.1520/D0854-10, www.astm.org.

Indraratna, B. and Ranjith, P. 2001. Hydromechanical Aspects and Unsaturated Flow in Joints Rock, A.A. Balkema, Lisse, pp. 1-39.

Obcheoy J., Aracheeploha S., Fuenkajorn K. 2011. Fracture permeability under normal and shear stresses, In Rock Mechanics, K. Fuenkajorn and N. Phien-wej, editor. Geomechanics Research Unit, Suranaree University of Technology, Thailand, pp 133-140.

Papp J.E. 1996. Sodium bentonite as a borehole sealant. In Sealing of Boreholes and Underground Excavations in Rock, K. Fuenkajorn and J.J.K. Daemen, editor. Chapman and Hall, London, pp 280-297.

Tsang Y.W. 1992. Usage of Equivalent Apertures for Rock Fractures as Derived From Hydraulic and Tracer Tests. Water Res. 28(5), 1451-5.

LIST OF FIGURES

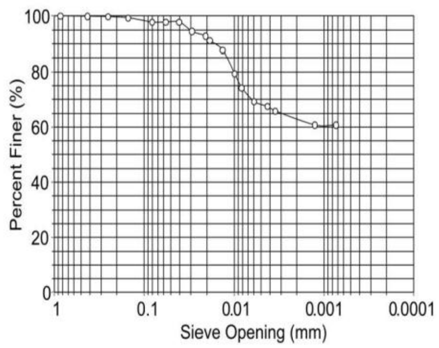

Figure 1. Grain size distribution of water treatment sludge

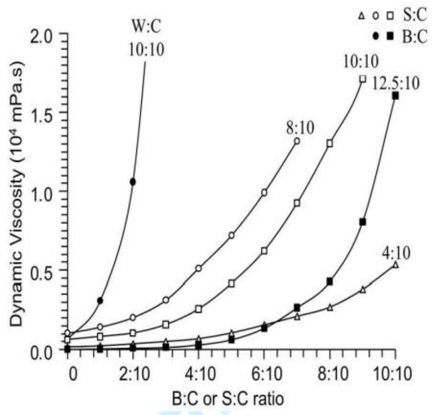

Figure 2. Dynamic viscosity of S:C and B:C for different W:C ratio.

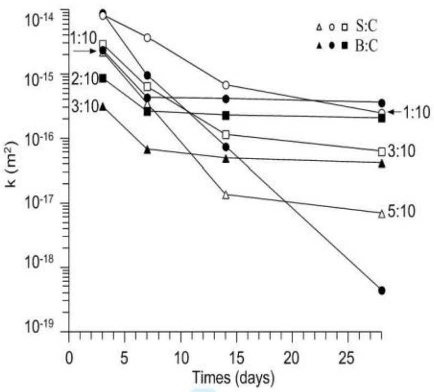

Figure 3. Intrinsic permeability as a function of time for pure cement (C), B:C, and S:C with W:C = 1:1.

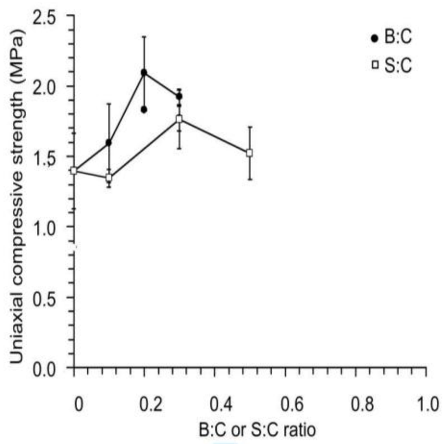

Figure 4. Uniaxial compressive strengths for B:C and S:C with W:C = 1:1.

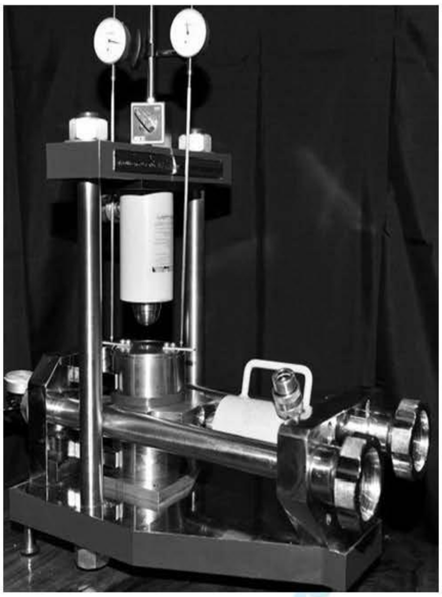

Figure 5. Laboratory arrangement for three-ring direct shear test.

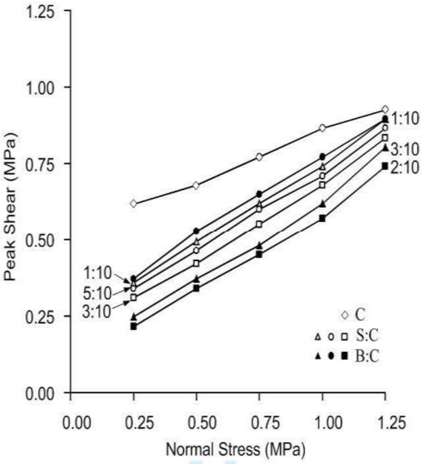

Figure 6. Normal stress and peak shear stress.

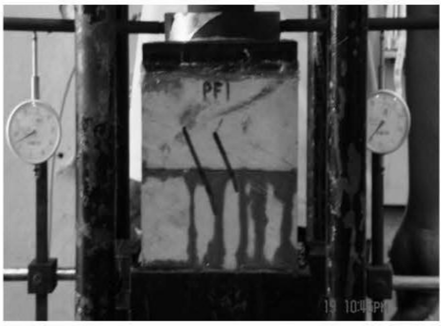

Figure 7. Laboratory arrangement for permeability testing of fractures.

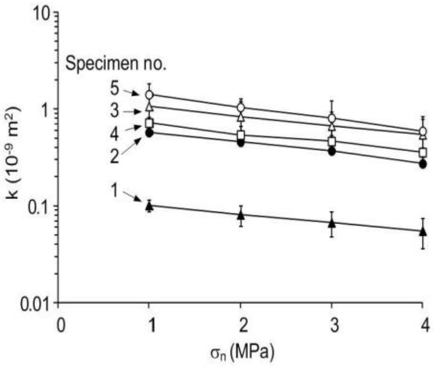

Figure 8. Intrinsic permeability (k) as a function of normal stress (σn) for fracture in Phu Kradung sandstone.

Figure 9. Permeability testing of grouting materials in rock fracture aperture 20 mm.

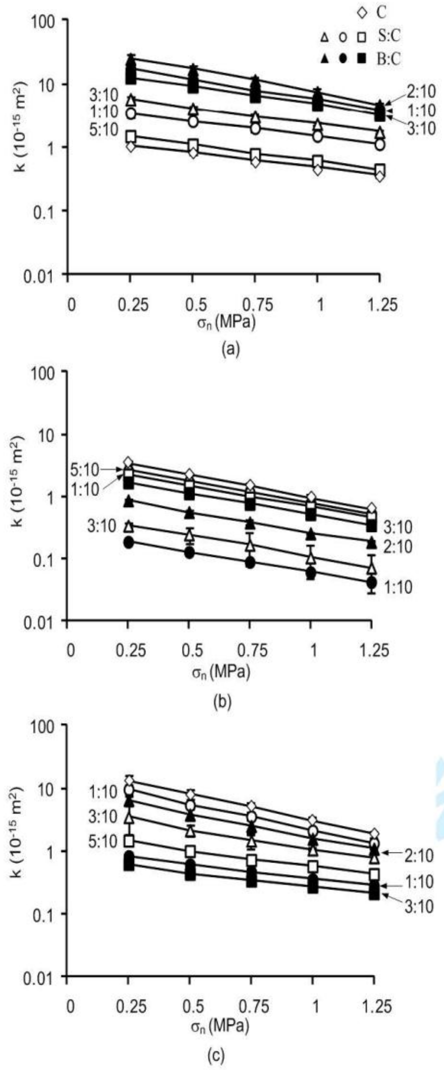

Figure 10. Intrinsic permeability (k) as a function of normal stress (σn) for fracture apertures (a) 2 mm (b) 10 mm and (c) 20 mm in Phu Kradung sandstones.

List of Tables

Table 1 Atterberg's limits and specific gravity of sludge and bentonite.

Atterberg Limits	Bentonite (%)		Sludge (%)	
	SUT *	ACC **	SUT *	TU ***
Liquid limit	357	478	55	69
Plastic limit	44	28	22	42
Plasticity index	313	449	23	28
Specific gravity	-	-	2.56	-

*SUT = Suranaree University of Technology Laboratory,
**ACC = American Colloid Company Technical Data,
***TU = Tummasart University Laboratory.

Table 2 Mechanical properties of grouting materials.

Type	Mix ratio	Number of Samples	Average density (g/cm^3)	Poisson Ratio ν	σ_c (MPa)	E (MPa)
C	0:10	5	0.83 ± 0.01	0.18	1.40 ± 0.27	212
B:C	1:10	5	1.35 ± 0.04	0.17	1.59 ± 0.28	193
B:C	2:10	5	1.38 ± 0.04	0.14	2.09 ± 0.26	275
B:C	3:10	5	1.33 ± 0.02	0.16	1.92 ± 0.05	228
S:C	1:10	5	1.91 ± 0.06	0.15	1.35 ± 0.06	190
S:C	3:10	5	1.81 ± 0.07	0.21	1.77 ± 0.21	224
S:C	5:10	5	1.79 ± 0.06	0.16	1.52 ± 0.19	261

BIOGRAPHY

Mr. Khomkrit Wetchasat was born on the 3rd of March 1977 in Chaiyaphum province. He earned his Bachelor's Degree in Civil Engineering in 1998 and Master's Degree in Geotechnology in 2002. Both degrees are from the Suranaree University of Technology (SUT). He continued with his Doctor of Philosophy Program in Geotechnology, Institute of Engineering at SUT with the major in Geological Engineering. In 1999-2002, he served in position of assistant civil engineer at the Chaiyaphum Provincial Public Works Office, and a teaching and research assistant at SUT. Since 2003, he has been working full-time as an engineer at the Metropolitan Waterworks Authority. Here, his responsibility is on the water treatment, and sludge waste disposal. Moreover, he has a part-time lecturer at SUT, Rajamangala University of Technology Suvarnabhumi, Rajamangala University of Technology Krungthep, Rajamangala University of Technology Thanyaburi, and Ramkhamhaeng University teaching Geological Engineering, Geology for Engineers, Soil Mechanics, Mechanics of Materisals, Surveying, Water Supply Engineering and Building Sanitation. He earned his registered Professional Engineer with proficiency in Civil Engineering (Reg. No. 8851) and Environmental Engineering (Reg. No. 211). His expertise is in the areas of soil and rock mechanics, nuclear waste disposal, sludge utilization and water loss management.